Stability and Mobility of Foam Generated by Gas-Solvent/Surfactant and Gas-Solvent/Nanoparticles under Reservoir Conditions

by

Chao Wang

A thesis submitted in partial fulfillment of the requirements for the degree of

Master of Science

[in

Petroleum Engineering]

Department of Civil and Environmental Engineering
University of Alberta

ABSTRACT

Foam can be a feasible means to remedy the low sweep efficiency of solvent flooding (e.g., CO_2 and/or C_3H_8) resulting from viscous fingering and gravity segregation. It works as a good mobility control agent that decreases the mobility difference between the displaced oil and the displacing agent. Solvent-alternating-surfactant is a feasible way to create foam under reservoir conditions. However, most of the surfactant-stabilized foams are normally unstable and thermally degradable, especially with the presence of salt and oil at high temperatures. To recover more oil from a depleted reservoir, the foam needs to maintain a long-term stability in the reservoir. With the continuing innovation of nanoparticle technologies, the challenges encountered by surfactant-stabilized foam can be remedied by using nanoparticles instead of surfactant as foaming agents. Solid particles need high energy to be adsorbed to, and desorbed from the fluid interfaces; therefore, the nanoparticle-stabilized foam can be highly stable even under harsh conditions (e.g., elevated temperature and the presence of oil).

In this study, firstly, the static foam stability and dynamic mobility of solvent/surfactant/pseudo-heavy-oil system under reservoir conditions have been examined experimentally by using a pressure/volume/temperature (PVT) system and a glass beadpack, respectively. The following factors are considered in the static foam stability experiments: surfactant concentration, salinity, temperature, and the presence of pure n-$C_{16}H_{34}$ as pseudo-heavy oil. It is found that increasing surfactant (Triton X-100) concentration contributes to an increase in C_3H_8 foam stability; C_3H_8 foam stability is insensitive to surfactant concentration when the surfactant concentration is above the threshold CMC. The stability of C_3H_8 foam is negatively affected by an increasing salinity, temperature, and the presence of oil. The C_3H_8 foam is much more stable than CO_2 foam at any conditions. In addition, it is found that alternating injection of C_3H_8 and Triton solution

(SAG) results in a larger pressure difference, hence leading to a higher mobility reduction effect than alternating C_3H_8 and water (WAG) through the porous media.

Secondly, the static foam stability of nanoparticle-stabilized C_3H_8 foam is examined under different reservoir conditions. Nanocrystalline cellulose (CNC), which is naturally hydrophilic and cannot act as foam stabilizer alone, has been chosen as the nanoparticle for foam stabilization purpose. Cationic CTAB is used to modify the surface of bare anionic CNC in situ from being hydrophilic to relatively hydrophobic and surface active. We examine the effects of particle coating, surfactant concentration, salinity, temperature, and the presence of oil on C_3H_8/CNC/CTAB foam stability. It is found that the stability of CTAB-coated CNC stabilized foam increases with an increase in CTAB concentration, salinity and temperature. It is less sensitive to the presence of oil. Other foams formed by recipes of C_3H_8/CNC/Tween 20, C_3H_8/CNC/Tween 80, and C_3H_8/CNC/Triton X-100 are also tested to explore the synergistic effect on foam stability due to the use of CNC and non−ionic surfactants. It is found that, if a non-ionic surfactant is a foaming agent, the synergistic effect of CNC nanoparticle and non-ionic surfactant enhances the foam stability. In other words, a stable foam can be formed by introducing both foam forming agent (surfactant) and foaming booster (nanoparticle). By comparing the stability of foam formed by CTAB-coated CNC and CNC/non-ionic surfactant mixtures, foam stability of CTAB-coated CNC stabilized foam is stronger than that of CNC/non-ionic surfactant mixtures. This is probably because the electrostatic interaction of CTAB with CNC is stronger than the synergistic effect due to the use of non-ionic surfactant and CNC, leading to a more stable foam thereof. Finally, the dynamic mobility of foam flow through porous media is examined by alternatively injecting C_3H_8 and CTAB-coated CNC or CNC/non-ionic surfactant mixtures (SAG). The experimental results indicate that if a non-ionic surfactant

is used as a foaming agent, the synergistic effect of CNC and non-ionic surfactant enhances the reduction in foam mobility. In addition, foam formed by alternatively injecting CTAB-coated CNC and C_3H_8 shows a higher mobility reduction effect than that formed by alternatively injecting CNC/non-ionic surfactant and C_3H_8, which is consistent with the results of the static stability tests. In the SAG tests (either CTAB/CNC or Triton X-100/CNC stabilized C_3H_8 foam) conducted with an oil-saturated beadpack, the presence of CNC nanoparticles is able to enhance the oil recovery due to a mobility control mechanism.

DEDICATION

This dissertation is dedicated to my dearest parents, Mrs. Xiaoli Gao and Mr. Zhenhai Wang.

ACKNOWLEDGEMENTS

I would like to express my deepest gratitude to my supervisor, Dr. Huazhou Andy Li for providing me a precious opportunity to work under his supervision through my graduate studies. He equipped me with brilliant ideas, academic and technical knowledge that is helpful in the future. I would like to extend my gratitude to his encouragement and unconditional support during my graduate studies.

I would also like to thank the following individuals or organizations for their help during my study at the University of Alberta:

- A Discovery Grant from the Natural Sciences and Engineering Research Council (NSERC) to Dr. Huazhou Andy Li;
- University of Alberta Start-up Fund for New Faculty to Dr. Huazhou Andy Li;
- Dr. Yang Liu for using the Ultrasonifier and Optical Microscope apparatus and Dr. Ravin Narain for introducing some chemicals to be used.
- The technician, Mr. Todd Kinnee, in Petroleum Engineering Department for his technical assistance on the PVT setup;
- Dr. Li's group members: Mr. Yueliang Liu, Mr. Lanxiao Hu, Mr. Bailu Teng, Mr. Jialin Shi, Mr. Dashun Wang, Ms. Jianyi Gao, Ms. Ruixue Li, Ms. Wanying Pang and Ms. Siyuan Yi;
- Faculty and staff in Petroleum Engineering Department for giving me a happy time at the University of Alberta;
- My dearest friends and families for their friendship, understanding, love and constant help.

TABLE OF CONTENTS

LIST OF FIGURES

LIST OF TABLES

CHAPTER 1 INTRODUCTION

1.1. Overview

The BP Statistical Review of World Energy shows that, at the end of 2013, total world proved oil reserves reach 1687.9 billion barrels, 60% of which are trapped in formations after primary and water flooding (BP Statistical Review, 2014). Such large quantity of residual oil is being expected to be recovered by many enhanced oil recovery (EOR) technologies. Enhanced oil recovery, also called as tertiary recovery, is the process to reduce the residual oil saturation by gas injection, chemical injection, and thermal recovery methods. At present, gas solvent flooding technique (e.g., CO_2 or C_3H_8 based solvent) has attracted much attention in heavy oil and bitumen recovery (Li *et al.*, 2013; Upreti *et al.*, 2007). However, the high mobility ratio between the displacing gas phase and the displaced oil phase is a critical challenge encountered in solvent-flooding EOR process. In other words, such low-viscosity gas is more mobile than displaced oil or water in the reservoir; therefore, it channel through the reservoir, resulting in the early breakthrough of gas with large volume of hydrocarbon trapped in reservoir. In addition, the low-density gas fluid relative to oil will readily result in the gravity segregation, which inhibits the contact between the displacing gas and deeper hydrocarbon zones. The above problems of viscous fingering and gravity segregation are considered to be an unfavorable displacement condition; because in this case, large quantities of oil in the formation will be bypassed and the formation residue oil saturation will still be high at gas breakthrough (Smith, 1988). In order to achieve a lower mobility ratio of solvent to reservoir oil, it is necessary to find a mobility control method to make the displacement sustain a uniform displacement front.

Foam has been widely used in tertiary oil recovery due to its capability of decreasing the gas-phase mobility, which can be considered as a mobility control agent. Therefore, generating foam *in situ* can be a viable approach to mitigating the sweep inhomogeneity and increase the sweep efficiency of solvent flood due to the foaming mechanism. The high apparent viscosity of foam contributes to a low mobility of the displacing fluid, i.e., gas solvent, which is critical to improving the volumetric sweep efficiency of solvent flood so as to improve the oil recovery. Conventional foam, generated *in situ* by surfactant-alternating-solvent injection (SAG), is widely used in the oil and gas industry. Surfactant is considered as an effective foam forming agent due to its amphiphilic property. In other words, the hydrophilic head of surfactant has the affinity to the water phase, while its hydrophobic tail has the affinity to gas or oil.

However, most foam generated by surfactant can be naturally unstable and thermally degradable; therefore, they cannot maintain long-term stability before fulfilling the duty, especially at elevated temperatures or with the presence of brine or oil. In addition, surfactant also has potential to be adsorbed to the rock, resulting in a high surfactant retention (Grigg and Mikhalin, 2007). Recently, with a growing interest in nanotechnology applications in the petroleum industry, employing the nanoparticles to replace the surfactant is an alternative way for generating foam, which can partially remedy the limitations of the traditional surfactant-stabilized foam.

1.2. Literature Review

Foam can be used to displace the trapped oil in formations, and it needs to maintain a long-term stability to fulfill its duty under the reservoir conditions.

1.2.1. Stability of Foam Formed by Surfactant

The low-density gas used for displacing oil in a reservoir hardly contacts the deeper part of the reservoir due to the gravity segregation. Its low viscosity also makes it easily channel through the formation due to a high mobility ratio between the displacing phase the displaced phase. The mobility ratio (M) is defined as:

$$M = \frac{\lambda_{displacing}}{\lambda_{displaced}} = \frac{\left(\frac{k_r}{\mu}\right)_{displacing}}{\left(\frac{k_r}{\mu}\right)_{displaced}} \quad (1)$$

where λ is the mobility, k_r is the relative permeability, and μ is the viscosity. Based on Equation (1), as to reduce the mobility ratio (M), i.e., overcome the gravity segregation and fingering or channeling problem, it is not practical to increase the density of displacing phase or decrease the permeability of displacing phase in the formation. The most feasible way is to increase the viscosity of the displacing phase via using foam. Extensive studies have focused on foam stability of surfactant-stabilized foam by a conventional way of solvent-alternating-surfactant method. The earliest idea of using foam to displace oil was suggested and patented by Bond and Holbrook in 1958 (Bond and Holbrook, 1958). Soon after, Fred (Fred, 1961) conducted extensive laboratory experiments to further confirm that the foam can perform as a blocking agent to reduce the mobility of the displacing solvent. Following Fred's laboratory work, Bernard and Holm found that the conventional CO_2 flooding method could easily bypass large quantities of oil in the reservoir, resulting in a disappointing recovery. In 1967, they patented a notion that uses foam for mobility control in CO_2 recovery method. They noticed that the sweep efficiency was more satisfactory by just adding a small quantity of surfactant into CO_2-water

flood process compared to conventional CO_2 flooding. Although the increased sweep efficiency achieved, there exists a difficulty in dissolving the Triton X-100 in CO_2 (Bernard and Holm, 1967). Surfactant-stabilized foam readily suffers from the surfactant degradation due to the high temperature, high salinity and the presence of oil and the surfactant absorption onto the formation rock. The use of nanoparticles to replace surfactant can overcome such limitations so as to enhance the foam stability.

1.2.2. Stability of Foam Formed by Nanoparticles

As to remedy the lack of the capability of providing stable foam over a long period by surfactant under harsh reservoir conditions, the surfactant can be replaced by nanoparticles to generate foam with outstanding foam stability. Colloidal particles on the nanoscale, behaving like surfactant, can act as a foam stabilizer by spontaneously residing at fluid interfaces. Nanoparticles can be irreversibly attached to the immiscible gas-liquid or liquid-liquid interfaces due to their high adsorption energy. Such high adsorption energy of nanoparticles might enable the foam to tolerate challenging conditions including high temperature, high salinity, and he presence of oil.

In order to achieve long lasting foams, nanoparticles need to exhibit a certain contact angle at the interfaces, indicating a strong free energy of adhesion to the fluid interfaces (Binks, 2002; Binks and Horozov 2006). As for spherical particles, the minimum free energy of particle detachment (E) is given as:

$$E = \pi r^2 \gamma (1 \pm cos\theta)^2 \qquad (2)$$

where r is spherical particle radius; γ is interfacial tension; and θ is contact angle. Equation (2) shows that the particle detachment energy increases as contact angle increases until it reaches

90^o, and then decreases with a further increase in contact angle. When the contact angle is around 90^o, nanoparticles can be irreversibly trapped into the liquid interface with an energy thousand times of k_BT. As for non-spherical particles, the particle orientation and aspect ratio need to be considered in the detachment energy. Binks and Horozov (2006) also reported that particles with a disklike-shape exhibit a higher detachment energy than those with a rodlike-shape, and rodlike-shape particles have a higher detachment energy than the spherical particles.

There are extensive new researches associated with the nanoparticle-stabilized foams. The pioneering idea of nanoparticle-stabilized foams or emulsions, also called as pickering emulsion, was suggested by Ramsden (Ramsden, 1903) and Pickering (Pickering, 1907) in the early twentieth century. Studies by Alargova *et al.* (2004) demonstrated that the hydrophobic polymer microrods can generate super-stabilized aqueous foams, which can keep a constant foam volume for many days, in contrast to a few hours' lifetime of foam generated by sodium dodecyl sulfate (SDS) surfactant. Soon after, Binks and Horozov (2005) hydrophobized the fumed silica to test the foam stability with varied particle hydrophobicity. Their findings showed that particles with an intermediate hydrophobicity are surface active and tend to have a higher chance of being attached to the fluid interfaces. However, most raw nanoparticles are inherently hydrophilic; thus it is necessary to modify the wettability of these colloidal particles from being hydrophilic to being more hydrophobic. Espinoda *et al.* (2010) obtained very stable in-situ supercritical CO_2-in-water foams by co-injecting the CO_2 and the dispersion of hydrophilic fumed silica coated with polyethylene glycol (PEG) through a glass-beads pack with 180 um glass beads. The resistance to flow calculated from the measured differential pressure of the capillary tube showed that the viscosity of silica-stabilized foam is two to eighteen times than fluids without nanoparticle. Later on, Yu *et al.* (2012) studied the effect of total injection rate and phase ratio of CO_2/silica

dispersion on the foam mobility through glass beads. The results showed that the higher the total flowrate and phase ratio of CO_2/silica dispersion, the higher the foam mobility. Worthen *et al.* (2012) employed the partially hydrophobic silica modified by methyl silyl ligands to achieve a long-term CO_2 in water foam, which revealed greater foam stability than that formed by PEG-coated silica.

However, surface treatment of non-surface-active nanoparticles through chemical modification may be expensive and complicated. Later, some researchers found that altering the particle surface via physiochemical adsorption is also an effective method. Zhang *et al.* (2008) reported that the combination of inherently hydrophilic laponite clay with non-ionic surfactant $C_{12}E_4$ created a synergistic effect on stabilization of foam. Recently, static tests by Singh *et al.* (2014) revealed that foam stabilized by mixture of silica and anionic surfactant is more stable at elevated temperature and with the presence of oil than the surfactant-stabilized foam.

Up to date, most previous works were focused on determining experimentally the foam stability generated by N_2 or CO_2; however, C_3H_8 is also a commonly used rich gas in the solvent flooding, none of the researches have focused on C_3H_8 stabilized foam. The gas type may have a significant effect on the foam stability. In addition, most of the previous studies only focused on exploring the foam stabilization mechanism of spherical nanoparticles. No research has been conducted on foam stabilized by one unique type of non-spherical nanoparticles, i.e., cellulose nanocrystals (CNC). CNC is derived from low-cost, environmental-friendly and abundant fibre materials. Besides, only a few of studies examined the foam stability of foam generated either by surfactant or nanoparticles under harsh reservoir conditions, such as high salinity, elevated temperature, and presence of oil (Zhang *et al.* 2008; Espinoda *et al.* 2010; Yu *et al.* 2012; Worthen *et al.* 2012). Therefore, it is highly necessary to test the foam stability of foam

generated by C_3H_8 in both conventional (surfactant-stabilized foam) and nonconventional (nanoparticle-stabilized foam) way under reservoir conditions.

1.3. Objectives

The objective of this study is to systematically test the static stability and dynamic mobility of C_3H_8 foam stabilized by surfactant and nanoparticle experimentally by using a pressure/volume/temperature (PVT) setup and a glass beadpack, respectively. Static foam stability test is conducted by recording the foam height as a function of time. Dynamic mobility test is conducted by recording the pressure drop across the porous glass beadpack. The detailed objectives are listed as follows,

1) To conduct the static foam stability test of foam generated by C_3H_8/Triton X-100 under different surfactant concentrations, salinities, temperatures and absence and presence of pure *n*-$C_{16}H_{34}$, as compared to CO_2/Triton X-100 foam;
2) To test the static foam stability of C_3H_8 foam stabilized by silica/Triton X-100, CTAB modified CNC, or CNC/nonionic surfactant mixture. The influencing factors including concentration, salinity and temperature are considered. The effect of presence of oil on foam stability is only considered for the CNC/CTAB system.
3) To test the mobility of SAG-generated foam and NAG-generated foam (nanoparticle alternating gas) by allowing the foam to flow through a porous glass beadpack.

1.4. Thesis Outline

This Thesis is divided into five chapters and organized as follows:

Chapter 1 provides an overview of the foam flooding technology, updated literature review and

background on stability of foam stabilized either by gas/surfactant or gas/nanoparticle, and the major research objectives.

Chapter 2 discusses the static stability and dynamic mobility of foam generated by gas solvent/surfactant (Triton X-100) mixtures. In the static tests, the effect of surfactant concentration, salinity, temperature, and absence and presence of pure *n*-$C_{16}H_{34}$ as the pseudo-heavy oil on foam stability, have been investigated. Two types of foams have been considered in the static foam-stability test for comparison purpose: C_3H_8 foam and CO_2 foam. Then the optimized surfactant concentration in bulk test is used to test the mobility of SAG-generated foam flowing through a glass beadpack.

Chapter 3 discusses and compares the static foam stability of C_3H_8 foam stabilized by silica/Triton X-100, cationic CTAB modified CNC, or CNC/nonionic surfactant mixture under different concentrations, salinities, and temperatures. The effect of presence of oil on CNC/CTAB foam is also tested.

Chapter 4 covers the mobility test results by alternately injecting C_3H_8 and CTAB modified CNC, or alternately injecting C_3H_8 and CNC/nonionic surfactant mixtures, through a porous glass beadpack.

Chapter 5 provides the conclusions of the current research as well as the recommendations and suggestions for future work.

CHAPTER 2 STABILITY AND MOBILITY OF TRITON X-100-STABILIZED C_3H_8 FOAM UNDER RESERVOIR CONDITIONS

2.1. Introduction

Although it is a widely accepted method to use commercially available gas, i.e., CO_2 or C_3H_8, to recover oil in the formations, its low density and low viscosity, resulting in an unfavorable recovery, is nonnegligible. Generating foam in situ can be used to overcome such problems by alternately injecting surfactant and gas, i.e., SAG. The stability and mobility of surfactant-stabilized foam under reservoir conditions is worth of study. This chapter is organized as follows: Section 1 discusses the static foam stability of Triton X-100-stabilzied C_3H_8 foam under reservoir conditions with the variations of surfactant concentration, salinity, temperature, and with and without the presence of oil, by using a pressure/volume/temperature (PVT) setup. Section 2 compares Triton X-100-stabilized C_3H_8 foam with Triton X-100-stabilized CO_2 foam. Section 3 applies the optimum conditions obtained in the bulk stability tests to conduct the flow mobility experiments by alternately injecting Triton X-100 and C_3H_8 through a porous media.

2.2. Experimental Section

2.2.1. Materials

The surfactant used in this study is the non-ionic polyoxyethylene octylphenyl ether with purity of 100%, also called as Triton X-100 (See Figure 2-1 for its molecular structure with n=10). Triton X-100 has been considered as an excellent foaming agent in previous studies. This product is supplied by Sigma-Aldrich. The solid sodium chloride (NaCl), provided by Fisher Scientific Acros Organics, with purity greater than 99%, is used in experiments for salinity control. CO_2

(Praxair, Canada) and C_3H_8 (Praxair, Canada) with 99.5% purity, are used to generate foam. C_3H_8 and CO_2 maintain gas phase as they are injected into PVT. *n*-$C_{16}H_{34}$ with 99% purity is chosen as the pseudo-oil to simulate heavy oil for studying the effect of oil presence on foam stability. This product is supplied by Fisher Scientific Acros Organics. *n*-$C_{16}H_{34}$ is chosen, instead of heavy oil, because heavy oil is opaque such that it will be stuck on the glass cylinder, making the visual reading of the foam height very difficult. The weight of Triton X-100 and NaCl are weighed by an electronic balance. The fresh sample solutions with different surfactant concentrations and salinities are prepared separately by dissolving them into de-ionized water right before each test and the concentrations in the aqueous phase are expressed in w/v (weight over volume fraction). No further modification has been applied to the chemicals mentioned above.

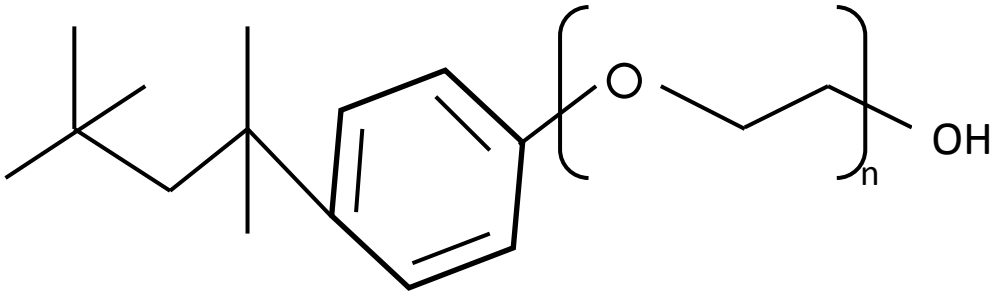

Figure 2-1 Molecular structure of Triton X-100 surfactant with *n*=10 (Supplied by Sigma-Aldrich)

2.2.2. Experimental Setup

2.2.2.1. Static Foam Stability Tests

The experimental apparatus used for studying the static foam stability is a mercury-free DBR PVT system (Schlumberger, Canada), as shown in Figure 2-2. The PVT cell, also called visual

cell, is a transparent glass column embedded in a PVT system with a total volume of 112 ccs. There is a mobile isolation piston inside the cell separating the cell into two chambers: the hydraulic oil chamber above and the sample chamber below. The sample chamber volume can be changed by compressing or expanding the upper hydraulic oil so that the piston can move up or down. The cell can withstand a pressure up to 15,000 psi that is controlled by the positive displacement pump (DBR Pump, Schlumberger, Canada). The cell can tolerate a temperature range of -10ºC to 200ºC that is controlled by a microprocessor temperature controller. A magnetic stir is installed at the bottom of the cell to rock and mix the sample. A vacuum pump (1400, Welch Vacuum, USA) is used to vacuum the PVT cell. The fresh surfactant solution is first prepared and then placed in a small transfer cylinder. It will later be transferred into the bottom chamber of PVT cell. One charging vessel is used to store the *n*-$C_{16}H_{34}$ that will be later transferred into the PVT cell by using the DBR Pump. The fluid height in the visual cell is accurately measured by a cathetometer with a resolution of 0.002 cm.

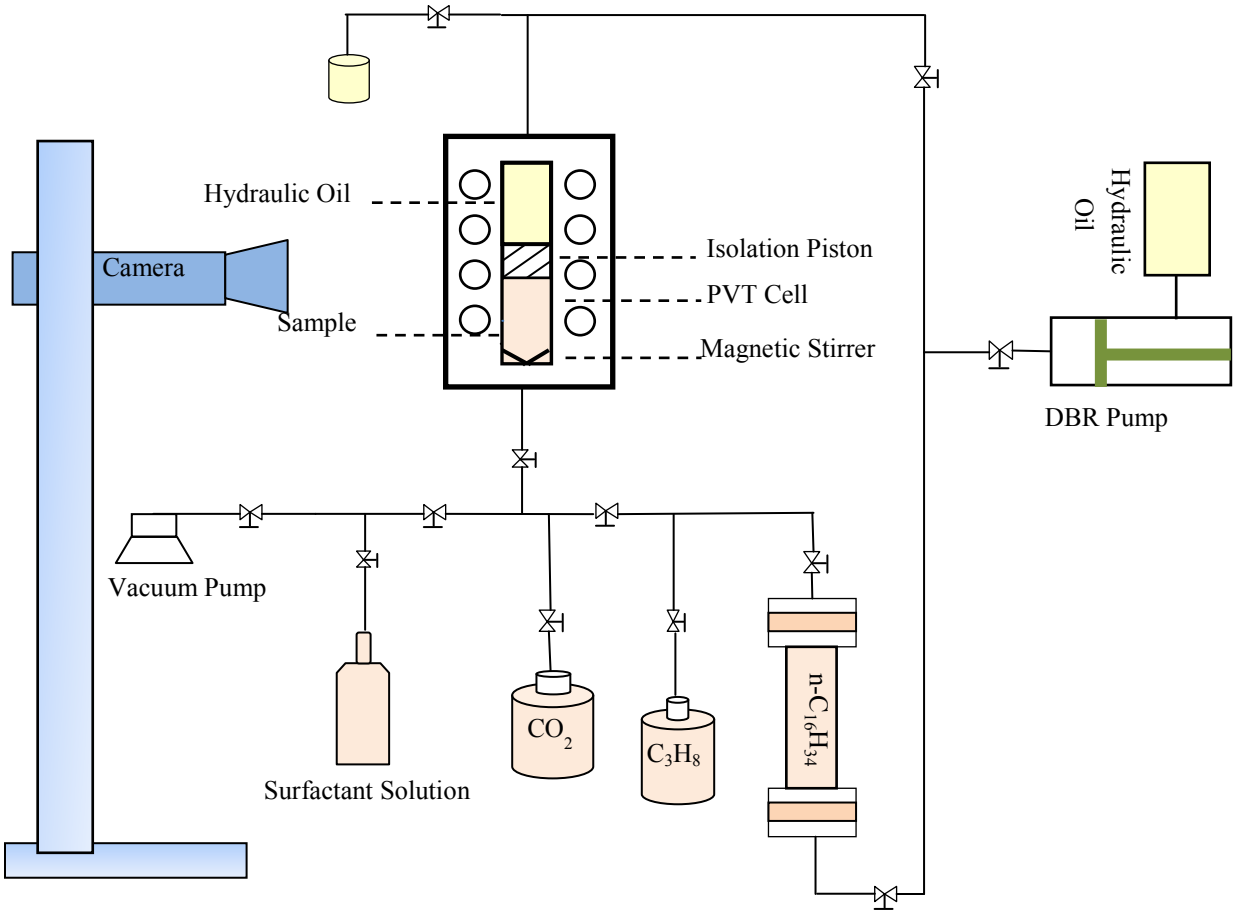

Figure 2-2 Schematic of the PVT experimental setup for foam stability tests

2.2.2.2. Mobility of Foam through Porous Media

Figure 2-3 shows a diagram of the experimental apparatus used to test the mobility of foam generated using the SAG method. A 38.400-cm long stainless steel tube with 0.386 cm inner diameter has been packed tightly with 177 μm to 250 μm spherical glass beads. Glass beads are sealed in place by metal screens attached to the tubing ends. For a constant flowrate, surfactant solution is placed in a transfer cylinder and injected by a syringe pump and gas is injected from a gas tank through a mass flow controller. The dynamic pressure difference is measured by a differential pressure gauge (PM, Heise, USA) that is connected to the two ends of the glass

beadpack. A mass flow controller (RK 32907-57, Cole-Parmer, Canada) is used to control the injection rate of C_3H_8.

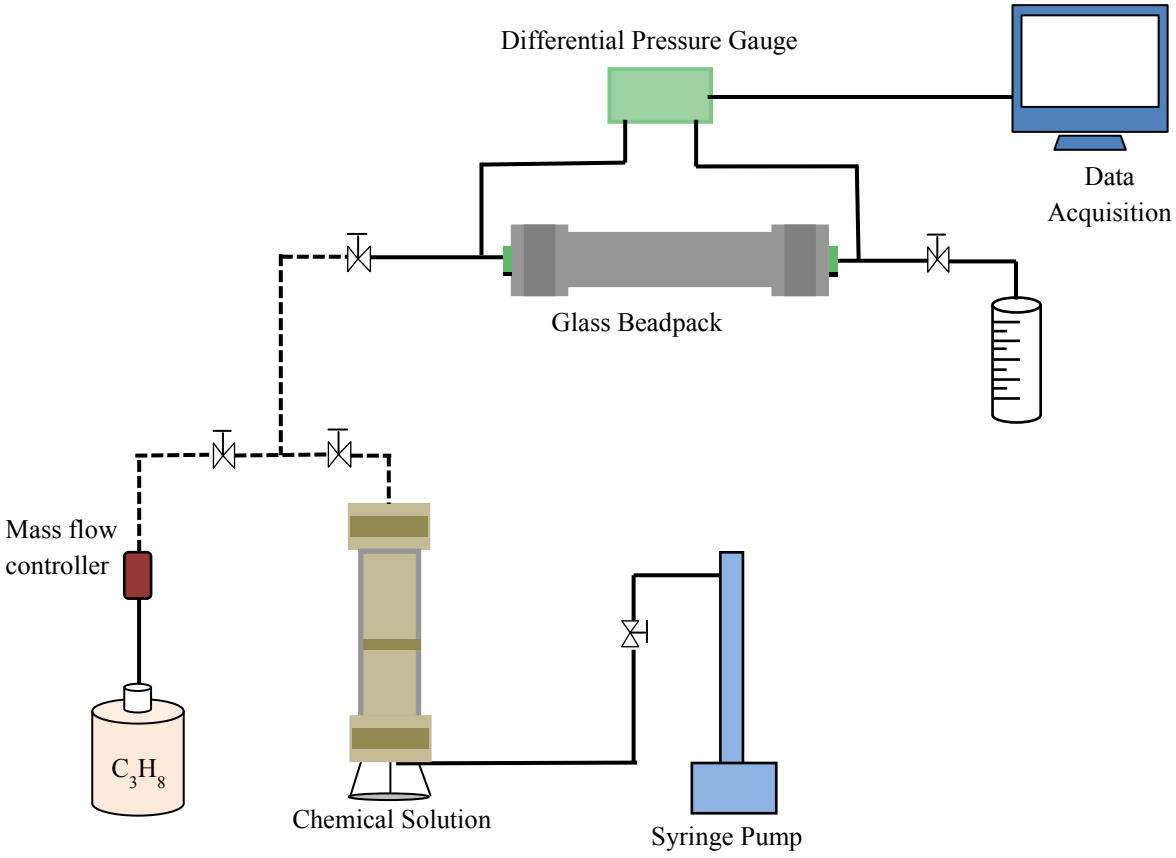

Figure 2-3 Schematic of the experimental setup for studying foam flow through porous media

2.2.3. Experimental Procedure

2.2.3.1. Static Foam Stability Tests

Prior to each test, the PVT cell and tubings are cleaned with de-ionized water for three times and then evacuated by a vacuum pump. In addition, at least 12 hours is needed to allow the cell temperature to reach the desired temperature. Each sample is first freshly prepared and then

placed in the transfer cylinder before each test. During the experiment, about 15 cc of the prepared surfactant solution in transfer cylinder is firstly transferred into the PVT cell. Next, C_3H_8 gas is discharged into the PVT cell at a constant pump flow rate of 500 cm^3/hr. The resulting volume ratio of C_3H_8 gas to surfactant solution is kept as 2:1. Then the magnetic stir is turned on for 2 min right after the gas injection terminates in order to generate cloudy foam. When mixing stops, the initial height of foam is recorded. Then foam will decay and collapse as time elapses. The heights of foam above liquid phase and below gas phase at different times can be recorded in order to inspect the foam decay. The time, when the foam height reduces to half of its initial height, is called half-life ($t_{1/2}$). A longer half-life represents a more stable foam. In the experiments with oil presence, there is an additional step to introduce 5 cm^3 oil into the PVT cell at a rate of 500 cm^3/hr just after the stirring is terminated. As for the experiments with oil presence, the PVT cell needs to be cleaned with toluene twice before cleaning with water to remove any traces of oil. The bubble size and foam uniformity can also be visually observed during the tests. As for the CO_2-stabilized foam, CO_2 is used to replace C_3H_8 gas.

As for the C_3H_8 foam, the maximum initial foam height under room temperature and 700 kPa is firstly tested by running the experiments three times at three surfactant concentrations of 0.0155 w/v, 0.0194 w/v and 0.0310 w/v, respectively. Secondly, the foam stability tests are performed by using such validated critical micelle concentration (CMC) at different salinities of 200 ppm, 5,000 ppm, 50,000 ppm and 100,000 ppm, respectively, and under the same temperature and pressure conditions (i.e., 20ºC and 700 kPa). The solution with the validated CMC and 5,000 ppm salinity is used to test the foam behavior at 50ºC and 80ºC. Some representative tests mentioned above are selected to test the stability of CO_2 foam.

2.2.3.2. Dynamic Foam Mobility Tests

Prior to each experiment, the tubing containing newly packed glass beads is first evacuated and flooded by 15 PV of freshly prepared surfactant solution. Foam is then generated *in situ* by alternatively injecting C_3H_8 gas and surfactant solution into the beadpack. The duration of either C_3H_8 or surfactant injection is set as 2 min. C_3H_8 is injected at a rate of 6 cm^3/min, while the surfactant solution is injected at a rate of 3 cm^3/min (SAG ratio of 1:2) or 2 cm^3/min (SAG ratio of 1:3). During the tests, pressure differences are recorded as a function of time. The permeability of the beadpack is measured to be 34.16 Darcy by recording the steady-state pressure differences when water is flowing through the beadpack at different rates. Other properties of the glass beadpack are detailed in Table 2-1. The fluid mobility can be calculated by applying Darcy's law:

$$\lambda = \frac{qL}{A\Delta p} \tag{3}$$

where λ is the fluid mobility in Darcy/cp; q is the volumetric flow rate of fluid in cm^3/s; L is the beadpack length in cm; A is the cross-sectional area of the beadpack in cm^2; Δp is the differential pressure along the beadpack in atm. All these foam mobility tests are conducted at the room temperature of 20ºC.

Table 2-1 Properties of the glass beadpack used in the experiments

Length (cm)	38.400
Diameter (cm)	0.386
Pore volume (cm^3)	1.823
Porosity	40.58%
Permeability (Darcy)	34.16

2.3. Results and Discussion

2.3.1. C_3H_8-Foam Stability

2.3.1.1. Surfactant Concentration Effect on C_3H_8-Foam Stability

Surfactants are able to form an aggregation, also called as a micelle, in a solution above a critical value of surfactant concentration (called as CMC). At high surfactant concentrations, the foamability becomes independent of concentrations; therefore, defining CMC during the experiments is meaningful to prevent forming the micelle and reduce the cost spent on the extra surfactant. The CMC of Triton X-100 lies in the range between 0.0155 w/v and 0.0200 w/v (Fisher Scientific Acros Organics, Canada) at room temperature. Hence, three different concentrations of 0.0155 w/v, 0.0194 w/v and 0.0310 w/v are selected in the foam tests to confirm the actual CMC of the Triton X-100 used. Figure 2-4 plots the initial foam height as a function of Triton X-100 surfactant concentration. The previous study indicates that the foamability, initial height of foam, increases with an increase in surfactant concentration until its CMC is reached; then there will be little increment in the initial foam height as the concentration increases above such CMC. This is because the further increase of surfactant concentration does not change the amount of free molecules of the surfactant (Chiang *et al.*, 1980). All three selected concentrations show good foamability during foam formation; however, the initial foam height increases as the concentration increases from 0.0155 w/v to 0.0194 w/v and then gently decreases as the concentration increases to 0.0310 w/v. The initial height is highest at 3.449 cm with 0.0194 w/v surfactant concentration at room temperature, which can be considered as an effective CMC concentration in this case. Above this effective CMC, a further increase in surfactant concentration shows little effect on foam height. It is efficient and economical to use

surfactant concentration at CMC during enhanced oil recovery applications because unnecessary increase in the surfactant cost can be otherwise incurred. According to the experimental results, the validated CMC from tests is within the range of recommended CMC by the supplier.

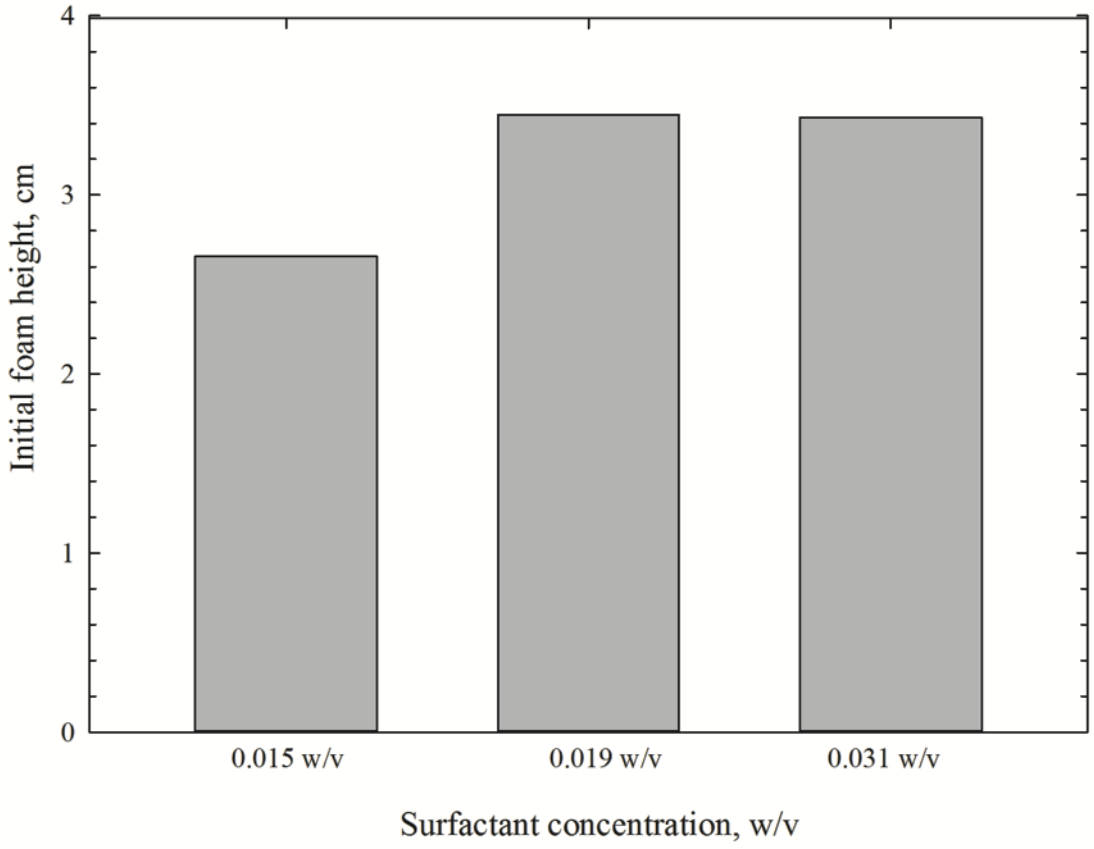

Figure 2-4 Comparison of initial heights of C_3H_8 foam under different Triton X-100 concentrations (0 ppm salinity and 20°C)

Figure 2-5 plots the change of foam height as a function of time at different surfactant concentrations, which demonstrates that the foam decay trend is milder at concentrations of 0.0194 w/v and 0.0310 w/v compared to the sharp decay of foam at 0.0155 w/v surfactant solution. With an increase in the surfactant concentration above CMC, foam stability will not increase anymore and be generally insensitive to surfactant concentrations. The stability of foam

depends on two main factors - film drainage and film rupture. The rapid initial foam column reduction at the beginning is due to the gravity drainage effect. This means that, after foam is generated, the liquid drains downward through the liquid film of bubbles due to gravity force (Simjoo *et al.*, 2013). As the gravitational flow becomes slow, film drainage is dominated by liquid discharging at plateau borders. Then, as the liquid travels into the plateau boarder from lamella, lamella becomes thinner and eventually ends up with rupturing. The random distortion of foam can also lead to film rupturing (Shaw, 1992). The visual observation reveals that, at or above CMC, bubbles maintain stable spherical structures and the bubble size is distributed homogeneously with a diameter smaller than 1 mm. Bubble coalescence process is not visible through the glass column. For bubbles at a surfactant concentration below CMC (0.0194 w/v), the rupture process still cannot be observed, but the bubble size increases to 1-2 mm in diameter. Therefore, the foam tends to be smaller, denser and more narrowly distributed at a higher surfactant concentration.

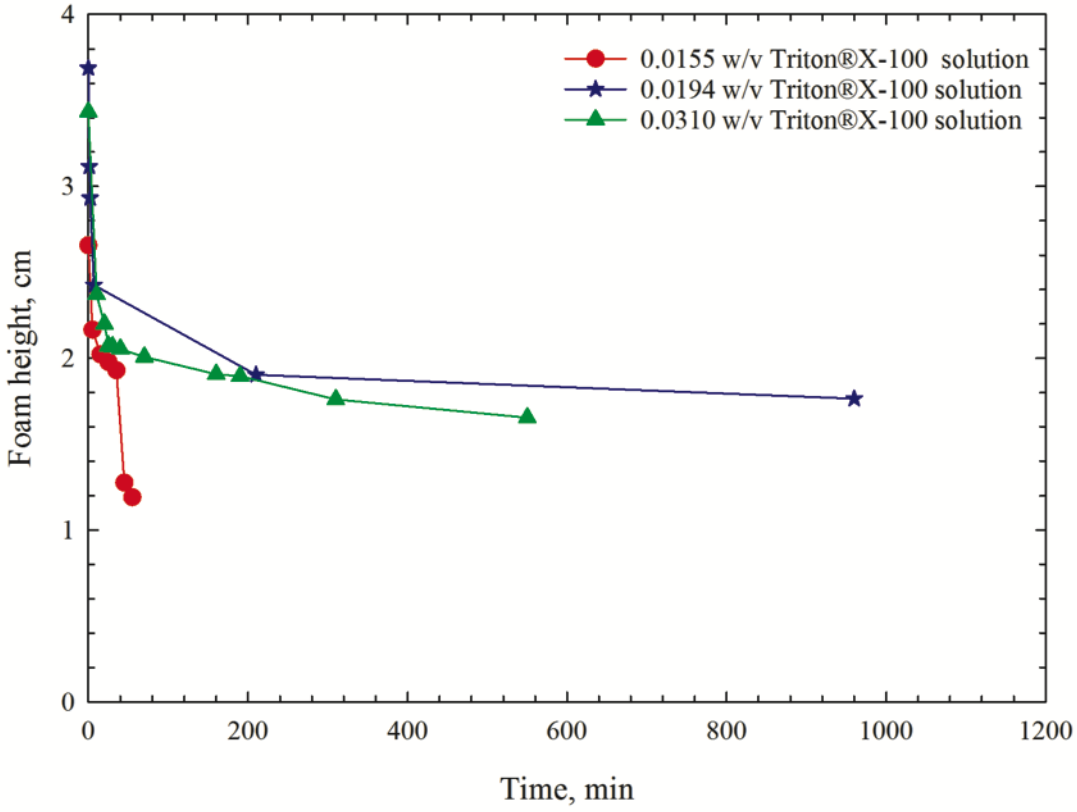

Figure 2-5 Comparison of C_3H_8-foam stability measured at different Triton X-100 concentrations (0 ppm salinity and 20°C)

2.3.1.2. Salinity Effect on C_3H_8-Foam Stability

In an oil reservoir, the connate water contains naturally generated electrolytes. Several studies demonstrate that the presence of electrolytes has an influence on the stability of the surfactant-stabilized foam. The foam stability tests are then conducted with different salt (NaCl) concentrations of 200 ppm, 5,000 ppm, 50,000 ppm and 100,000 ppm, respectively. The other operating conditions are: surfactant concentration: 0.0194 w/v (validated CMC), temperature: 20°C and absolute pressure: 700 kPa. Figure 2-6 shows that the foams at all tested salinities can be considered as stable foams. All foams exhibit a short period of fast foam-draining process, i.e.,

around 2 min, followed by a long period of the gentle foam-decay process. Table 2-2 summarizes the measured initial height and half-life of the foams formed at different salinities. It clearly indicates that the foamability or foam's initial height decreases as salinity increases. When salting-out electrolytes (NaCl) are added to the nonionic surfactant solution, the foam foamability or stability may decrease in a minor scale (Schott, 1988). The addition of NaCl salts out some surfactant from the solution. Therefore, it reduces the effective surfactant concentration, resulting in a reduced foamability.The half-life of foam column is a common method to show foam stability. A longer half-life represents a more stable foam. As shown in Table 2-2, as salinity increases, half-life decreases slightly, except the case at 50,000 ppm with a half-life of 50 min more than that of 5,000 ppm case. These observations add up to a general conclusion that the addition of electrolytes leads to a reduced foam stability to a small degree, but, in general, the C_3H_8 foam is stable at all salinities and is less sensitive to electrolytes.

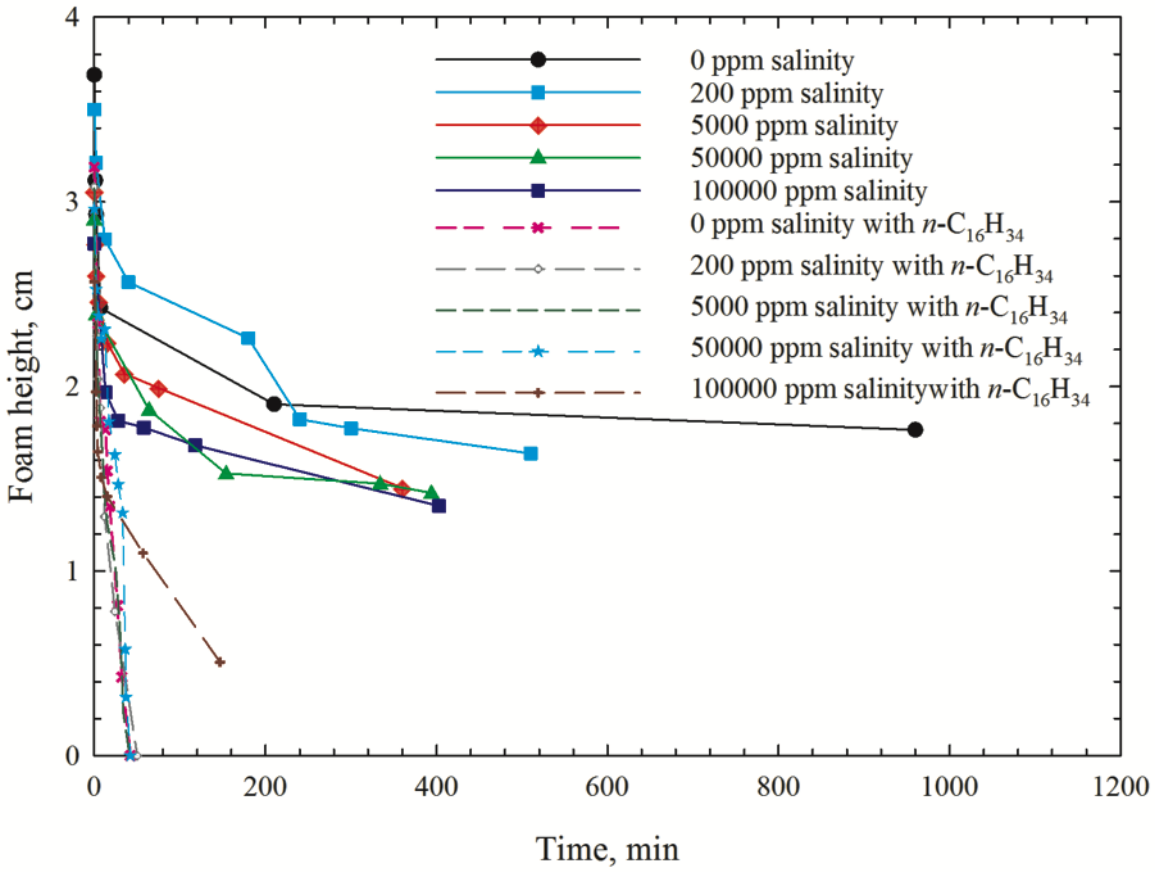

Figure 2-6 Comparison of C_3H_8-foam decay profile as a function of time at different salinities with and without the presence of *n*-$C_{16}H_{34}$ (0.0194 w/v Triton X-100 and 20°C)

Table 2-2 Foamability and half-life of foams generated at different salinities at 0.0194 w/v surfactant concentration at 20°C in oil and non-oil cases.

Salt concentration, ppm	without *n*-$C_{16}H_{34}$		with *n*-$C_{16}H_{34}$	
	Initial height, cm	Half-life, min	Initial height, cm	Half-life, min
0	3.688	585	3.189	15
200	3.500	360	3.080	10
5000	3.053	304	3.072	11
50000	2.903	354	2.962	25
100000	2.775	302	2.568	13

2.3.1.3. Effect of Temperature on C_3H_8-Foam Stability

Many previous studies have demonstrated that foam is a thermodynamically unstable fluid due to its high interfacial area (Belhaij *et al.*, 2014); therefore, it is necessary to test the foam stability of Triton X-100 at elevated temperatures. Foam stability in Triton X-100 solution with a concentration of 0.0194 w/v and 5,000 ppm salinity is tested at temperatures of 20°C, 50°C and 80°C, respectively. Figure 2-7 shows only minor changes in foamability occur with the rising temperature from 20°C to 50°C; however, foam column shortens rapidly with time at elevated temperatures, indicating a reduced stability as temperature increases. At 80°C, the temperature is too high to generate foam. The decay trend of foam at 50°C is different from the one at 20°C: the foam height drops dramatically as time elapses without any gentle decrease at a later time. According to the half-life measurement (Table 2-3), the half-life of foam at 20°C is around 25 times higher than that at 50°C, confirming a consistent observation as shown in Figure 2-7 that a high temperature is quite detrimental to the foam stability for Triton X-100 solution. Figure 2-8a and 2-8b show the snapshots of long foam column generated 20 min after the mixing termination at 20°C and short column at 50°C, respectively, The texture of foam at 20°C is characterized with fine bubbles (smaller than 1 mm in diameter) and uniform bubble size distribution; while the texture of foam at 50°C is characterized by relatively coarse bubbles and a wider bubble size distribution (1-3 mm in diameter). A similar result has been found in previous studies, showing that the bubble size increases as the temperature increases (Sharma *et al.*, 1985). Since foam is thermodynamically unstable, its interfacial area tends to be reduced, therefore decreasing its interfacial free energy by bubble coalescence process (Wang and Yoon, 2006). Bubble coarsening by bubble coalescence is one type of foam destabilization mechanism. When the gas pressure inside the small bubbles exceeds the pressure inside large bubbles, gas will diffuse into

the large bubbles from small bubbles through the liquid film, resulting in bubble coarsening and consequently bubble rupturing (Cervantes, 2008). By comparing the textures of foam at different temperatures, one can conclude that foam is thermodynamically unstable, which shows a faster bubble-collapse rate at higher temperatures than that at the room temperature.

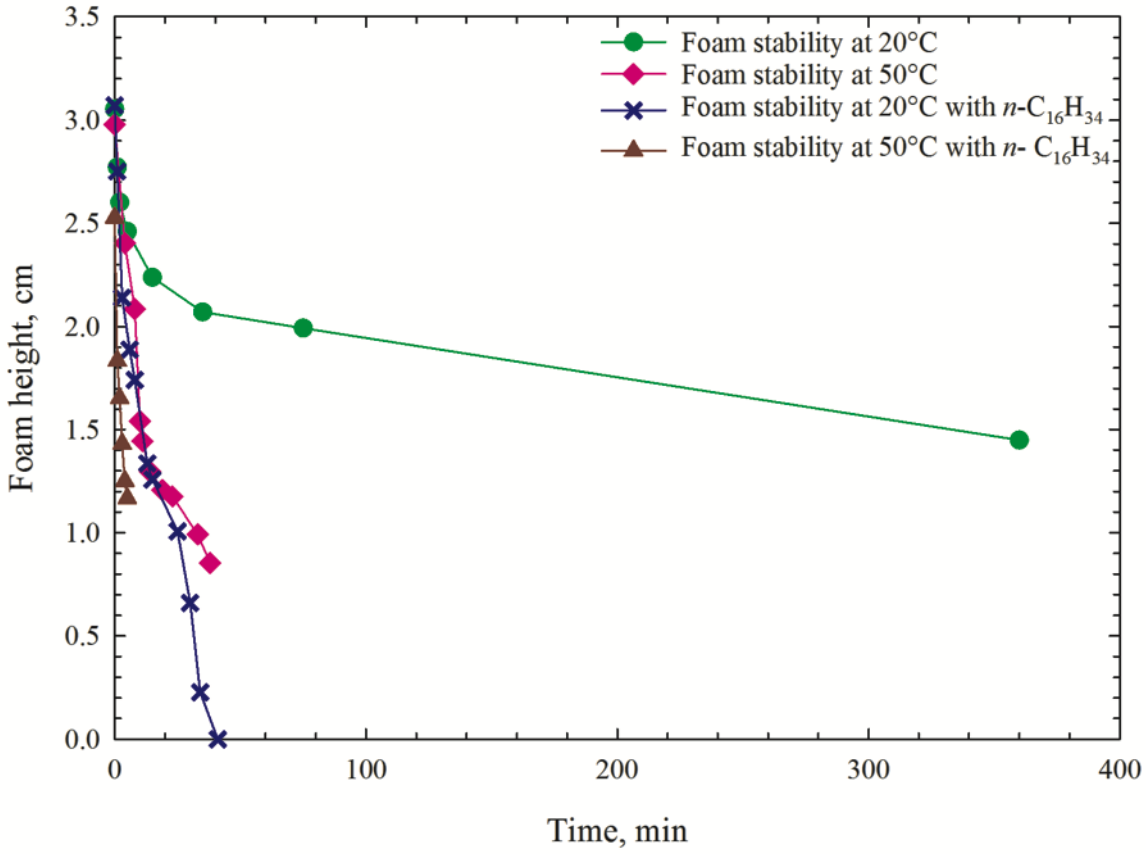

Figure 2-7 Comparison of temperature effect on C_3H_8-foam stability with and without the presence of *n*-$C_{16}H_{34}$ (0.0194 w/v Triton X-100 and 5,000 ppm salinity)

Table 2-3 Half-life of foam generated by 0.0194 w/v surfactant and 5,000 ppm salinity at different temperatures.

Temperature, °C	Half-life (without *n*-$C_{16}H_{34}$), min	Half-life (with *n*-$C_{16}H_{34}$), min
20	304	11
50	11	4
80	N/A	N/A

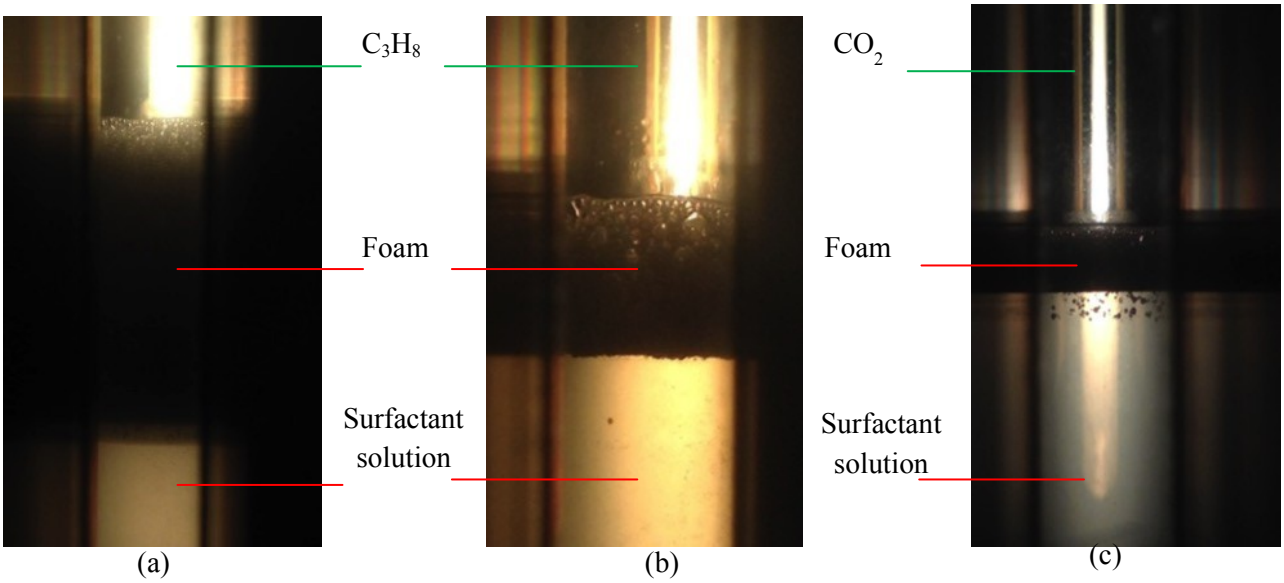

Figure 2-8 Digital images of foam column stabilized by 0.0194 w/v Triton X-100 and 5,000 ppm salinity, 20 min after mixing termination: (a) C_3H_8 foam at 20°C, (b) C_3H_8 foam at 50°C, and (c) CO_2 foam at 20°C, respectively

It is noted that, at 50°C, with an increase in surfactant concentration, the initial foam height increases rapidly until reaching a certain surfactant concentration (0.0400 w/v). Above such threshold concentration, the initial foam height fluctuates at a very small scale (See Figure 2-9). As observed during experiments, the foam height at 50°C generated by 0.5000 w/v surfactant concentration, 5 min after mixing termination, is less than half of its initial height. This is

contradictory to the results suggested by previous studies that the foam volume is greater than 80% of its initial volume with the same concentration and surfactant at an even higher temperature (100°C) (Demiral and Okandan, 1987). Such low stability result is different from the previous conclusion that Triton X-100 is with high foam stability at elevated temperatures. The cause for such difference is probably due to the different gases used: C_3H_8 gas is used in this study, while N_2 is used in the previous study, which, however, needs further experimental investigation. Compared to the effective CMCs of surfactant concentrations at 20°C and 50°C, the effective CMC of 0.0400 w/v is higher at 50°C than 0.0194 w/v at 20°C. The results imply that at a higher temperature, in order to generate a long foam column, surfactant concentration needs to be increased until reaching the effective CMC. In order to acquire data at 80°C, experimental runs are conducted at 80°C by increasing surfactant concentrations from 0.0194 w/v to 0.5000 w/v. However, no foam can be generated at 80°C with any selected surfactant concentration.

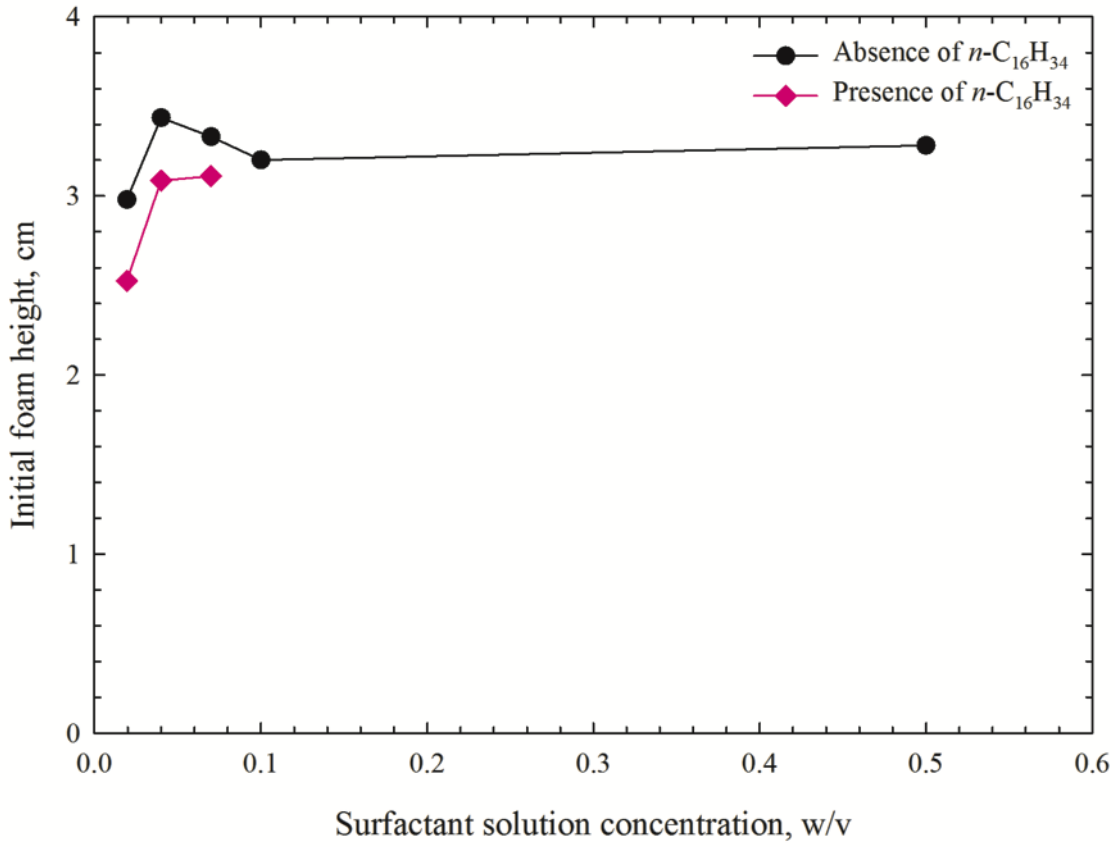

Figure 2-9 Comparison of initial C_3H_8-foam heights at different Triton X-100 concentrations with and without the presence of n-$C_{16}H_{34}$ (5,000 ppm salinity and 50°C)

2.3.1.4. Effect of Oil Presence on C_3H_8-Foam Stability

Since the foam is to be used to displace the trapped oil in formations, the foam needs to maintain its long-term stability to fulfill its duty under the reservoir condition with the presence of oil (Mannhardt *et al.*, 2003). There is a major concern to use foam as a displacing fluid for mobility control in oil saturated reservoir because extensive coreflood experiments have suggested that oil is detrimental to foam stability (Schramm, 1994). This might be especially the case for C_3H_8, because it has high solubility in oil (Luo *et al.*, 2007; James *et al.*, 2012). Some of the

aforementioned C_3H_8-foam experiments are tested again in the presence of pseudo-oil *n*-$C_{16}H_{34}$. Foam half-life is used as the measurable index to compare the oil case and non-oil case.

In order to test the destabilizing effect of oil on foam stability of C_3H_8 system, several tests are conducted again over the previous salinity range. The other test conditions are: surfactant concentration of 0.0194 w/v, 20°C, 700 kPa, and the presence of *n*-$C_{16}H_{34}$. Test results summarized in Table 2-2 indicates that at room temperature, the presence of hydrocarbon significantly reduces the foam heights with a half-life more than 30 times shorter than the one without oil; and this is universally true for all the salinity scenarios. Figure 2-6 compares the change in foam height as a function of time with and without *n*-$C_{16}H_{34}$, showing that foam decays extremely rapidly with oil's presence, while foam is decaying rapidly initially, and then decaying gently afterward for the oil-free case. Therefore, the foam generated by C_3H_8 is not stable to oil and can be easily diminished by oil phase. A visual observation (Figure 2-10) compares the foam column height, bubble size and size distribution 30 min after mixing termination with and without oil presence. Large bubbles and a wider bubble-diameter distribution (ranging from 1 mm to 5 mm) could be observed with the presence of oil; however, the bubble size is distributed more homogenously in the oil-free case. The foam height of the oil case is much shorter than the one without oil at the same time after mixing stops, suggesting that the foam enters into the decay regime faster in the oil-presence case. It can be clearly observed by naked eyes that as soon as the oil comes into contact with the foam column, foam enters into its decay regime rapidly with drastic coalescing and rupturing of bubbles at the upper and lower parts of the foam column. Farajzadeh *et al.* pointed out that surfactant partition into the oil reduces the surfactant concentration in aqueous phase (Farajzadeh *et al.*, 2012). In this study, the negative effect of oil addition on foam stability is probably because Triton X-100 is easy to be

partitioned into the oleic phase, resulting in a reduction in the effective amount of surfactant that stabilizes foam. Another explanation is found to be that once oil droplets continually enter into the gas/water interface, it alters the original gas/liquid/gas film into gas/liquid/oil film, which is likely unstable (Farajzadeh *et al.*, 2012). In addition, C_3H_8 solvent has a large solubility in the oil, accelerating the rupturing process of C_3H_8 foam.

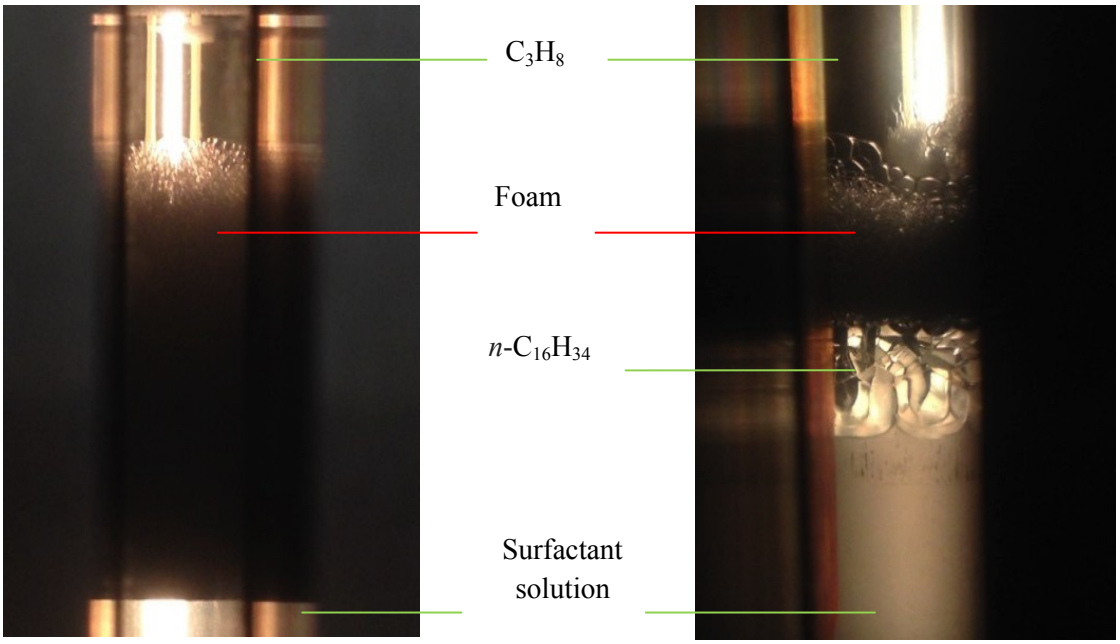

Figure 2-10 Digital images of C_3H_8-foam column stabilized by 0.0194 w/v Triton X-100 and 5,000 ppm salinity with (right) and without (left) the presence of n-$C_{16}H_{34}$, respectively, 30 min after the mixing is terminated at room temperature

As shown in Table 2-3, at high temperatures, the half-decay time of foam with oil is much shorter than the one without oil. The half-life for the oil-case is 4 min at 50°C, in comparison to 11 min for the oil-free case. This result is consistent with previous researches that showed the extremely short half-life of foam generated by Triton X-100 and N_2 at elevated temperatures with the presence of oil (Demiral and Okandan, 1987). Therefore, at any given temperature, oil imposes a detrimental impact on foam stability. Figure 2-7 plots the change of foam height as a

function of time at both 20°C and 50°C with and without the presence of oil. The sharp decay trend at 50°C clearly indicates the foam enters into the decay regime and bubble rupturing occurs drastically right after the mixing is terminated.

Based on the experimental results shown above, foam generated by Triton X-100 and C_3H_8 is most stable at the optimum conditions that reservoir temperature is around 20°C and salinity below 200 ppm. Since the foam stability shows a general decreasing trend as salinity increases, such foaming technique can also be applied to low-salinity and intermediate-salinity conditions. Although the foam stability is low in the presence of oil, such foam can be used to block the large pore throats in high permeable zones where most of the oil is already displaced. Thus, C_3H_8 can be diverted to smaller pore throats in low permeable zones where little foam is generated due to the existence of oil. This will enable the contact between C_3H_8 and heavy oil, leading to diluting of the trapped residue heavy oil due to the high solubility of C_3H_8 in oil. Consequently, more trapped residue heavy oil can be recovered.

2.3.2. CO_2-Foam Stability

The experimentally tested CMC of 0.0194 w/v of Triton X-100 in C_3H_8 system is firstly selected to conduct the CO_2 foam stability at the room temperature. Unfortunately, there is no foam produced at absolute pressures of 1321 kPa, 1755 kPa, and 2596 kPa, which means that the bubbles rupture quickly and cannot entrap CO_2 gas within the bubbles at low pressures. As the pressure increases to 3464 kPa and 5201 kPa, the foamability increases. The height of foam column as a function of time is plotted in Figure 2-11 at the above two different pressures. As can be seen, right after the mixing terminates, with pressure increasing from 3464 kPa to 5201 kPa, the initial foam height increases from 0.444 cm to 4.022 cm. In both cases, all foams start to

decay slowly when foam drops to the height below 1 cm. Beyond 22 min, almost all the foam disappears when pressure is at 3464 kPa, while there is still a short foam column with a height of 0.454 cm as observed in the PVT cell at 5201 kPa. Since, at 5201 kPa, the CO_2 foam stability is most stable among all the pressures with 0.0194 w/v, such pressure is used in the following tests.

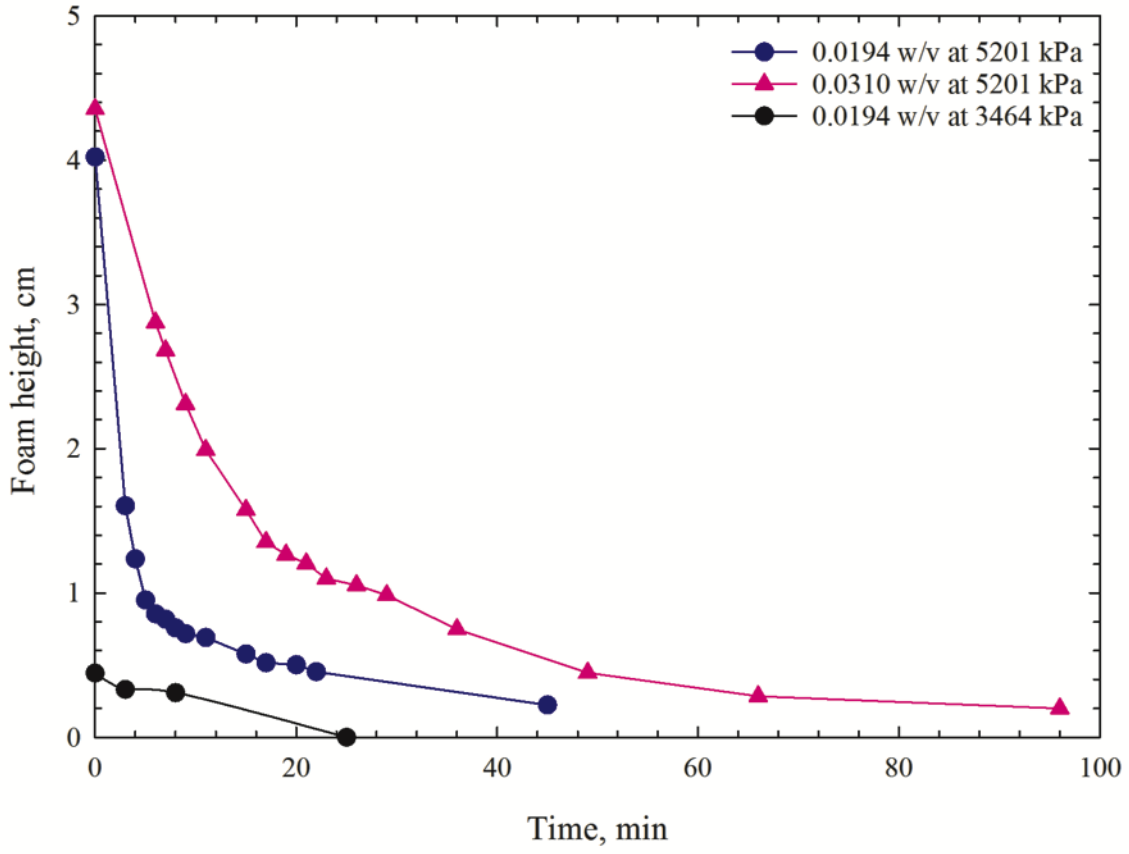

Figure 2-11 Comparison of CO_2-foam stability at different pressures and surfactant concentrations, without addition of salt and oil at 20°C

The CO_2 foam with 0.0194 w/v Triton X-100 enters into the decaying regime so fast with just 3 min of half-life; therefore, it is necessary to test the foam stability with increased surfactant concentrations. Digital images in Figure 2-12 show the initial foam column (left) and the column

4 min after mixing termination (right). It can be observed that within the short 4-min duration, foam height drops dramatically. Figure 2-11 compares the foam profiles changing as a function of time at surfactant concentrations of 0.0194 w/v and 0.0310 w/v. It points out that the foam column is always higher at 0.0310 w/v than 0.0194 w/v, no matter at the beginning of decay or during the decay. The half-life of foam increases from 3 min to 10 min as surfactant concentration increases to 0.0310 w/v, as shown in Table 2-4. Table 2-4 compares the initial height and half-life of CO_2 foam and C_3H_8 foam formed at above two different surfactant concentrations. The foamability of CO_2 foam at both concentrations is slightly higher than those of C_3H_8 foam. But, the half-life for C_3H_8 foam is found to be about 190 times and 30 times of that for CO_2 foam at 0.0194 w/v and 0.031 w/v concentrations, respectively. By comparing the foam decay trend and half-life of C_3H_8 foam and CO_2 foam, one can conclude that C_3H_8 provides much more stable foam than CO_2.

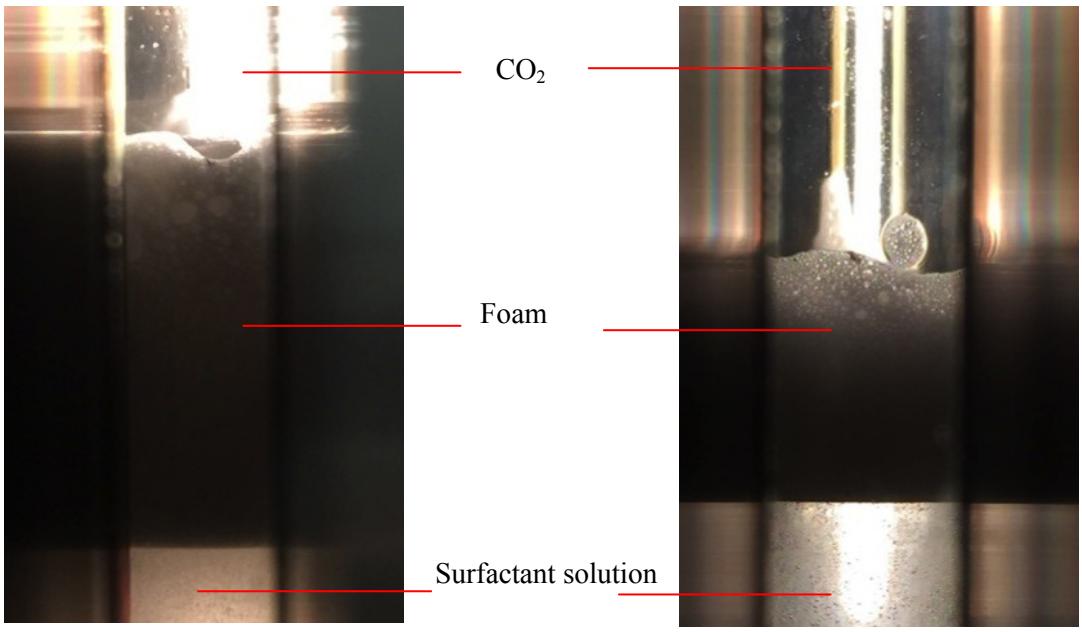

Figure 2-12 Digital images of foam columns stabilized by 0.0194 w/v Triton X-100 at 20°C right after mixing termination (left) and 4 mins after mixing termination (right)

Table 2-4 Initial height and half-life of foam at different conditions for both 5201 kPa-CO_2 and 700 kPa-C_3H_8 gases

Surfactant concentrations, w/v	Salinity, ppm	Temperature, °C	CO_2 foam		C_3H_8 foam	
			$H_{initial}$, cm	$t_{1/2}$, min	$H_{initial}$, cm	$t_{1/2}$, min
0.0194	0	20	4.022	3.0	3.688	585
0.0310	0	20	4.355	10.0	3.434	310
0.0194	5,000	20	4.433	3.2	3.053	304
0.0194	50,000	20	4.326	2.8	2.903	354
0.0194	5,000	50	1.740	< 0.5	2.980	11
0.0194	5,000	80	N/A	N/A	N/A	N/A

Figure 2-13 illustrates the effect of salinity on the stability of CO_2-foam with 0.0194 w/v Triton X-100 at room temperature. As the salinity increases from 0 ppm to 5,000 ppm, the initial foam height increases slightly; with the continuous increasing of salinity from 5,000 ppm to 50,000 ppm, the foam height decreases slightly. This is probably because the addition of much NaCl will reduce the effective concentration of surfactant in the solution, hence leading to a reduction in the foam height or foam stability (Schott, 1988). Half-life can be a good indicator on foam stability in this case. In Table 2-4, the half-life of foam increases from 3.0 min to 3.2 min as salinity increases from 0 ppm to 5,000 ppm, and then decreases to 2.8 min at 50,000 ppm salinity. The difference in the half-lives of CO_2 foams at the three salinity cases is found to be small, which indicates that CO_2 foam has a relatively low sensitivity to salinity change. By comparing the half-life of both CO_2 foam and C_3H_8 foam in Table 2.4, it can be clearly found that, at any tested salinity, the half-life of C_3H_8 foam is more than 100 times of that of CO_2 foam, although CO_2 foam has a higher foamability than the C_3H_8 foam. Image of foam column (Figure 2-8c) is captured 20 min after mixing CO_2 with 0.0194 w/v surfactant solution with 5,000 ppm salinity at room temperature. One can observe the vivid comparison of the higher C_3H_8-foam column and the much shorter CO_2-foam (See Figures 2-8a and 2-8c).

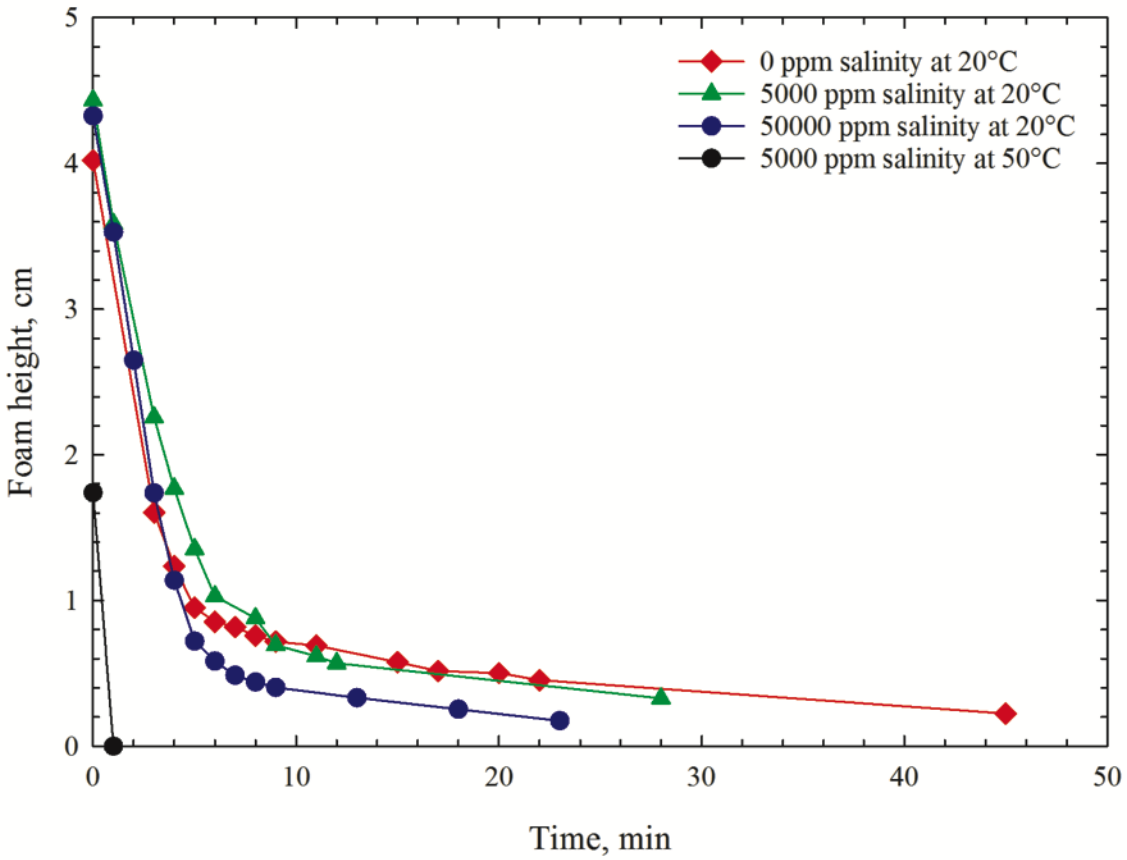

Figure 2-13 Comparison of CO_2-foam decay profiles as a function of time at different salinities and temperatures (0.0194 w/v Triton X-100)

To investigate the temperature effect on CO_2-stabilized foam, experiments are then conducted with 0.0194 w/v surfactant concentration and 5,000 ppm salinity at 20°C, 50°C and 80°C, respectively. The foam variation versus time at 20°C and 50°C has been plotted in Figure 2-13, respectively. No foam can be generated at 80°C due to the high sensitivity to temperature. At 20°C, the foam can maintain a 0.328 cm column beyond 28 min, while the foam disappears within 1 min at 50°C. Table 2-4 compares the test results on foam half-life for CO_2 foam and C_3H_8 foam, respectively, at different temperatures. The half-life of C_3H_8 foam is 90 times and 20 times of that of CO_2 foam at 20°C and 50°C, respectively. To summarize, the stability of CO_2

foam decreases as temperature increases. The foam produced in C_3H_8 system exhibits a much better foam stability compared to CO_2 generated foam at the tested temperature conditions.

Based on the experimental results shown above, foam generated by Triton X-100 and CO_2 does not exhibit good stability. At any tested condition (surfactant concentration, salinity, and temperature), the half-life of CO_2 foam is found to be on the scale of several mins, while the C_3H_8 foam created at similar conditions can exist over a much longer duration. The observed difference in the foam stability between CO_2 and C_3H_8 can be partially because that C_3H_8 has lower solubility in Triton X-100 than CO_2 since more gas dissolved in solution during foaming can result in a lower foaming capability (Farajzadeh *et al.*, 2014). As a whole, gas with a lower solubility in the surfactant solution tends to create more stable foam.

2.3.3. C_3H_8-Foam Mobility in Porous Media

Based on our results of static tests, C_3H_8 gas and 0.0194 w/v of Triton solution with 0 ppm salinity at room temperature are the optimized conditions for generating a stable foam. Therefore, the foam mobility experiments are conducted by alternately injecting 0.0194 w/v of Triton solution and C_3H_8 into the porous media every 2 min to generate foam *in situ*. Two runs are conducted by injecting surfactant solution at a rate of 3 cm^3/min (SAG ratio of 1:2) and 2 cm^3/min (SAG ratio of 1:3), respectively. Another test, water-alternating-gas (WAG) injection with water-to-gas ratio of 1:2, is also conducted, which serves as a baseline case for comparison with SAG. Figure 2-14 shows the measured differential pressures across the beadpack in the three tests. In Figure 2-14, the ascending segments represent the surfactant-solution flooding stage, and the descending segments represent the C_3H_8 flooding stage. Figure 2-14 clearly indicates that a steady-state SAG gives a maximum pressure of around 514 kPa, which is much

higher than that given by WAG, i.e., 169.4 kPa. The high-pressure difference in SAG indicates C_3H_8 forms a substantial amount of foam within the beadpack when it comes into contact with the surfactant solution. Figure 2-15 compares the fluid mobility measured by different tests; the ascending segments represent the C_3H_8 flooding, and the descending segments mean the surfactant-solution flooding. According to Figure 2-15, the minimum mobility in the SAG test is about 2 Darcy/cp, 4 times lower than that in the WAG test. The foam generated *in situ* increases the viscosity of the fluid through the beadpack, thus greatly reducing the mobility of C_3H_8. Figure 2-14 and 2-15 also show the effect of SAG ratios on the pressure drop and fluid mobility, respectively. It can be seen from these two figures that a higher SAG ratio results in a larger differential pressure as well as a higher degree of mobility reduction. This is attributed to the fact that more foam can be generated *in situ* when more surfactant is present in the porous media.

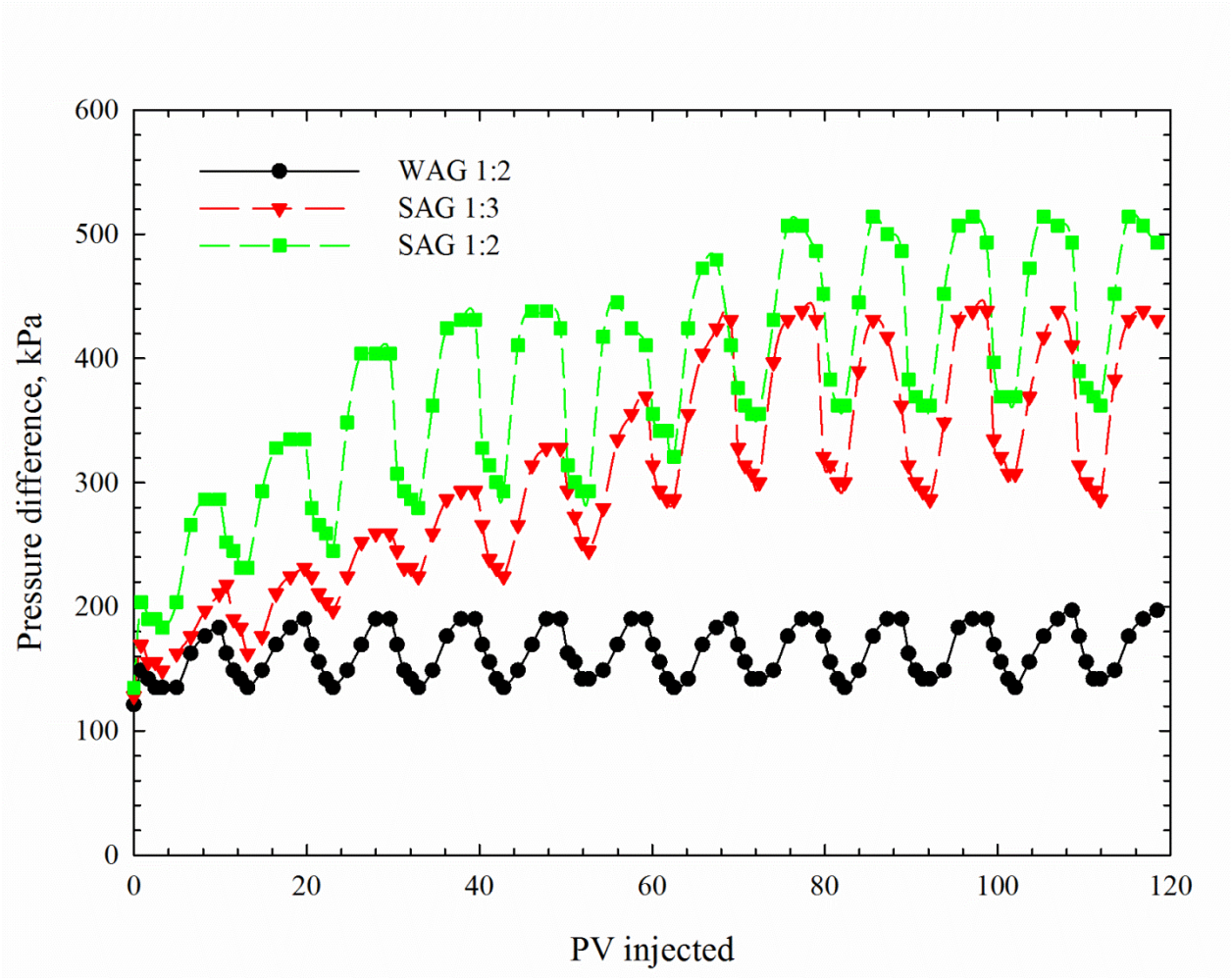

Figure 2-14 Comparison of pressure drops measured in SAG tests (0.0194 w/v Triton X-100, 20°C, SAG ratios of 1:2 and 1:3) and WAG tests (WAG ratio of 1:2)

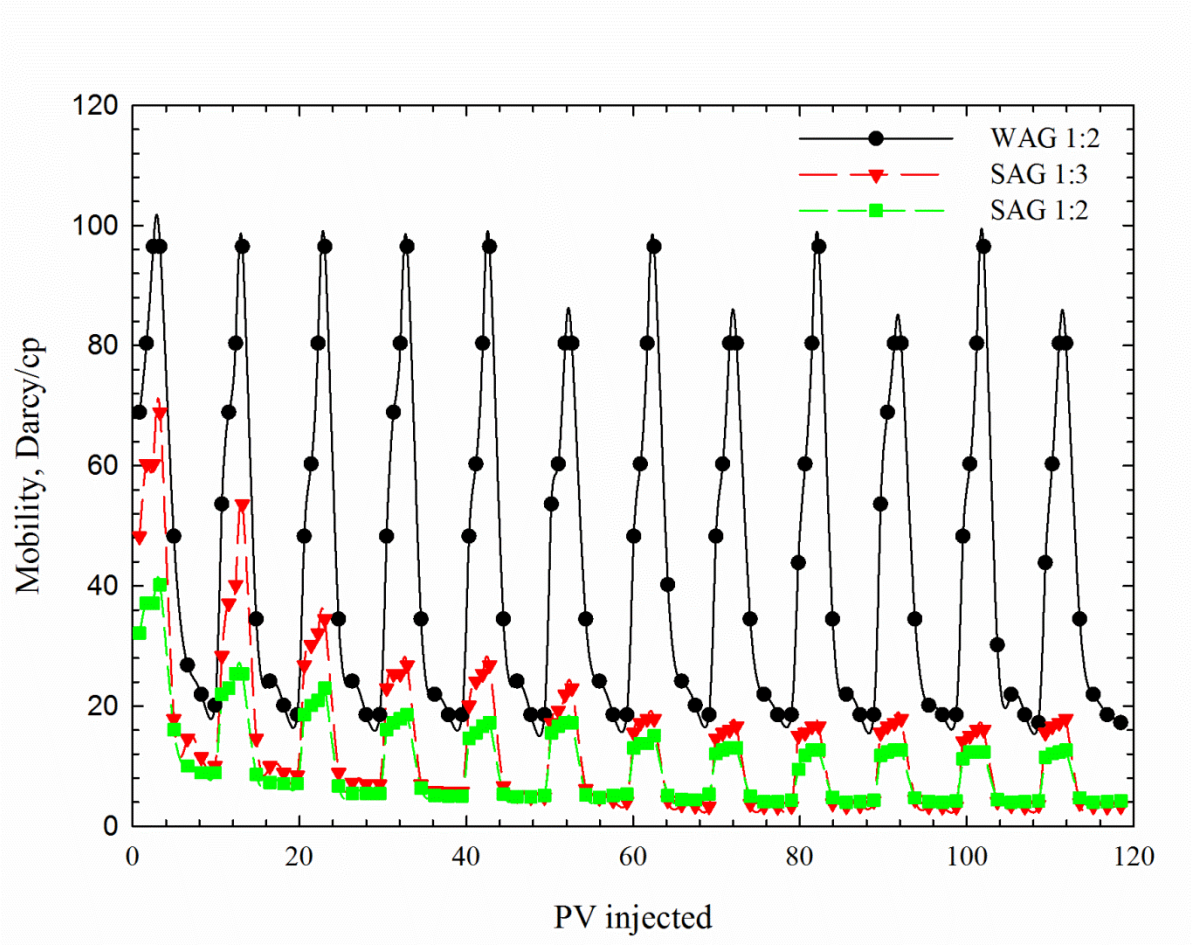

Figure 2-15 Comparison of foam mobility measured in SAG tests (0.0194 w/v Triton X-100, 20°C, SAG ratios of 1:2 and 1:3) and WAG tests (WAG ratio of 1:2)

2.4. Conclusions

In this study, foam stability generated by gas-solvent/surfactant mixtures is experimentally examined by using a PVT setup, while the foam mobility in porous media is assessed by conducting flow experiments with a glass beadpack. The following conclusions can be obtained:

1) At any given temperature, foam stability of C_3H_8 foam increases as the surfactant concentration increases until reaching the effective surfactant concentration (effective

CMC), above which foam stability keeps almost the same. Such effective CMC also increases with an increase in temperature.

2) C_3H_8 foam shows the highest stability without the addition of salt and generally decreases with an increase in salinity. The deteriorated foam stability due to salinity increase is probably because the addition of salt salts out the surfactant in solution. Overall, the foam is found to be stable at different salinities.
3) A higher temperature leads to much lower stability of C_3H_8 foam. Furthermore, the presence of *n*-$C_{16}H_{34}$ (pseudo-heavy-oil) has a detrimental effect on foam stability under all conditions tested.
4) C_3H_8 foam is much more stable than CO_2 foam at any tested conditions. In the CO_2-stabilized foam, foam stability increases with an increase in surfactant concentration and decreases in temperature. The stability of CO_2-foam is not very sensitive to salinity since the foam stability fluctuates slightly as salinity increases.
5) Alternate injection of C_3H_8 and surfactant solution provides a much larger pressure drop than that given by WAG. The C_3H_8 foam generated *in situ* increases the viscosity of the fluid through the beadpack, thus greatly reducing the mobility of C_3H_8.
6) A larger differential pressure, as well as a higher degree of mobility reduction, can be obtained by increasing the SAG ratio.

CHAPTER 3 FOAM STABILITY OF NANOPARTICLE-STABILIZED C_3H_8 FOAM UNDER RESERVOIR CONDITIONS

3.1. Introduction

As discussed in the prior chapter, the surfactant-stabilized foam is very sensitive to high temperature, high salinity and the presence of oil. Colloidal particles, such as silica, are known as the long-term effective foam stabilizer in stabilizing foam. As the particles are attached to the liquid-gas interface, it prevents the bubble coalescing, so as to enhance the foam stability at reservoir conditions. The nanoparticles with intermediate wettability tend to be surface active; while most bare nanoparticles are hydrophilic in nature. The wettability of nanoparticles can be surface modified from being hydrophilic to being more hydrophobic, which is able to stabilize the foam (Binks and Horozov, 2005). CNC, fibrous nanocrystalline cellulose, has the environmental advantages than other nanoparticles because it is derived from wood pulp. This chapter presents the research results using CNC for stabilizing C_3H_8 foam. This chapter is organized as follows: Section 1 discusses the stability of C_3H_8 foam stabilized by silica/Triton X-100 under different reservoir conditions. Section 2 discusses the stability of C_3H_8 foam stabilized by cationic CTAB-coated CNC under different reservoir conditions. The effects of surface coating, salinity, temperature and presence of oil have been considered. In section 3, the stability of C_3H_8 foam stabilized by the synergistic effect of CNC with different non-ionic surfactants is performed and compared.

3.2. Experimental Section

3.2.1. Materials

The bare silicon dioxide nanoparticle is purchased from Sigma-Aldrich in a powder phase with an average particle diameter of 12 nm. CNC is fibrous anionic-type nanocrystalline cellulose derived from wood pulp, which potentially offers environmental advantages than other nanoparticles. Both of the nanoparticles are hydrophilic in nature. Triton X-100 (See Figure 3-1(a) for its molecular structure with n=10) is the non-ionic polyoxyethylene octylphenyl ether surfactant with a purity of 100%, purchased from Sigma-Aldrich. CTAB (See Figure 3-1(b)), also called as hexadecyltrimethylammonium bromide, is a cationic surfactant, supplied by Sigma-Aldrich in a powder phase with >=99% purity. Nonionic surfactant Tween 20 (See Figure 3-1(c)) and Tween 80 (See Figure 3-1(d)) with purity of 100% are purchased from Sigma-Aldrich. Solid sodium chloride (NaCl) with >99% purity is provided by Acros Organic. Liquid C_3H_8 (Praxair) with 99.5% purity is depressurized into the gas phase in PVT cell prior to foam generation. To investigate the effect of heavy oil presence on foam stability, n-$C_{16}H_{34}$ with 99% purity is chosen as the pseudo-oil to simulate heavy oil for studying. The nanoparticles, surfactants and NaCl are all weighed by an electronic balance and their concentrations are expressed in w/v (weight over volume fraction) in the aqueous phase.

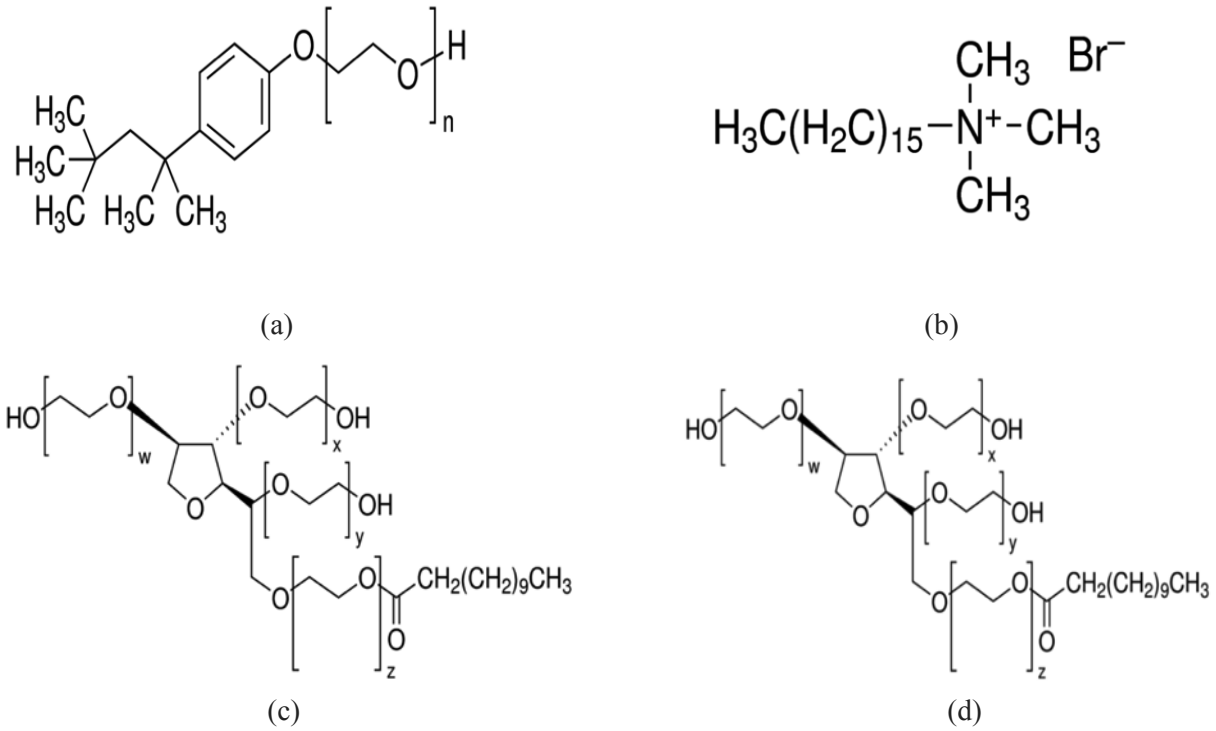

Figure 3-1 Molecular structures of (a) Triton®X-100 surfactant with *n*=10; (b) CTAB surfactant; (c) Tween 20 surfactant; (d) Tween 80 surfactant (Supplied by Sigma-Aldrich)

3.2.2. Experimental Setup

The mercury-free DBR PVT system (Schlumberger, Edmonton, Alberta, Canada), as shown in Figure 3-2, is the experimental apparatus used to test foam stability. Embedded in a PVT system is a transparent PVT cell, which can withstand pressures up to 15000 psi. The cell temperature, controlled by the microprocessor temperature controller fitted in the air bath, can tolerate a temperature range of -10^{o}C to 200^{o}C. The cell is separated into two isolated chambers by a mobile piston, above and below which are a hydraulic oil chamber and a sample chamber, respectively. The sample chamber volume is changeable by moving the piston up and down through a positive displacement pump (DBR pump). The bottom of the sample chamber is equipped with a magnetic stir that can stir the sample at different rates. Two charging vessels are

used to transfer the solution samples and n-$C_{16}H_{34}$ into the PVT cell. A Vacuum Pump (1400, Welch Vacuum, USA) is used to vacuum the PVT cell. A cathetometer with a resolution of 0.002 cm is used to measure the fluid height in the visual cell.

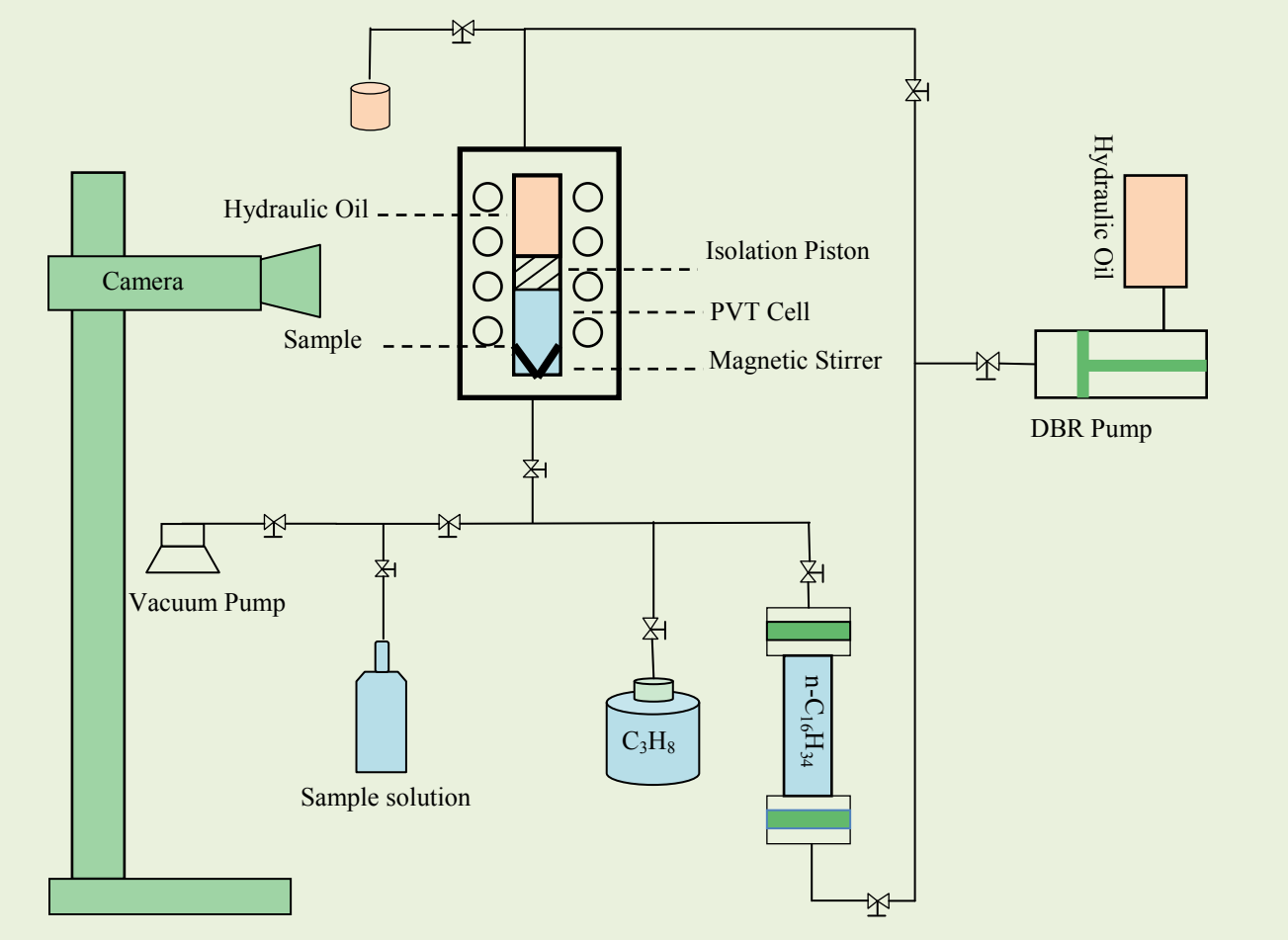

Figure 3-2 Schematic of the PVT experimental setup used for foam stability tests

3.2.3. Experimental Procedure

Preparation of Nanoparticles Dispersion. Each sample is freshly prepared prior to each test. To prepare the aqueous dispersion, 0.5 w/v bare silica or 0.3 w/v bare CNC are prepared by dispersing the particles in de-ionized water for 40 min by using an Ultrasonifier (FS30, Ultrasonic Cleaner, USA). To prepare the silica/Triton X-100 mixture, 0.0194 w/v Triton X-100

is added into the silica dispersion. Since anionic CNC is hydrophilic due to the presence of hydroxyl groups, a cationic surface modifier, CTAB, with 0.002 w/v, 0.010 w/v, or 0.015 w/v, is added into bare CNC dispersion to change the wettability of CNC from being hydrophilic to more hydrophobic, as shown in Figure 3-3. To prepare CNC/nonionic surfactant mixtures, Tween 20, Tween 80, and Triton X-100 are added into the bare CNC dispersion, respectively, at their CMCs. Sodium chloride solution is prepared at desired concentrations and mixed into nanoparticle solutions. All the above particle/surfactant dispersions are stirred for 30 min to ensure the mixture homogeneity.

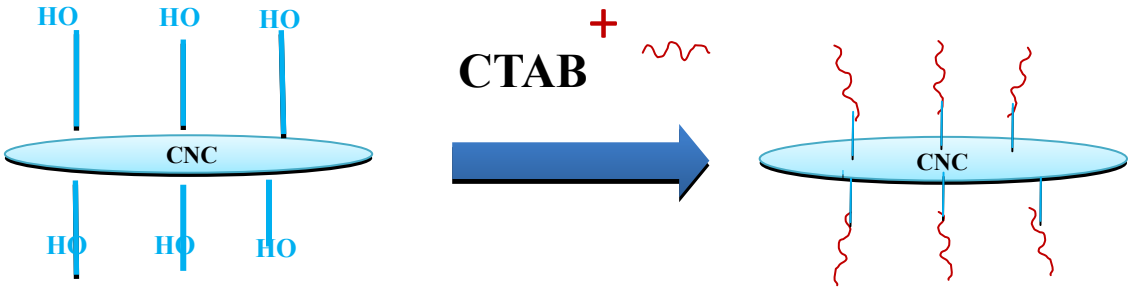

Figure 3-3 Schematic showing how to perform surface modification of bare CNC by CTAB

Foam Stability Determination. The PVT cell and tubing are carefully cleaned with toluene and de-ionized water, followed by an evacuation by a vacuum pump before each test. As for temperature control, the air bath temperature is set at a desired value, followed by at least 12 hours to ensure a constant temperature. Freshly prepared 15 cc of solution sample is initially transferred into PVT cell via the charging vessel. Then C_3H_8 is injected from the bottom of the sample cell at a constant flowrate of 500 cc/hr. The volume ratio of C_3H_8 gas to sample solution is kept as 2:1 throughout all tests. Right after the gas sparging terminates, static foam can be generated by stirring the solution for 2 min with the stirrer. Then quantitative evaluation of the

foamability is achieved by measuring the initial foam height just after the mixing terminates. The foam stability can be evaluated by recording the foam height as time elapses. In the tests with the presence of oil, 5 cc of oil is introduced into PVT cell at a rate of 500 cc/hr exactly after the mixing terminates. The bubble size and foam uniformity can be observed with naked eyes through PVT cell during the tests.

Transmission electron microscope (TEM) (Morgagni 268, Philips) and optical microscope are used to observe the particle shape, distribution, and bubble structure. In this case, the foam is formed by handshaking the solution with air, since it is difficult to collect C_3H_8 foam out of the PVT cell. TEM imaging is carried out as follows. First, a small volume of sample foam is placed on 1 cm diameter stub and dried in an oven. Then the sample is transferred into TEM chamber, followed by a vacuum process. Then TEM image can be acquired.

3.3. Results and Discussion

3.3.1. Foam Stabilized by Mixture of Triton X-100 and Silica Dispersion

In order to investigate whether the silica dispersion can generate foam or not, silica dispersions with concentrations of 0.1 w/v, 0.5 w/v and 1.0 w/v are tested, respectively, at room temperature (20^oC) and 700 kPa. However, none of the bare silica at the selected concentrations can generate foam, which is consistent with previous studies that bare silica is too hydrophilic to be attracted into the liquid interfaces (Binks and Horozov, 2006).

Foam stability tests are carried out for the case where 0.5 w/v silica is dispersed in 0.0194 w/v Triton X-100. The decay trends of foam generated by silica/Triton X-100 mixture and Triton X-100 alone are plotted in Figure 3-4. Table 3-1 details the foamability and foam stability test results for different combinations of silica/Triton X-100 mixtures. Our previous study reported

that foam formed by C_3H_8 and 0.0194 w/v Triton X-100 alone showed a 3.688 cm height at beginning and 1.765 cm height after 12 hours (Wang and Li, 2014). The foam formed by the silica/Triton X-100 (Table 3-1 and Figure 3-4) shows an initial height of 1.484 cm, which is two times lower than the foam formed by using Triton X-100 alone. The height of foam generated by silica/Triton X-100 is 0.730 cm after 12 hours, which is half of the height formed by Triton X-100 alone. Although the foamability is higher by using Triton X-100 alone than using the mixture, both foams exhibit about 580 min of half-life. Figures 3-5 (a) and (b) compare the heights of foams generated by these two systems, 20 min after mixing terminates. By observing the foam texture with naked eyes, it can be seen that the bubble size increases from 1 mm to 1.5-3 mm as time elapses. All the above observations indicate that Triton X-100 exhibits a better foamability than the mixture, but both foams show a good foam stability. Unfortunately, no obvious synergistic effect on foamability and foam stability are observed for the Triton X-100/silica mixture. Increased concentrations of silica and Triton X-100 are then used for further testing; however, with the increase of both concentrations, very thick flocculates are formed. Two factors may lead to the low foamability formed by the mixture of 0.5 w/v silica and 0.0194 w/v Triton X-100. Firstly, it is assumed that Triton X-100 is the main contributor to stabilize the foam in both cases; however, some of the surfactants is adsorbed onto the particle surfaces, resulting in a reduced surfactant concentration. Secondly, particles may not be surface active even with the presence of surfactant (Zhang, 2008). Figure 3-4 shows that foam stabilized by either Triton X-100 or the silica/Triton X-100 decays drastically in the beginning, but decays gently after 7 min.

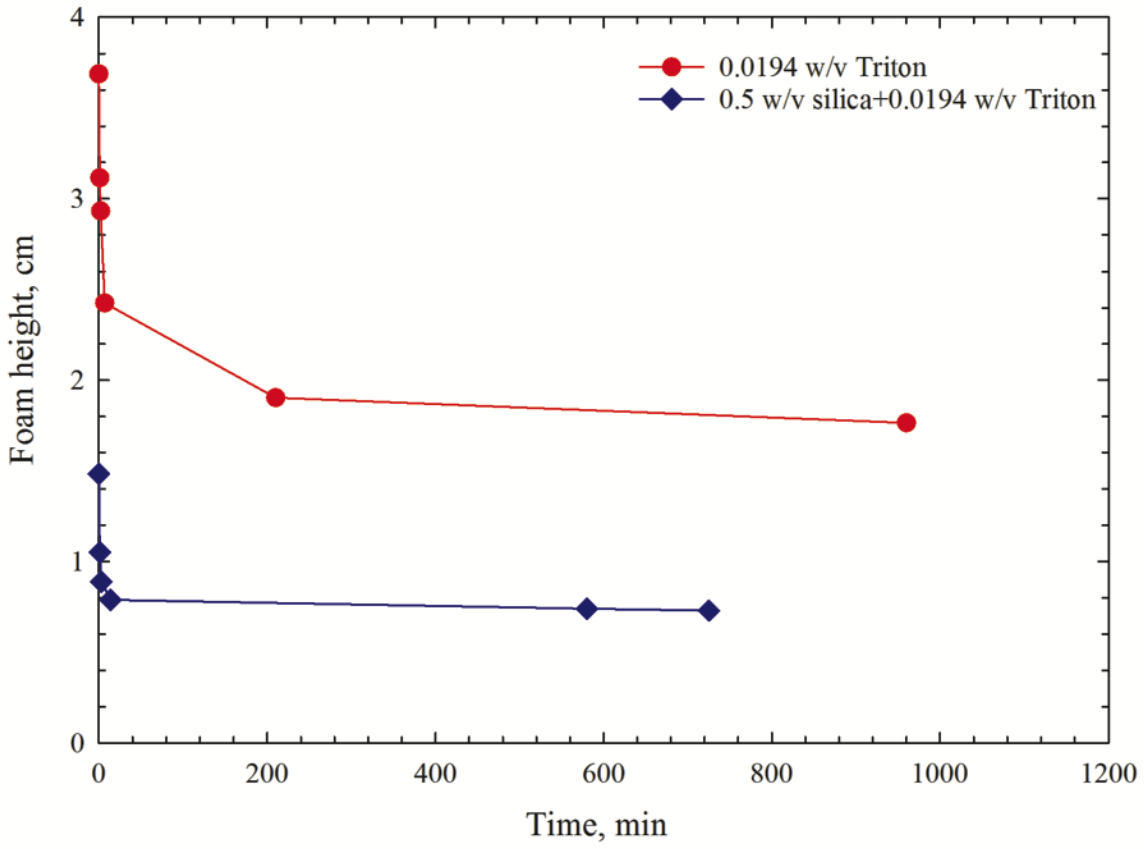

Figure 3-4 Stability of foams generated by silica/Triton X-100 mixture and Triton X-100 alone (20°C, 700 kPa)

Table 3-1 Foamability and foam stability of foams formed by different combinations of TritonX-100/silica dispersion at different salinity and temperatures.

Silica concentration, w/v	Triton X-100 concentration, w/v	Salinity, ppm	Temperature, °C	Initial foam height, cm	H_{12}, cm	Mixed dispersion
0	0.019	0	20	3.688	1.765	Foam
0.5	0	0	20	0	0	No foam
0.5	0.019	0	20	1.484	0.730	Foam
0.5	0.019	5000	20	2.258	1.112	Foam + flocculate
0.5	0.019	5000	50	1.786	0.680	Foam +flocculate

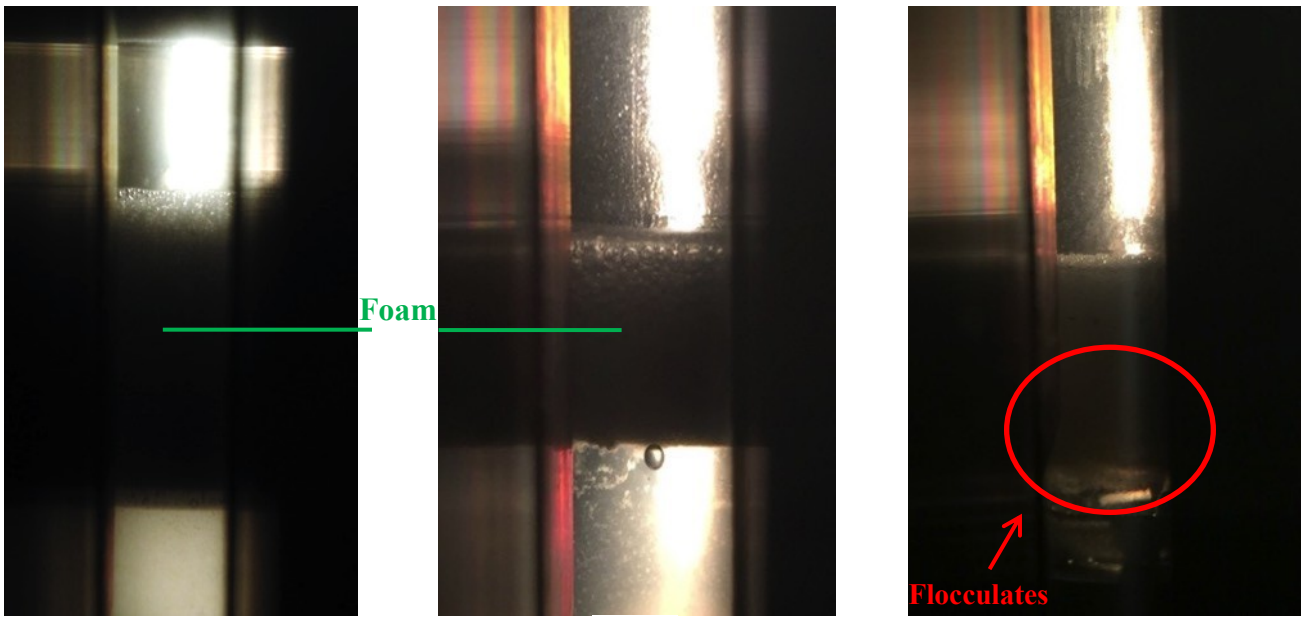

Figure 3-5 Digital images of foam stabilized by (a) 0.0194 w/v Triton X-100 (Wang and Li, 2014); (b) mixture of 0.0194 w/v Triton X-100 with 0.500 w/v silica; (c) flocculates formed by mixture of 0.0194 w/v Triton X-100 and 0.500 w/v silica at 5000 ppm salinity

Table 3-1 also details the results of foam stability tests at increased brine concentration and temperature. With the addition of 5000 ppm of salt into the silica/Triton X-100 mixture, thick flocculates are formed below the thin foam column as the mixing terminates. It is hard to find an interface between the foam and flocculates as shown macroscopically in Figure 3-5 (c). This phenomenon also happens at an elevated temperature of 50^{o}C. Therefore, at increased salinity and temperature for such mixture concentration, foam stability test cannot be obtained due to the forming of flocculates.

3.3.2. Foam Stabilized by CNC Hydrophobized with CTAB

3.3.2.1. Effect of surface coating on foam stability

Several bare CNC solutions with concentrations of 0.05 w/v, 0.3 w/v, and 0.5 w/v are mixed

with C_3H_8 to generate foam at 20°C and 700 kPa; however, no foam is generated by CNC alone without addition of surfactant as a surface modifier. Based on the previous study (Binks and Horozov, 2006), particle can act as a foam stabilizer only when wettability of nanoparticle surface is partially hydrophobic and partially hydrophilic, which allows the particles to disperse in water due to the hydrophilic property and to be adsorbed at liquid interfaces due to the hydrophobic property. The formation of foam requires adsorption of solids at air/water interface; therefore, it is necessary to select a suitable surface modifier that can render the CNC surface be modified from being hydrophilic to partially hydrophobic via either electrostatic or ligand exchange reactions. Since CNC is negatively charged, the cationic hydrophobic surfactant CTAB can be coated onto its surface via electrostatic interaction to modify the surface wettability of CNC particles, as shown in Figure 3-3. Here, CNC with a constant 0.3 w/v concentration is coated by adding surface modifier CTAB with concentrations of 0.02 w/v, 0.010 w/v, and 0.015 w/v, respectively, at 20°C and 700 kPa. And the foamability and foam stability of CNC/CTAB-stabilized foams are compared with CTAB-stabilized foam at the same conditions. Table 3-2 and Figure 3-6 shows the foam stability test results for foam stabilized by 0.3 w/v CNC coated with different CTAB concentrations. It shows an encouraging result that the coated CNC increases the foam stability. No foam can be formed solely by 0.002 w/v CTAB surfactant, while a short and stable column of foam can be formed when 0.3 w/v CNC is coated by 0.002 w/v CTAB in aqueous phase. This indicates that in-situ surface-coated nanoparticles are responsible for such foam generation. As shown in Figure 3-6, at increased CTAB concentrations (0.010 w/v and 0.015 w/v), foam prepared from CTAB solutions alone collapses completely within 12 hours; however, CNC/CTAB stabilized high-volume foam can retain 4/5 of the initial height after 12 hours. Images of foam columns (Figure 3-7) are captured, 3 hours after the mixing terminates, at

different concentrations of CTAB with and without the presence of CNC. It is found that, 3 hours after the mixing terminates, the coated CNC/CTAB foam exhibits a much thicker column than CTAB-stabilized foam. Figure 3-6 also compares the decay profiles of foams generated by CNC/CTAB and CTAB alone, respectively. CNC/CTAB-stabilized foam decays more gently in contract to the CTAB foam that shows a remarkable drop in foam height as time elapses. This is attributed to that surfactant-stabilized foam is easy to attach to and detach from the liquid interface; on the contrary, CNC-stabilized foam can be irreversibly attracted onto liquid interfaces due to its high adhesion energy (Binks and Horozov, 2006). Therefore, CNC particle-stabilized foam has a high adhesion energy that prevents itself from destabilization.

Table 3-2 Foamability and foam stability of foams formed by CTAB and 0.300 w/v CNC/CTAB at 20^{o}C. No foam could be generated solely by 0.300 w/v CNC dispersion.

CTAB concentration, w/v	Surfactant			Surfactant + CNC			Mixed dispersion
	Initial foam height, cm	H_{12}, cm	$T_{1/2}$, min	Initial foam height, cm	H_{12}, cm	$T_{1/2}$, min	
0.002	0	0	0	0.539	0	245	Stable foam
0.010	1.237	0	240	1.035	0.830	>1000	Stable foam
0.015	2.123	0	280	2.885	2.310	>1000	Very stable foam

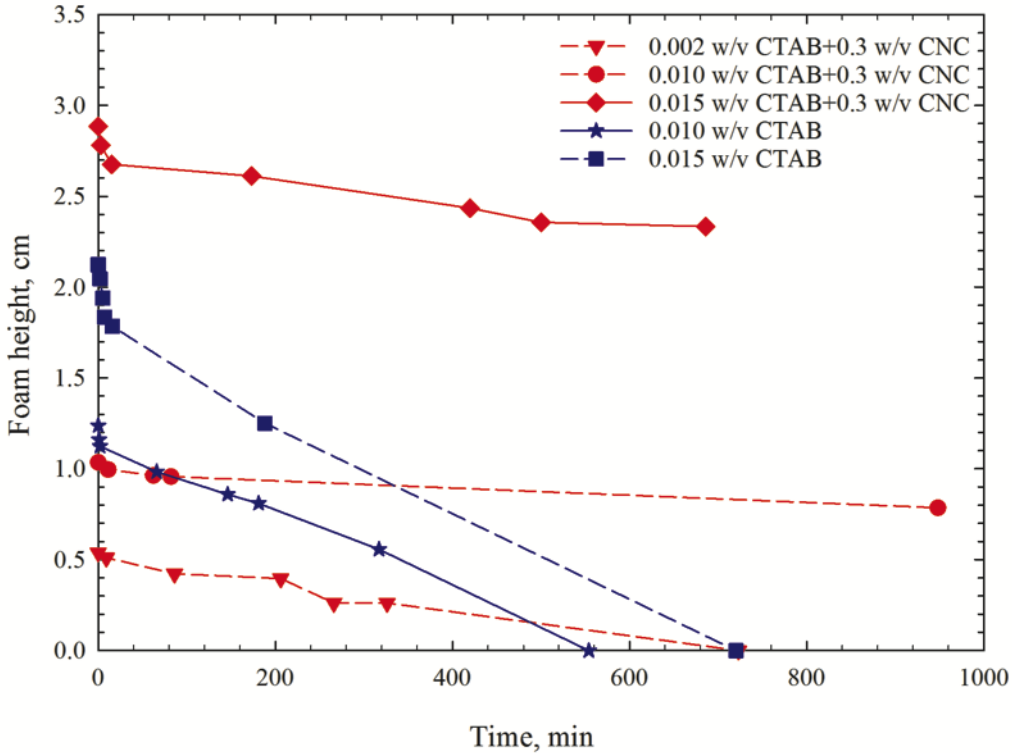

Figure 3-6 Effect of CTAB concentration on the stability of the CTAB/CNC-stabilized foam and CTAB-stabilized foam (20°C, 700 kPa)

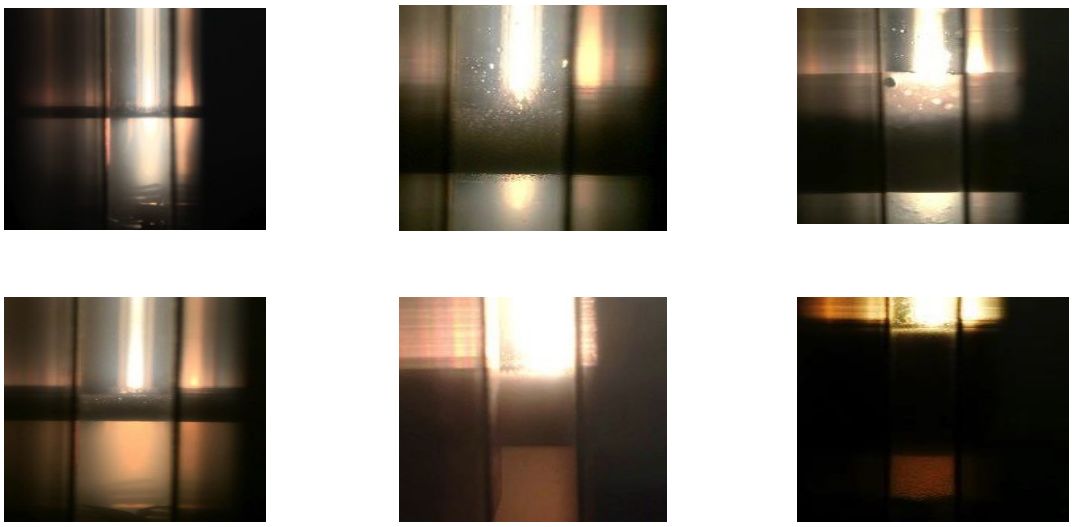

Figure 3-7 Digital images of foam stabilized by (a) 0.002 w/v CTAB (no foam formed); (b) 0.010 w/v CTAB; (c) 0.015 w/v CTAB; (d) 0.300 w/v CNC coated by 0.002 w/v CTAB; (e) 0.300 w/v CNC coated by 0.010 w/v CTAB; (f) 0.300 w/v CNC coated by 0.015 w/v CTAB (3 hours after the mixing was terminated, at 20°C and 700 kPa)

It is also found that (Table 3-2 and Figure 3-6), an increase in CTAB concentration from 0.002

w/v to 0.015 w/v leads to an increased foamability and foam half-life of CNC/CTAB foam. This is probably because: at lower surfactant concentrations, there are insufficient particle surfaces to be coated with hydrophobic surfactant, resulting in a relative low foamability compared to the high surfactant concentration cases. As surfactant concentration increases, more particle surfaces are altered to be partially hydrophobic; therefore strong attachment occurs onto interfaces, contributing to an increased foaming capability.

Macroscopic bubble characteristics are observed by naked eyes. In the presence of CNC particles, an uniform foam is observed in the PVT cell. The opaque white bubbles have a needle tip-like size with a diameter smaller than 1 mm. They are evenly packed in the beginning and maintain almost the same size (1 mm to 1.5 mm) and distribution as time elapses. However, in the absence of CNC particles, narrow packing of fine bubbles with a diameter smaller than 1 mm is observed initially; but the bubbles gradually coarsen to 2-3 mm as time elapses. The size of bubbles stabilized by CNC does not vary much as time goes by, which is consistent with the previous reports that particles can slow down the bubble coarsening process (Binks and Horozov, 2005). Bubble coarsening is one type of foam destabilization mechanism. When the gas pressure inside the small bubbles exceeds the pressure inside the large bubbles, gas will diffuse into the large bubbles from small bubbles through the liquid film, resulting in the bubble coarsening and consequently bubble rupturing (Cervantes, 2008). Hence, our study confirms that nanoparticle-stabilized foam is much more stable compared to the conventional surfactant-stabilized foam.

Figure 3-8 shows the microscopic examination applied to further quantify the size and distribution of both 0.010 w/v CTAB-stabilized foam and 0.3 w/v CNC/0.010 w/v CTAB-stabilized foam at ambient temperature and pressure. It is noticed that the average size of foams generated by CTAB alone is two to three times larger than that generated by coated CNC

nanoparticles. Most CTAB-stabilized foams are in donut-like shape with a diameter of 220 μm, while CNC stabilized foams are mostly 60 μm and 180 μm in diameter. Figure 3-9 shows that the fibrous bare CNC particles are dispersed in water, but coated CNC particles align along the films of foams by TEM imaging. For the bare CNC system, no foam is formed, so the CNC nanoparticles are randomly distributed. As for the coated CNC system, large quantities of foams are formed, and CNC nanoparticles are found to aggregate at the bubble films.

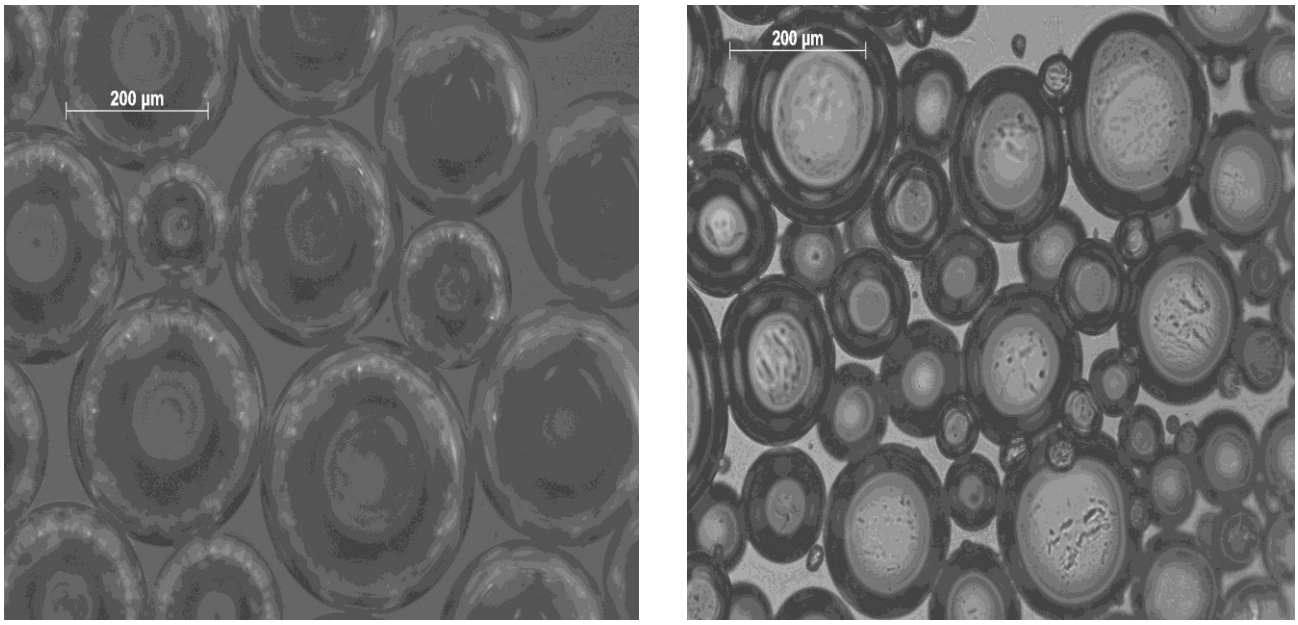

Figure 3-8 Optical microscopic images of aqueous foams stabilized by 0.010 w/v CTAB alone (left) and 0.300 w/v CNC coated by 0.010 w/v CTAB (right). Scale bars are given separately.

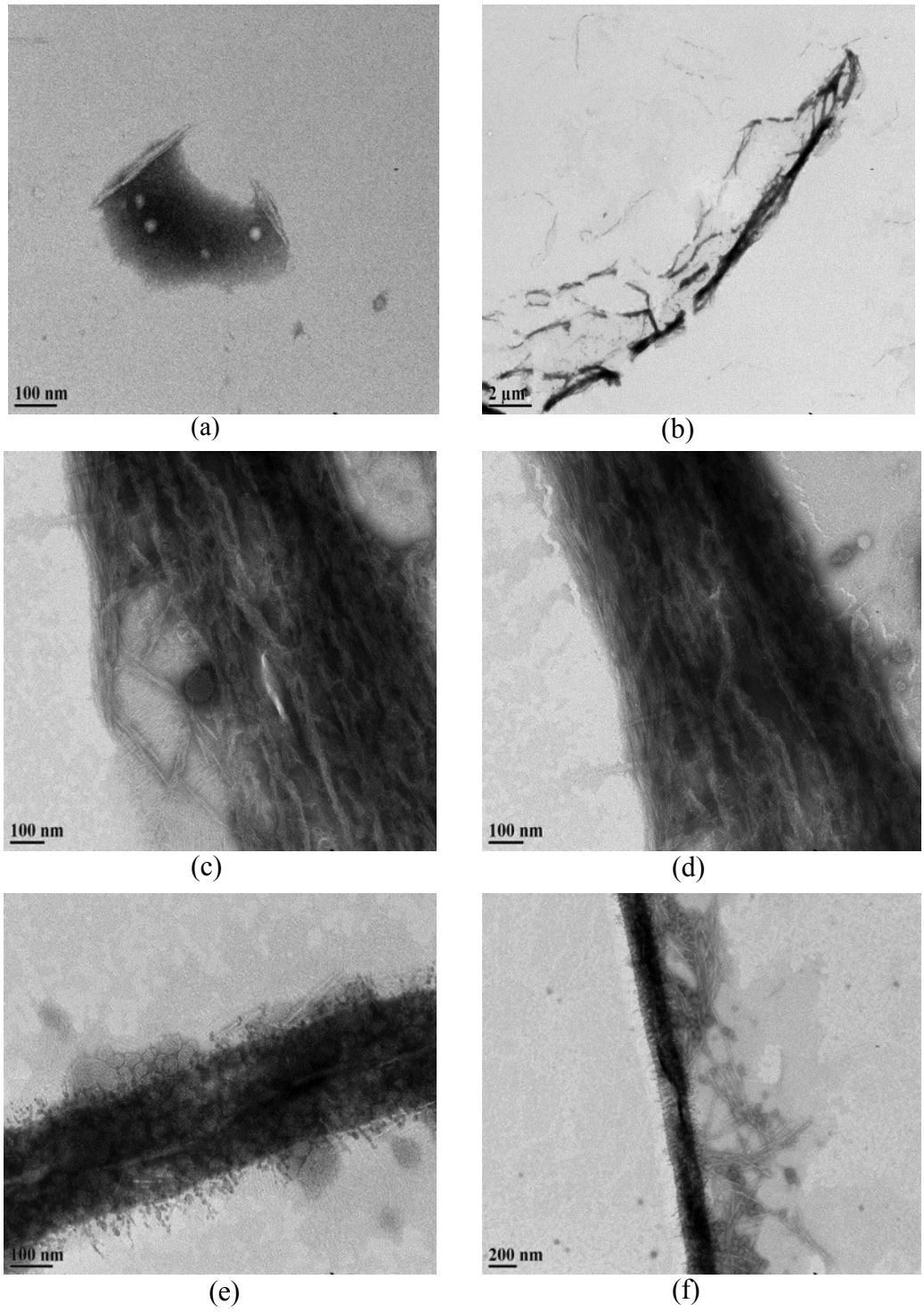

Figure 3-9 TEM images of (a) fibrous bare CNC dispersed in water; (b) (c) (d) dry and curved liquid film of bubbles with coated-CNC particles aligned along; (e) (f) another dry and curved liquid film of bubbles with coated-CNC particles aligned along. The CNC dispersion (a) was formed by using 0.300 w/v CNC particles alone; the others were formed by using 0.300 w/v CNC coated by 0.010 w/v CTAB. Scale bars are given separately.

3.3.2.2. Effect of salt concentration on foam stability

To investigate the salinity effect on foam stability, 10000 ppm of NaCl is added to the mixture of 0.3 w/v CNC and 0.010 w/v CTAB dispersion at 20°C and 700 kPa. Table 3-3 shows the initial conditions and test results on the foam formed by CTAB coated CNC under high brine concentrations. It is interesting to note that, compared with the case without salt, the presence of 10000 ppm salt increases the initial foam height from 1.035 to 2.803 cm but with a 0.560 cm column of flocculates below the foam column. The height of flocculates keeps a constant 0.560 cm during the foam decay. Such result is consistent with previous tests, which shows that fumed silica with 67% and 80% SiOH can stabilize foam when salt is present in the dispersion (Dickinson *et al*, 2004). With the presence of salt, a thick foam column is obtained, which is probably because the addition of monovalent ion neutralizes charges and increases hydrophobicity of particles, thus promoting the adsorption of CNC onto the liquid interfaces for generating more foam. The addition of salt to the solution not only increases the foam thickness but also results in finer foam texture with a uniform packing.

Table 3-3 Foamability and foam stability of foams formed by 0.300 w/v CNC coated with 0.010 w/v CTAB with addition of salt at 20°C.

Brine concentration, ppm	Surfactant + CNC			Mixed dispersion
	Initial foam height, cm	H_{12}, cm	$T_{1/2}$, min	
0	1.035	0.830	>1000	Stable foam
10000	2.803	2.306	>1000	Very stable foam (flocculate below the foam)

Figure 3-10 shows the foam decay profiles as a function of time for the tests with and without salt presence. Although the foam without the presence of salt exhibits a gentle and smooth slope, the foam without the presence of salt shows an even milder slope. The higher initial height and gentle decay trend of foam with the presence of salt indicate a higher foamability than the case

without salt presence. As mentioned by Deschenes (1997), there exists a hydrophobic force to rupture the liquid film. Therefore, a decrease in the hydrophobic force can result in an increase in foam stability. Craig (1993) reported that some common salts can inhibit bubble coalescence. He measured the bubble coalescence rate of foams formed by different electrolytes and found that the hydrophobic force decreased with an increase in the electrolyte concentration. It can be concluded that the presence of salt concentration might decrease the hydrophobic force on bubble coalescence, resulting in an increase in foam stability. Digital photographs are taken to record the change in foam height and foam texture over time. Figure 3-11 illustrates the foam texture generated with the addition of electrolyte concentration, showing a thicker foam column with larger bubble density and smaller bubbles. During the foam decay process, macroscopic observation reveals that with the addition of 10000 ppm salt into the dispersion, the bubble size is homogeneous and smaller than 1 mm initially, and increases to around 1 mm to 2 mm after 12 hours.

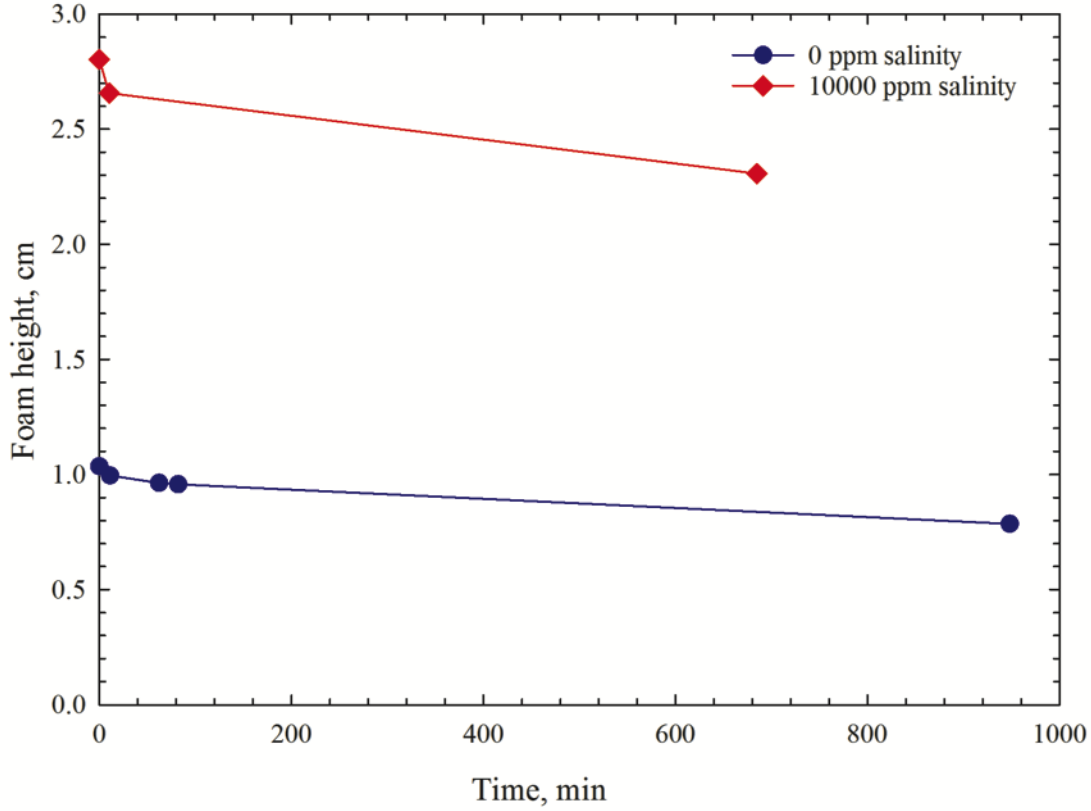

Figure 3-10 Effect of salinity on the stability of foam formed by CNC/CTAB (0.010 w/v of CTAB, 0.300 w/v of CNC, at 20°C and 700 kPa)

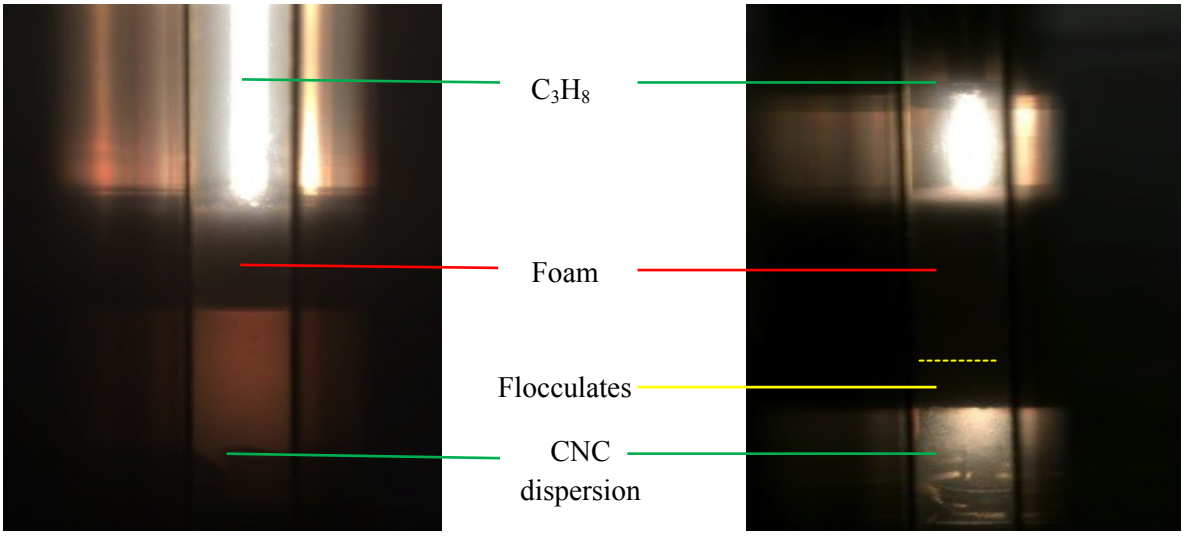

Figure 3-11 Digital images of CNC/CTAB stabilized foams (0.300 w/v CNC and 0.010 w/v CTAB) with (right) and without (left) adding 10000 ppm salt, respectively, at 20°C and 700 kPa, 5 hours after the mixing was terminated

3.3.2.3. Effect of temperature on foam stability

Foam is a thermodynamically unstable fluid, so it is worth of testing the foam stability formed by CTAB coated CNC at elevated temperatures. To investigate the temperature effect on foam stability, a series of experiments are conducted at temperatures of 20^{o}C, 50^{o}C, and 80^{o}C, respectively, but at 700 kPa by using 0.3 w/v CNC coated by 0.010 w/v CTAB or 0.010 w/v CTAB alone. Table 3-4 shows the foamability and foam stability for foams formed by CTAB and CTAB coated CNC at elevated temperatures. In the absence of CNC, foam solely formed by CTAB surfactant disappears completely within 12 hours at 20^{o}C and 50^{o}C (Table 3-4). And no foam is observed as temperature increases to 80^{o}C. It can be concluded that CTAB stabilized foam is very sensitive to temperature and the stability decreases with an increasing temperature. It is widely accepted that, since foam is thermodynamically unstable, a higher temperature tends to reduce its interfacial area and interfacial free energy via bubble coalescence (Wang and Yoon, 2006). Conversely, it is interesting to note that, in the presence of CNC, the initial height and the foam height after 12 hours at 20^{o}C is almost the same as those at 50^{o}C. When temperature increases to 80^{o}C, the foam becomes more stable with an initial height of 2.197 cm and a remaining height of 1.328 cm after 12 hours. It can be speculated that the adhesive strength of CNC particle and CTAB surfactant increases as temperature increases. To summarize, CTAB coated CNC foam keeps almost the same stability at 20^{o}C and 50^{o}C, while the foam stability increases as temperature increases from 50^{o}C to 80^{o}C. On the contrary, foam stability of CTAB stabilized foam decreases with an increase in temperature.

Table 3-4 Foamability and foam stability of foams formed by 0.010 w/v CTAB alone and 0.300 w/v CNC coated with 0.010 w/v CTAB at elevated temperatures.

Temperature, ^{o}C	Surfactant			Surfactant + CNC			Mixed dispersion
	Initial foam height, cm	H_{12}, cm	$T_{1/2}$, min	Initial foam height, cm	H_{12}, cm	$T_{1/2}$, min	
20	1.237	0	240	1.035	0.830	>1000	Stable foam
50	0.691	0	15	1.069	0.849	>1000	Stable foam
80	0	0	0	2.197	1.328	>1000	Stable foam

Half-life, the time it takes for the foam to decay to half of the initial height, is an alternative way to quantify the foam stability. The half-life of CTAB foam is 240 min at 20^{o}C and 15 min at 50^{o}C, while the half-life of CTAB coated CNC foam at 20^{o}C, 50^{o}C and 80^{o}C are all greater than 1000 min (Table 3-4). It is thus proven that surface modified nanoparticles can generate stable foams that are so strong that a high tolerance to temperature can be achieved. Figure 3-12 shows the evolution of foam height as a function of time at 3 different temperatures for both cases. It is clearly observed that the decay trend of foam stabilized by surfactant alone is much steeper, as compared to the nearly horizontal foam height stabilized by CTAB coated CNC. Specifically, at 50^{o}C, the foam formed by CTAB coated CNC remains a 0.893 cm height after 85 min, while the foam formed by CTAB alone completely disappears in 85 min.

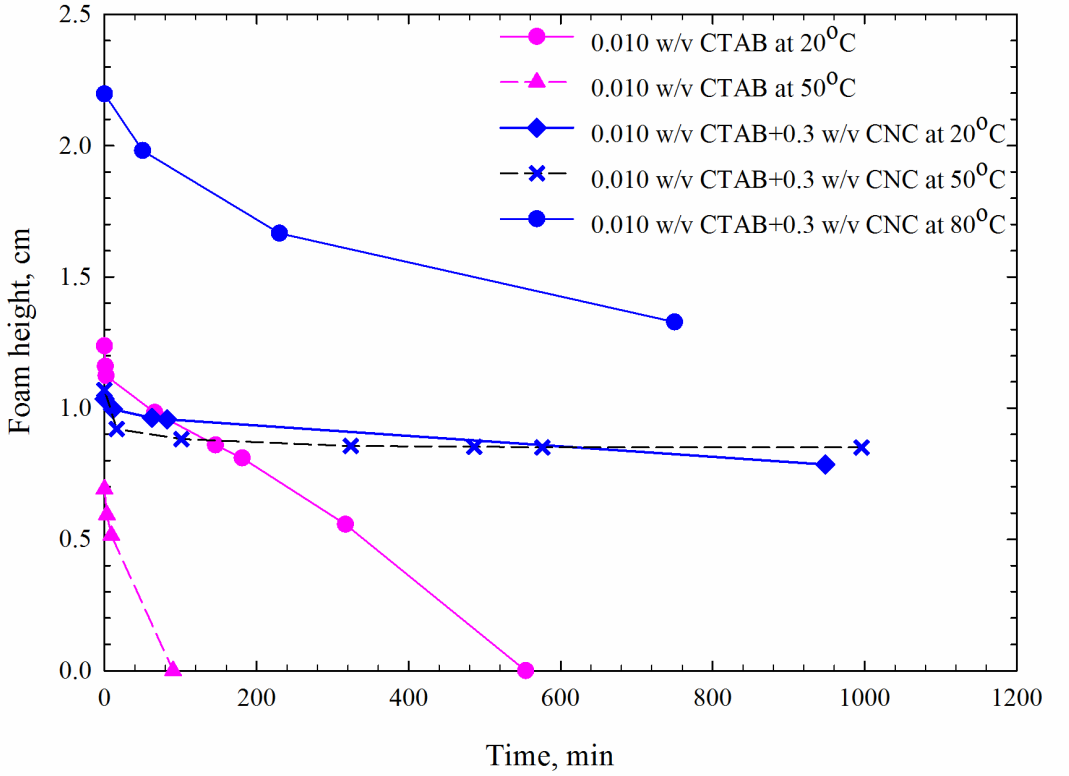

Figure 3-12 Effect of temperature on the stability of foam generated by CTAB (0.010 w/v) and CNC/CTAB (0.300 w/v CNC coated by 0.010 w/v CTAB), respectively.

3.3.2.4. Effect of presence of oil on foam stability

Since foam needs to be stable to displace oil under the reservoir conditions, the presence of oil on foam stability is worth of study. Extensive studies showed that the presence of oil could diminish the stability of surfactant/CO_2 foam (Schramm, 1994). Therefore, it is highly necessary to test the stability of foam stabilized by C_3H_8/CTAB coated CNC with the presence of oil. As the oil droplets replace the adsorbed surfactant on the interface, it reduces the surface elasticity of the foam (Pugh, 1996). In our previous tests, we tested the foam stability generated by C_3H_8/Triton X-100 with the presence of oil and found that the oil was detrimental to the foam stability since C_3H_8 was much more soluble in oil than CO_2 (Wang and Li, 2014). Tests are conducted by using 0.03 w/v CNC coated with 0.015 w/v CTAB and 0.015 w/v CTAB alone at 20°C and 700 kPa, with and without the addition of pure pseudo-oil *n*-$C_{16}H_{34}$. Figure 3-13

shows the foam decay profile of foams formed with and without the addition of oil. As illustrated in Figure 3-13, for both systems, foam stability is diminished by the addition of oil. Oil can be considered as a film breaker as it enters the gas/liquid interface and spreads over the bubble film, resulting in film rupturing (Pugh, 1996). By comparing the foams stabilized by CNC/CTAB and by CTAB alone, with the presence of oil, CNC/CTAB foam exhibits about 1000 min of half-life, which is 25 times of that for CTAB foam. This is probably because that the presence of CNC particles at the gas/liquid interface slows the process of oil droplets entering and spreading over the bubble film.

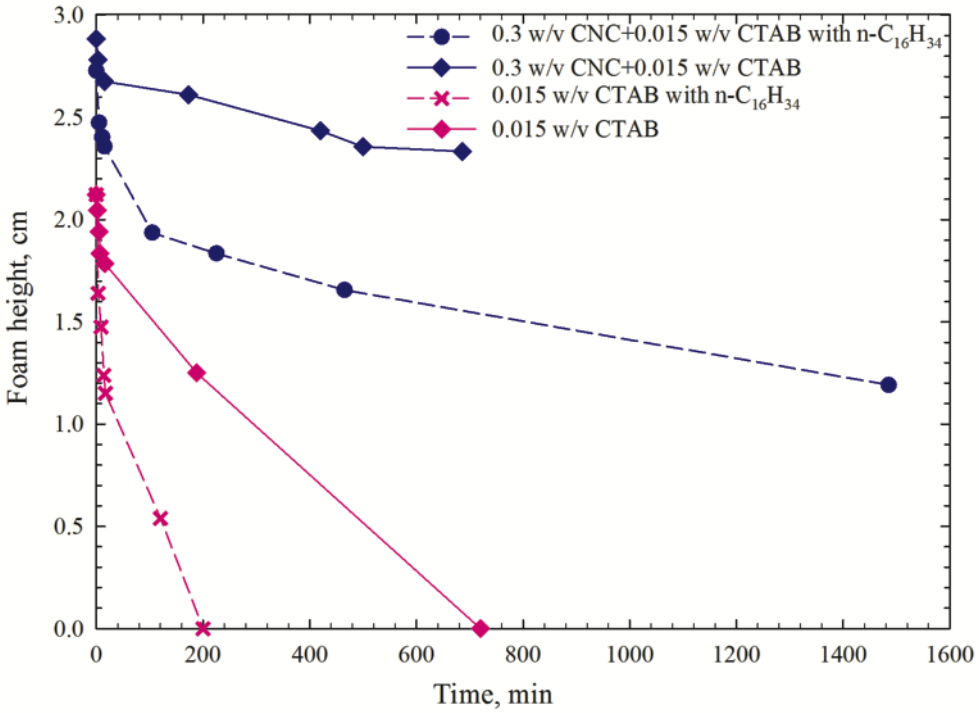

Figure 3-13 Effect of oil presence on the foam stability of foam generated by CTAB alone (0.015 w/v) and CNC/CTAB (0.300 w/v CNC coated by 0.015 w/v CTAB), respectively, at 20°C and 700 kPa

Figure 3-14 shows the image captured 8 hours after the introduction of oil to the CNC/CTAB foam, showing that the foam height decreases with the addition of oil. It can be observed that as soon as the oil comes in contact with the bottom part of foam, the oil spreads over the lamellas of

foam, resulting in an expedited rupturing of foam with time. These results indicate that the CNC-stabilized foam is sensitive to oil, but such foam is still very stable with a half-life of 1000 min.

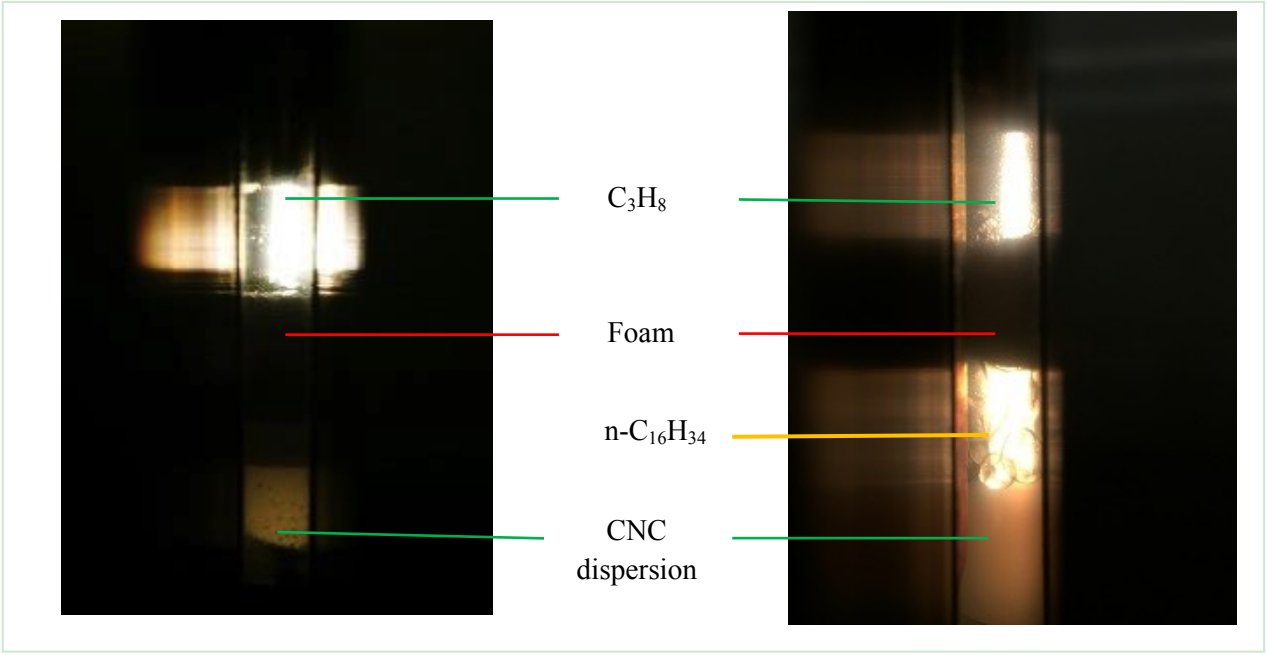

Figure 3-14 Digital images of CNC/CTAB stabilized foams (0.300 w/v CNC coated with 0.015 w/v CTAB) with (right) and without (left) presence of oil, respectively, at 20°C and 700 kPa, 8 hours after the mixing was terminated

3.3.3. Stability of Foam Generated by Non-ionic Surfactant and CNC

Nonionic surfactants Tween 20, Tween 80 and Triton X-100 at their CMCs are used, respectively, to mix with 0.3 w/v CNC dispersion to form a foam at 20°C. Another three foam stability tests are conducted by using these three surfactants alone, without adding CNC particles. Foams stabilized by these nonionic surfactants and surfactant/CNC are compared at the same conditions. Table 3-5 and Figure 3-15 show the test results on foam stability of foam formed by different combinations of surfactant with CNC at different temperatures. No foam is formed by Tween 80 and Tween 80/CNC at 20°C. The foam formed by Tween 20/CNC mixture shows a half-life two times longer than that formed by Tween 20 alone at 20°C, which indicates

that the addition of CNC particles in the nonionic surfactant solution increases the foam stability. No foam is generated by Tween 20 alone at 50°C, while there is a short column of 0.596 cm of foam formed by Tween 20/CNC mixture at the same condition. The Triton X-100/CNC foam also exhibits a longer half-life than the Triton X-100 foam tested previously at both 20°C and 50°C (Wang and Li, 2014). All these results add up to a conclusion that, if a surfactant can generate foam itself, then the surfactant/CNC mixture can form an even more stable foam under the same conditions.

Table 3-5 Foamability and foam stability of foams formed by different combinations of nonionic surfactant with 0.3 w/v CNC dispersion at different temperatures.

Type of surfactant	Surfactant concentration, w/v	With CNC	Temperature, °C	Initial foam height, cm	$T_{1/2}$, cm	Mixed dispersion
Tween 20	0.0071 (CMC)	without	20	0.677	360	Foam
Tween 20	0.0071 (CMC)	with	20	0.957	1179	Foam
Tween 20	0.0071 (CMC)	without	50	0	0	No foam
Tween 20	0.0071 (CMC)	with	50	0.596	33	Foam
Tween 80	0.0019 (CMC)	without	20, 50	0	0	No foam
Tween 80	0.0019 (CMC)	with	20, 50	0	0	No foam
Triton X-100	0.0194 (CMC)	without	20	3.688	585	Foam
Triton X-100	0.0194 (CMC)	with	20	2.627	1250	Foam
Triton X-100	0.0194 (CMC)	without	50	2.823	12	Foam
Triton X-100	0.0194 (CMC)	with	50	2.779	121	Foam

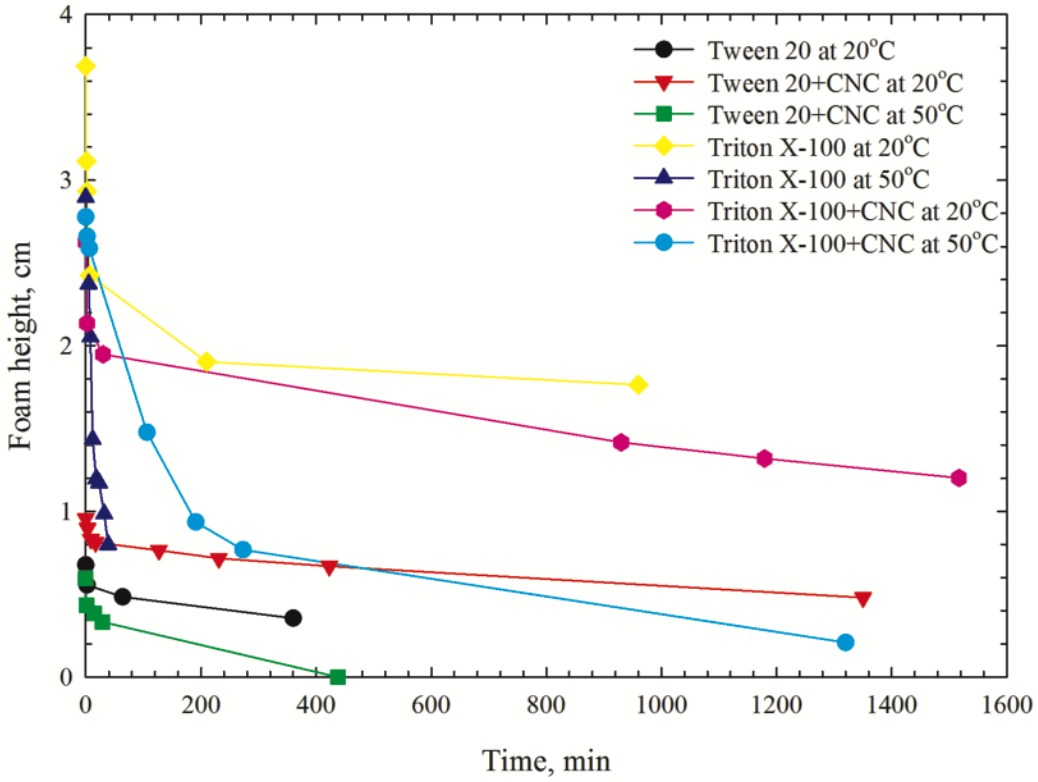

Figure 3-15 Comparison of stability of foams stabilized by a mixture of CNC with different nonionic surfactants (0.300 w/v CNC with surfactant at their CMCs, 20°C and 700 kPa)

According to Table 3-5, the initial heights of foam generated by Triton X-100 and Triton X-100/CNC are higher than those formed by Tween 20 and Tween 20/CNC mixture. This indicates that the foamability of the surfactant/CNC mixture is proportionally related to the foamability of surfactant alone. In other words, the nonionic surfactant can be considered as a foaming agent, and CNC nanoparticles function as a foam stability booster. As for nonionic surfactant/CNC stabilized foam, CNC boosts the foam stability.

By comparing the CTAB/CNC foam with nonionic surfactant/CNC foam, it is noted that CTAB/CNC foam is more stable than nonionic surfactant/CNC foam. This is probably because

the electrostatic interaction of CTAB with CNC is stronger than the synergistic effect due to the use of nonionic surfactant and CNC, providing a more stable foam as a result.

3.4. Conclusions

In this study, the stability of foams generated by C_3H_8/surfactant/nanoparticle mixtures is evaluated experimentally by using a PVT setup. The following conclusions can be obtained:

1. As for foam stabilized by silica/Triton X-100 mixture, no obvious synergistic effect is observed.
2. As for the CNC/CTAB stabilized foam, as the surface property of CNC changes from being hydrophilic to being relatively hydrophobic by adding cationic surfactant CTAB, more stable foams can be formed compared to the foam formed by CTAB alone.
3. As for the CNC/CTAB stabilized foam, its foam stability increases as salt concentration and temperature increase.
4. As for the CNC/CTAB stabilized foam, the presence of *n*-$C_{16}H_{34}$ (pseudo-oil) can only slightly decrease the foam stability.
5. If a surfactant is a foaming agent, the synergistic effect of CNC nanoparticle and non-ionic surfactant enhances the foam stability. In other words, a stable foam can be formed by introducing both foam forming agent (surfactant) and foaming booster (nanoparticle).
6. Foam stability of CNC/CTAB stabilized foam is stronger than that of CNC/non-ionic surfactant. This is probably because the electrostatic interaction of CTAB with CNC is stronger than the synergistic effect due to the use of non-ionic surfactant and CNC, leading to a more stable foam thereof.

CHAPTER 4 MOBILITY OF NANOPARTICLE-STABILIZED C_3H_8 FOAM

4.1. Introduction

The prior chapter systematically investigates the static stability of C_3H_8 foam formed by CTAB-coated CNC and CNC/non-ionic surfactant mixtures, respectively. However, the foam flow behavior in the porous media is also necessary to be tested. In this chapter, we attempt to study the mobility of C_3H_8 foam, formed by CTAB-coated CNC or CNC/non-ionic surfactant mixtures, when it flows through a glass beadpack. A series of flow experiments are conducted by alternately injecting C_3H_8 and CTAB/CNC or alternately injecting C_3H_8 and CNC/non-ionic surfactant dispersion through a porous beadpack. This chapter is organized as follows: Section 1 discusses the pressure drop and mobility reduction measured in SAG experiments without the presence of oil. In section 2, in order to determine the behavior of nanoparticle-stabilized C_3H_8 foam in the presence of hydrocarbon in the porous media, the foam mobility and foam's ability to improve oil recovery are investigated, again, using *n*-$C_{16}H_{34}$ as an oil phase.

4.2. Experimental Section

4.2.1. Materials

The materials used in the dynamic mobility test are the same as those used in the static foam stability tests in chapter 3. The nanoparticle used in the dynamic tests is the nanocrystalline cellulose, CNC, which is derived from wood pulp. This fibrous anionic and hydrophilic CNC has already been discussed in chapter 3. The cationic surfactant CTAB (Sigma-Aldrich), also called as hexadecyltrimethylammonium bromide (See Figure 3-1(b)), at a very low concentration, is used to modify the surface of CNC in the dispersion from being hydrophilic to being hydrophobic. The non-ionic surfactants (Sigma-Aldrich) at their CMCs used to form the

CNC/non-ionic surfactant mixtures are Tween 20 (See Figure 3-1(c)), and Triton X-100 (See Figure 3-1(a)), respectively. Since there is no foam formed by CNC/Tween 80 in our static foam stability test, Tween 80 is not selected to be used in the dynamic tests. C_3H_8 (Praxair) with 99.5% purity is used as the gas phase for foam generation. To investigate the effect of the hydrocarbon phase on the foam's flow behavior in the porous media, *n*-$C_{16}H_{34}$ is used to represent the oil phase in order to be consistent with the static stability tests. Concentrations of the above solutions are expressed in w/v (weight over volume fraction) in the aqueous phase.

4.2.2. Experimental Setup

A schematic of the apparatus used for foam flow through porous media test is shown in Figure 2-3. The components of the apparatus and the properties of porous media used have already been introduced in Table 2.1 in Chapter 1. Surfactant solution or nanoparticle dispersion is first placed in a transfer cylinder and then injected by a syringe pump at a constant rate into the beadpack. C_3H_8 gas is injected from a gas tank, the flowrate of which is controlled by a mass flow controller. A differential pressure gauge is used to measure the pressure difference on both ends of the beadpack.

4.2.3. Experimental Procedure

The beadpack is refilled with glass beads before each test. It is then flooded by 15 PV of the tested solution; the beadpack's permeability is observed to be almost the same in all tests. Initially, C_3H_8 and water are alternately injected into the system (WAG) with an injection period of 2 min for each stage, which is used as a baseline test. The injection rates for C_3H_8 and water are 6 cm^3/min and 3 cm^3/min (WAG ratio of 1:2), respectively. Then the experiments are repeated by alternately injecting C_3H_8 and CTAB-coated CNC or alternately injecting C_3H_8 and CNC/non-ionic surfactant mixture (SAG) under the same conditions as used in baseline WAG

test. The pressure difference across the beadpack, recorded during the experiments, is used to estimate the mobility of foam flowing through porous media. The fluid mobility can be calculated by applying the Darcy's law, which has been discussed in Chapter 1. All the aforementioned WAG and SAG tests are conducted at 20ºC.

In the tests with the presence of oil, a newly packed beadpack is firstly saturated with *n*-$C_{16}H_{34}$. Then surfactant solution or nanoparticle dispersion is alternately injected with C_3H_8 gas into the beadpack at the same injection conditions as used in the baseline WAG test. The duration of either chemical solution injection or C_3H_8 gas injection is kept as 2 min. The changes of differential pressures over time are monitored during the SAG process. Several graduated cylinders are used to collect the oil and solution at the outlet of the beadpack, in order to record how much oil has been produced. All the above experiments are conducted at 20 ^{o}C.

4.3. Results and Discussion

4.3.1. Mobility

4.3.1.1. Foam formed by CTAB-coated CNC

First, we carry out a water-alternating-C_3H_8 gas (WAG) injection test with a water-to-gas ratio of 1:2 through a glass beadpack 20 ^{o}C, which serves as a baseline case for comparison with the following SAG tests. Then, the experiments are repeated by alternately injecting CTAB or CNC/CTAB and C_3H_8 at the same conditions. The concentrations of CNC and CTAB are kept as 0.300 w/v and 0.010 w/v, respectively. Figure 4-1 shows the measured differential pressures and mobility across the beadpack in these three tests. In the differential pressure profiles, the ascending segments represent the liquid-solution flooding stage, and the descending segments represent the C_3H_8 flooding stage. In comparison, in the mobility profile, the ascending segments represent the C_3H_8 flooding stage, and the descending segments mean the liquid-solution

flooding stage. Figure 4-1 clearly indicates that both SAG (CNC/CTAB and CTAB alone) tests give higher pressure drops than the WAG test, indicating a substantial amount of foam within the beadpack is formed. As more and more foams are generated in the porous media, the pressure difference across beadpack will be increased until a steady state is reached (Yang and Reed, 1989). In the presence of CNC nanoparticles, CNC/CTAB stabilized C_3H_8 foam gives a maximum pressure drop of around 1000 kPa at the steady state, which is much higher than that given by CTAB stabilized foam with a maximum pressure drop of 650 kPa. As foam flows through a porous media, its dynamic behavior is controlled by bubble snap-off, coalescence, movement, and trapping. If the foam is unstable, foam coalescence and regeneration occur when it propagates through porous media (Holm, 1968). A higher pressure drop by CNC/CATB stabilized foam indicates an increased foam stability because CNC nanoparticles can be residing at the gas-quid interface, helping to prevent the foam from coalescence. As shown in Figure 4-1, CNC/CTAB stabilized foam shows a lower mobility than CTAB stabilized foam, and CTAB stabilized foam shows a lower mobility than the WAG case. This is because the addition of CNC nanoparticles forms more stable foam, which increases the apparent viscosity of the fluid and results in a higher mobility reduction effect. The key findings obtained from the mobility tests are consistent with those obtained in the former static foam-stability tests.

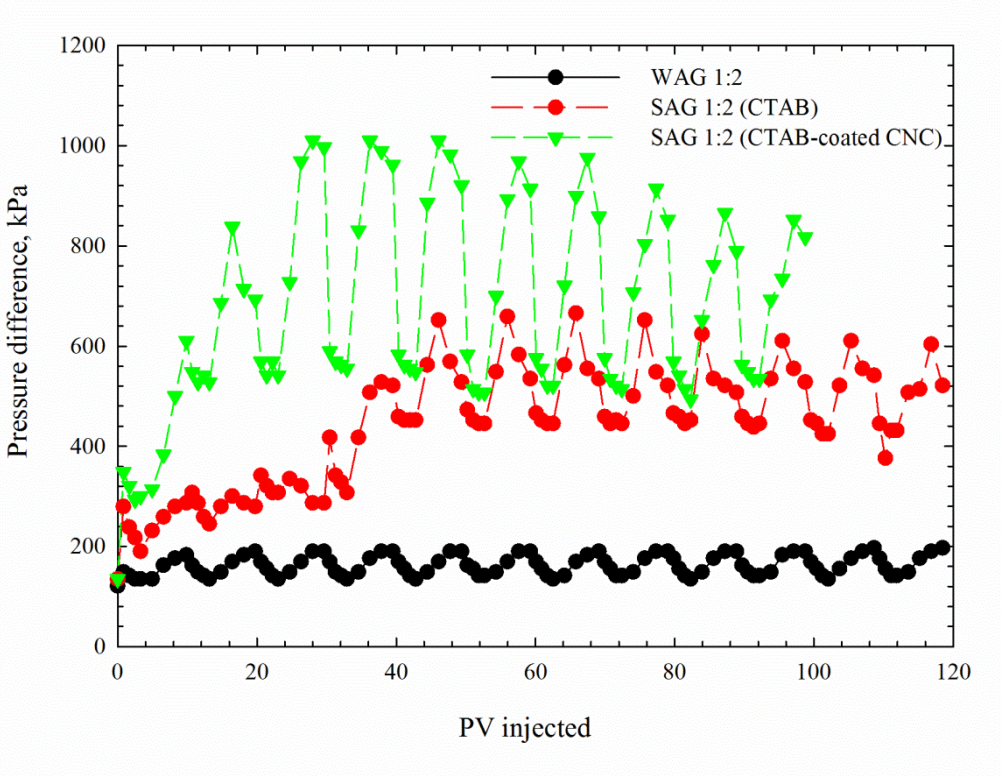

(a)

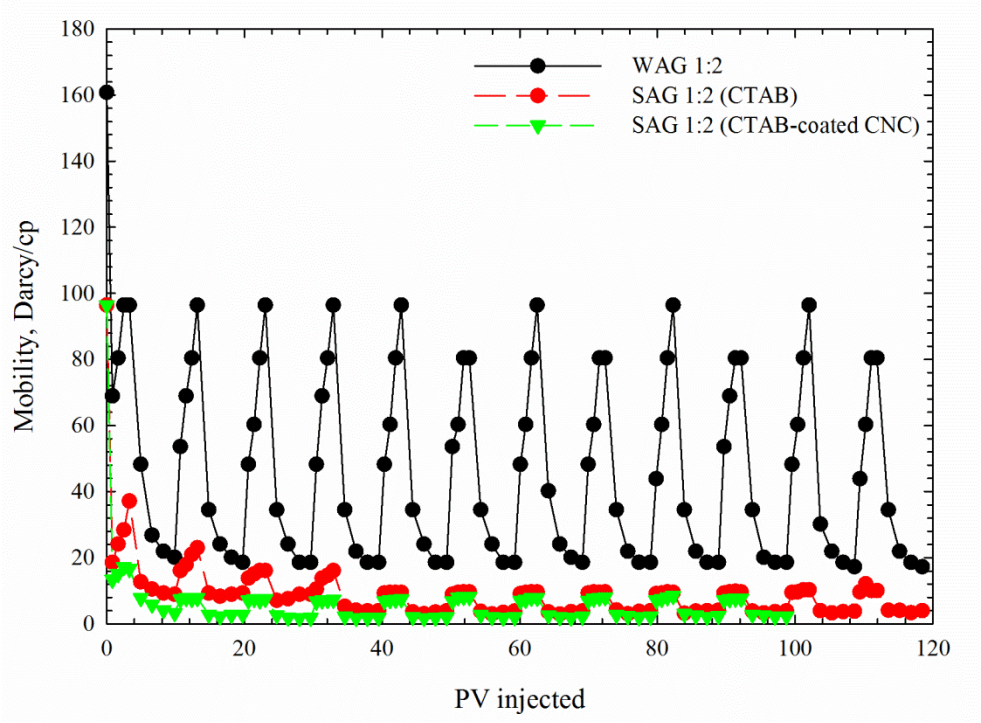

(b)

Figure 4-1 Comparison of pressure difference (a) and mobility (b) recorded in SAG tests (0.010 w/v CTAB, 0.3 w/v CNC, 20°C, SAG ratio of 1:2) and WAG tests (WAG ratio of 1:2)

4.3.1.2. Foam formed by CNC and nonionic surfactant mixture

Based on the static foam stability tests for CNC in combination with nonionic surfactants in the previous section, Tween 20 and Triton X-100 (at their CMCs) are chosen to mix with CNC nanoparticles in the foam mobility tests. Four series of SAG flow experiments with the use of Tween 20, CNC/Tween 20, Triton X-100, and CNC/Triton X-100, respectively, are conducted at the same flow conditions as before. Figure 4-2 shows the test results on the pressure drop and mobility obtained for different cases. It can be found from Figure 4-2 that the SAG with CNC/Tween 20 exhibits a higher mobility reduction effect than the SAG with Tween 20, indicating a substantial amount of foam has been formed within the beadpack. The SAG with Tween 20 shows mobility profiles similar to WAG, implying little foam has been created by Tween 20 alone in the beadpack. During the test, we also do not have any foam collected at the outlet of the beadpack. Therefore, the addition of CNC into the Tween 20 solution is able to create foam in the beadpack, leading to a lower mobility than Tween 20 alone.

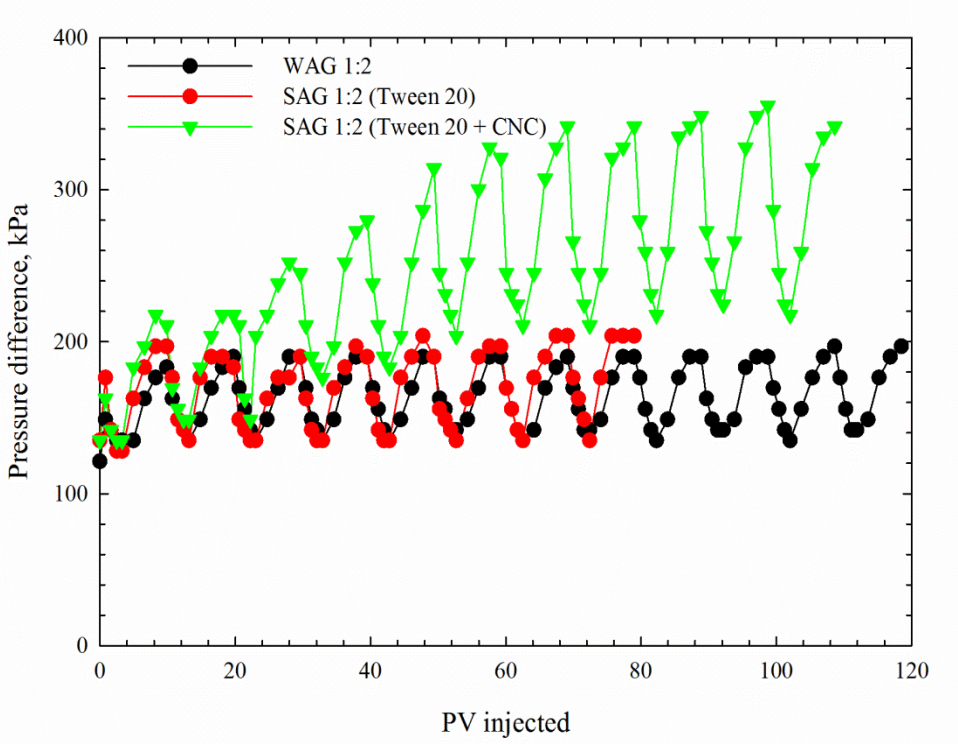

(a)

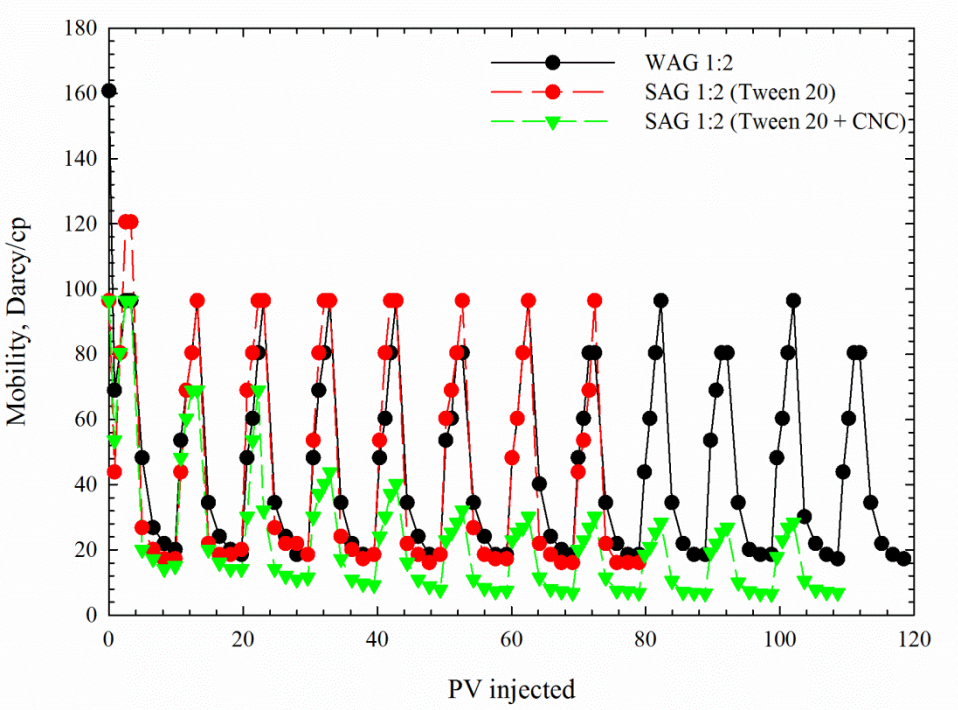

(b)

Figure 4-2 Comparison of pressure difference (a) and mobility (b) recorded in SAG tests (0.0071 w/v Tween 20, 0.3 w/v CNC, 20°C, SAG ratio of 1:2) and WAG tests (WAG ratio of 1:2)

We conduct further tests to examine the mobility of foam formed by Triton X-100 alone and CNC/Triton X-100 mixture, respectively. Figure 4-3 shows the test results on the pressure drop and mobility obtained for different cases. The maximum steady-state pressure drops given by CNC/Triton X-100 mixture and Triton X-100 alone are about 750 kPa and 490 kPa, which are around 3.5 and 2.5 times of that by WAG, respectively. This proves that foam is formed in both SAG test. A lower mobility of foam formed by CNC/Triton X-100 is obtained than that formed by Triton X-100 alone, which indicates that the addition of CNC into nonionic surfactant makes the foam more stable in the porous media.

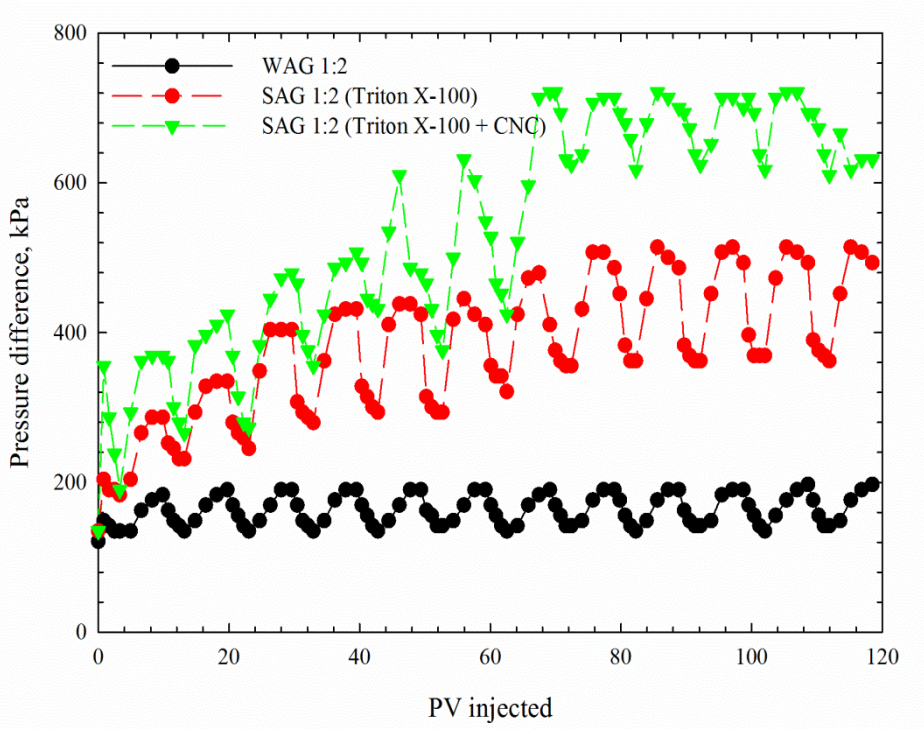

(a)

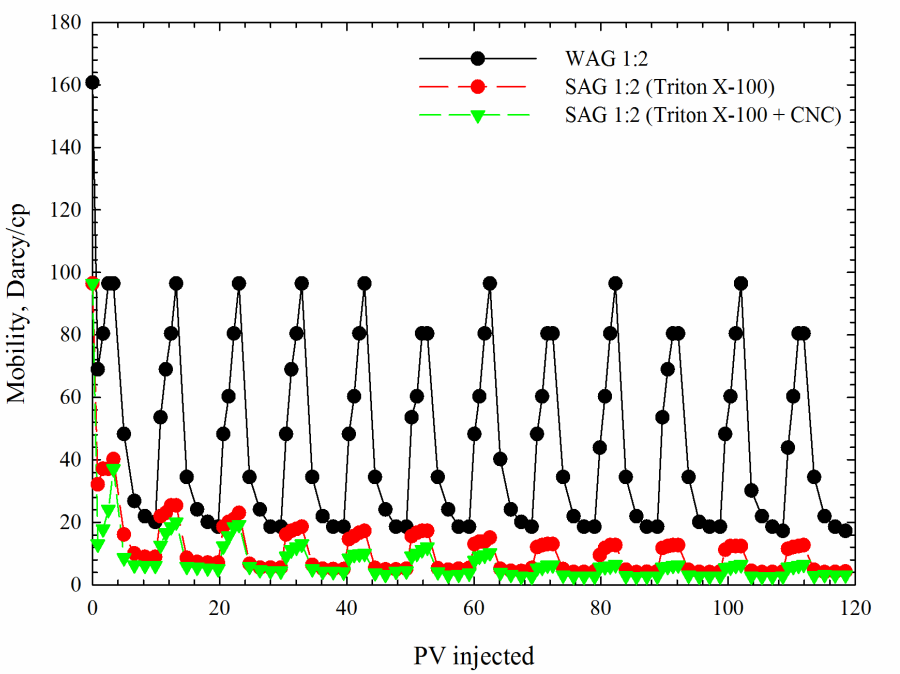

(b)

Figure 4-3 Comparison of pressure difference (a) and mobility (b) recorded in SAG tests (0.0194 w/v Triton X-100, 0.3 w/v CNC, 20°C, SAG ratio of 1:2) and WAG tests (WAG ratio of 1:2)

In summary, if a nonionic surfactant together with CNC is used as a foaming agent, the synergistic effect of CNC and a nonionic surfactant can lead to a lower mobility of foam in the porous media. Comparatively, when used together with CNC, CTAB displays a much better performance in terms of mobility reduction of foam than other nonionic surfactants; this is probably attributed to a stronger electrostatic interaction existing between anionic CNC and cationic CTAB, preventing CNC from detaching from the bubble films. All these findings obtained from the mobility tests are consistent with those obtained from the static foam-stability tests.

4.3.2. Oil recovery

In this section, further investigation on the ability of foam, formed by SAG, in recovering oil is carried out in *n*-$C_{16}H_{34}$ saturated beadpack under the same injection conditions as used in the

previous tests. Firstly, a baseline test case is performed by alternately injecting water and C_3H_8 gas (WAG) into the oil-saturated beadpack. Then two series of experiments are repeated by either injecting CTAB/C_3H_8 or CTAB-coated CNC/C_3H_8 under the same conditions. The measured pressure drop and mobility across the beadpack as a function of PV injected are shown in Figure 4-4. It clearly indicates that, in the absence of CNC nanoparticle, the pressure drop is lower than the case where CNC nanoparticles are present. The CTAB-coated CNC case yields the maximum pressure difference as high as 348 kPa, 80 kPa higher than the CTAB-only case and around 2 times of the WAG baseline case. It is observed that a notable amount of resistance is provided by CTAB-coated CNC-foam despite the presence of oil in the beadpack. SAG (CTAB-coated CNC) yields the highest mobility reduction than the CTAB-only SAG and the WAG baseline case, indicating more stable foams formed in the porous media by CTAB-coated CNC. A lower mobility given by the CTAB-coated CNC indicates that the CNC nanoparticles can serve as an mobility control agent with the presence of oil when they are coated by CTAB.

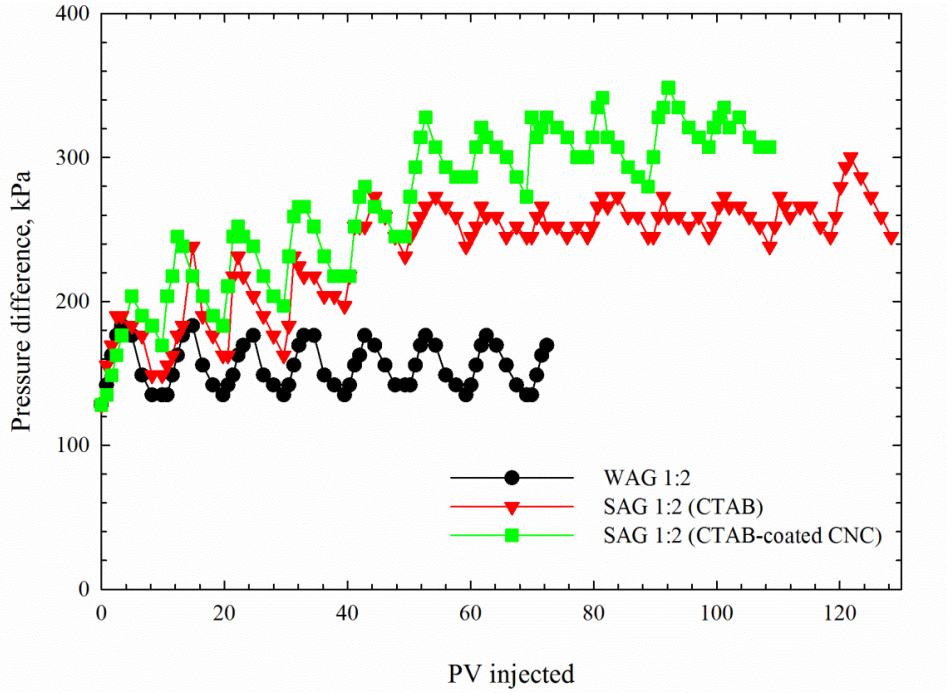

(a)

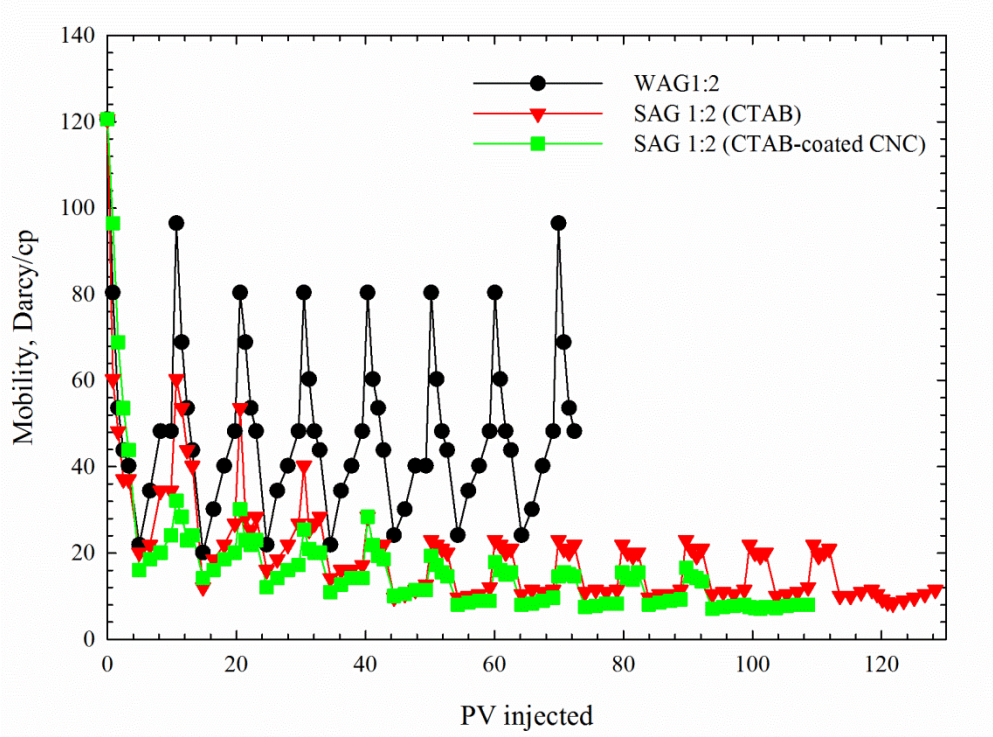

(b)

Figure 4-4 Comparison of pressure difference (a) and mobility (b) recorded in SAG tests (0.010 w/v CTAB, 0.3 w/v CNC, 20°C, SAG ratio of 1:2) and WAG tests (WAG ratio of 1:2) with the presence of oil

Non-ionic surfactant Triton X-100 is selected to test the behavior of C_3H_8 foam formed by the combination of CNC with Triton X-100 in the oil-saturated beadpack. Two series of tests are conducted by alternately injecting CNC/Triton X-100 and C_3H_8 through the porous media under the same conditions as used in the previous tests. The measured results on pressure drop and mobility as a function of pore volume injected are shown in Figure 4-5. The maximum pressure drop measured in the CNC/Triton X-100 case is found to be about 334 kPa, 50 kPa greater than the Triton-only case and around 2 times of the WAG baseline case. The experimental case using CNC/Triton X-100 exhibits a lower mobility than the Triton-only case or the WAG case. The above discussion shows that CNC is able to serve as a mobility control agent when it is used in conjunction with the non-ionic surfactant Triton X-100.

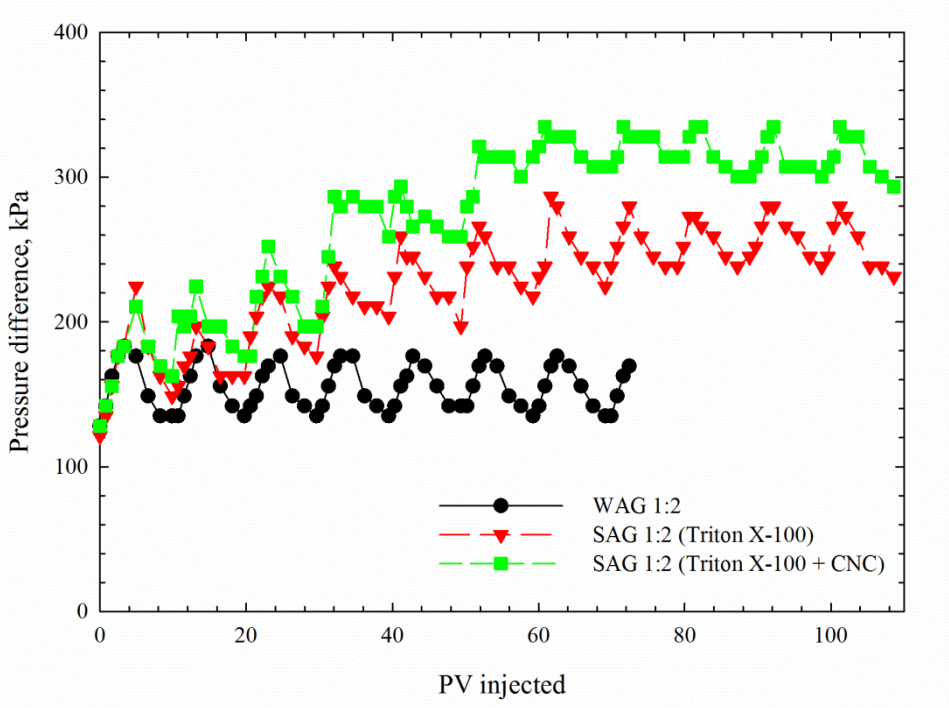

(a)

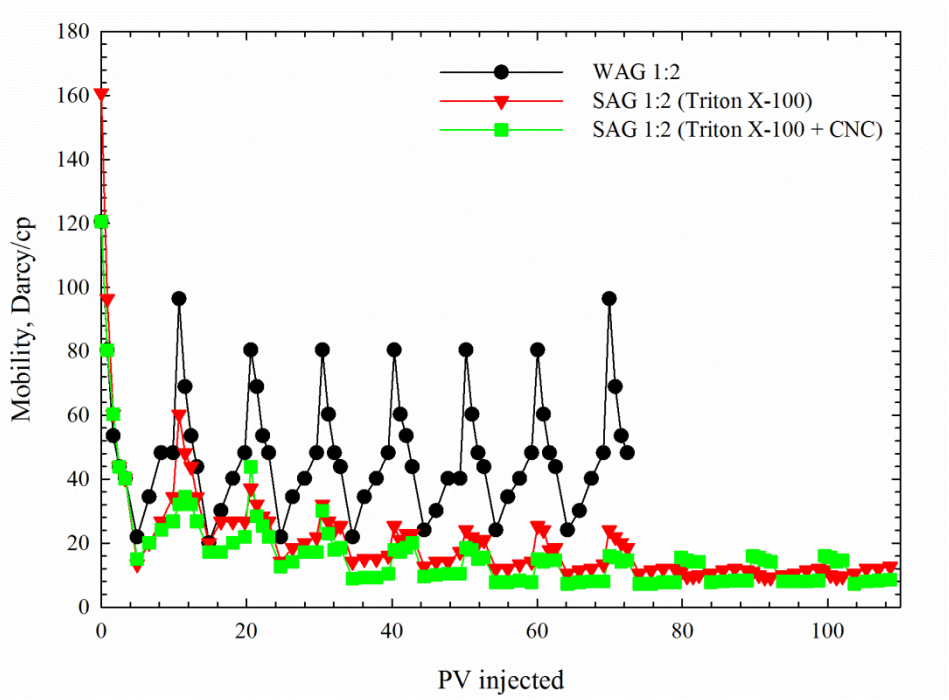

(b)

Figure 4-5 Comparison of pressure difference (a) and mobility (b) recorded in SAG tests (0.0194 w/v Triton X-100, 0.3 w/v CNC, 20°C, SAG ratio of 1:2) and WAG tests (WAG ratio of 1:2) with the presence of oil

During the SAG or WAG experiments, oil and chemical solution are collected from the outlet of the beadpack tube for further oil-recovery estimations. The cumulative oil recovery as a percentage of original oil in place (OOIP) is calculated for the WAG case and each SAG case. Figure 4-6 shows the oil recovery versus PV injected for the above 5 tests. Among all the cases, CTAB-coated CNC shows the best performance with an oil recovery of 97.8% OOIP, while water shows the lowest recovery with an oil recovery of 80% OOIP. The oil recovery given by the CTAB-coated CNC-stabilized foam (97.8%) is 15.6% OOIP more than that given by the CTAB-stabilized foam (82.2%). As for the test using Triton X-100/CNC dispersions, the addition of CNC leads to an additional oil recovery of 13.3% OOIP on top of the oil recovery given by Triton X-100. These results reveal that the foam formed by CNC nanoparticles can contribute to much more oil production than the foam generated by CTAB or Triton. In SAG, with the presence of oil, the nanoparticle-stabilized C_3H_8 foam reduces the residual oil saturation due to a mobility reduction mechanism.

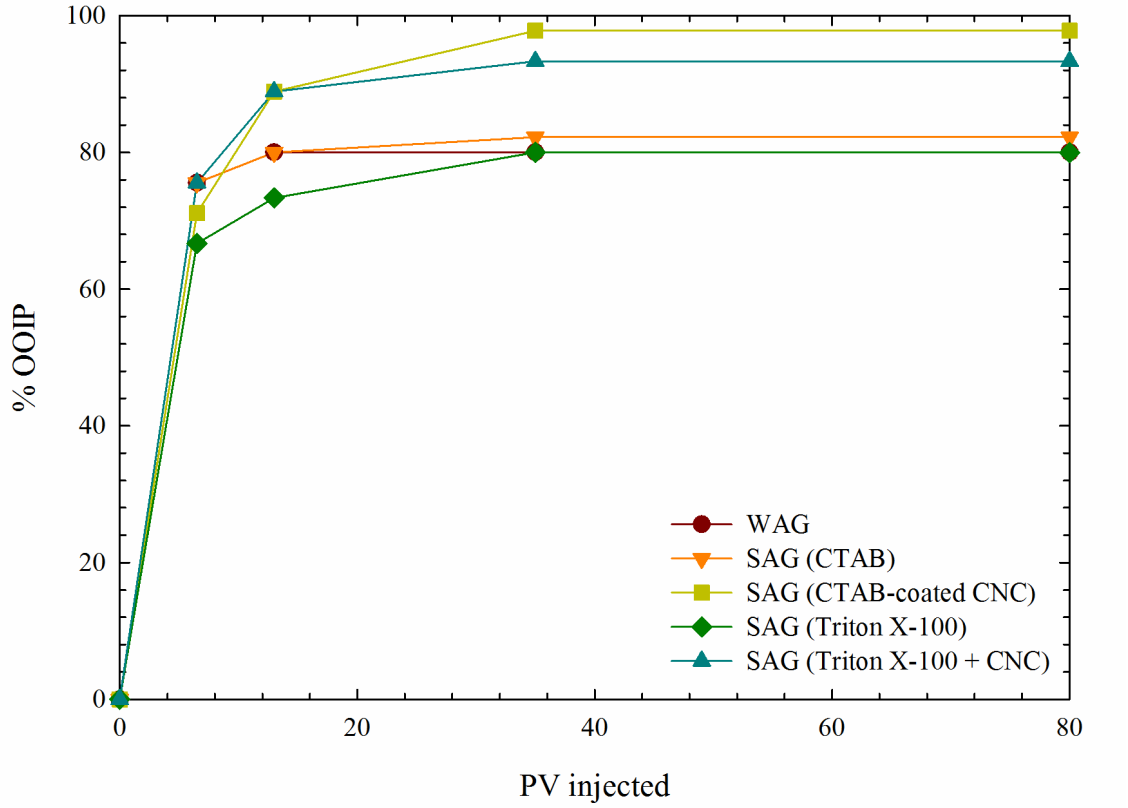

Figure 4-6 Comparison of total oil recovery profiles during WAG and different SAGs (CTAB, CTAB-coated CNC, Triton X-100, Triton X-100+CNC)

4.4. Conclusions

1. If a non-ionic surfactant is used as a foaming agent in SAG, the synergistic effect of CNC and non-ionic surfactant enhances the reduction in fluid mobility, even under the influence of the hydrocarbon phase.
2. The foam formed by alternately injecting CTAB-coated CNC and C_3H_8 shows a higher mobility reduction effect than that formed by alternately injecting CNC/nonionic surfactant and C_3H_8.
3. In the SAG test (either CTAB-coated CNC or Triton X-100/CNC stabilized C_3H_8 foam)

conducted with oil-saturated beadpack, the presence of CNC nanoparticles enhances the oil recovery due to the lowered foam mobility.

CHAPTER 5 CONCLUSIONS AND RECOMMENDATIONS

5.1. Conclusions

In this experimental study, the static stability and dynamic mobility of C_3H_8 foam have been evaluated by using two types of foam agents: surfactants and nanoparticles. Static foam stability and dynamic mobility tests are conducted by using a pressure/volume/temperature (PVT) setup and a porous glass beadpack, respectively. The following conclusions can be obtained:

Key observations from static foam stability tests:

1) As for the Triton X-100 stabilized C_3H_8 foam, its foam stability increases as surfactant concentration increases until reaching the CMC value.
2) As for the Triton X-100 stabilized C_3H_8 foam, its foam stability decreases at higher temperatures, higher salinities or with the presence of oil.
3) As for the foam stabilized by Triton X-100, C_3H_8 foam is much more stable than CO_2 foam at any tested conditions.
4) As the surface property of CNC changes from being hydrophilic to being relatively hydrophobic by adding cationic surfactant CTAB, the CNC/CTAB stabilized C_3H_8 foam tends to be more stable compared to the foam formed by CTAB alone.
5) As for the CNC/CTAB stabilized C_3H_8 foam, the foam stability increases with an increase in salinity or temperature. The presence of *n*-$C_{16}H_{34}$ (pseudo-oil) can only slightly decrease the foam stability.
6) If a surfactant is a foaming agent, the synergistic effect of CNC nanoparticle and non-ionic surfactant enhances the foam stability. In other words, a stable foam can be formed by introducing both foam forming agent (surfactant) and foaming booster (nanoparticle).

7) Foam stability of CNC/CTAB stabilized foam is stronger than that of CNC/non-ionic surfactant stabilized foam.

Key observations from dynamic foam mobility (SAG) tests:

8) In the SAG tests using C_3H_8 with Triton X-100 solution, a larger mobility reduction effect is achieved than WAG. A higher SAG ratio tends to further reduce the mobility of foam.
9) If a non-ionic surfactant is used as a foaming agent in SAG, the synergistic effect of CNC and non-ionic surfactant enhances the reduction in foam mobility.
10) The foam formed by alternately injecting CTAB-coated CNC and C_3H_8 shows a higher mobility reduction effect than that formed by alternately injecting CNC/nonionic surfactant and C_3H_8.
11) In the SAG test (either CTAB-coated CNC or Triton X-100/CNC stabilized C_3H_8 foam) conducted with oil-saturated beadpack, the presence of CNC nanoparticles enhances the oil recovery due to the lowered foam mobility.

5.2. Recommendations

- In the static foam stability test, an environmentally friendly cationic surfactant should be used to replace CTAB.
- SAG injections through glass beadpack should be carried out at higher temperatures, similar to reservoir conditions.
- The permeability of the glass beadpack should be decreased as low as possible to better simulate the property of actual reservoirs.

- The SAG injection can be conducted using two parallel beadpacks with different permeability. Hence, the effect of heterogeneity on the foam mobility can be quantified.
- SAG injections for EOR using real cores should be performed.
- The generation and propagation of foam in the porous media can be visually studied using micromodels, which could lead to a better understanding of how surfactant-stabilized foam or nanoparticle-stabilized foam behaves under various conditions.
- Different injection rates of SAG should be used in the experiments to better understand the effect of SAG ratio on foam generation and migration mechanisms.

REFERENCES

Alargova, R.G.; Warhadpande, D.S.; Paunov, V.N.; Velev, O.D. Foam superstabilization by polymer microrods. Langmuir 2004, 20 (24), 10371-10374.

Belhaij, A.; AlQuraishi, A.; Al-Mahdy, O. Foamability and foam stability of several surfactants solutions: the role of screening and flooding. Paper SPE 172185 presented at the SPE Saudi Arabia Section Technical Symposium and Exhibition, Al-Khobar, Saudi Arabia, April 21-24, 2014.

Bernard, G.G.; Holm, L.W. Method for recovering oil from subterranean formations. U.S. Patent No. 3342256, 1967.

Bond, D.C.; Holbrook, O.C. U.S. Patent 2866507, 1958.

BP Statistical Review of World Energy 2014. May 2015. http://www.bp.com/en/global/corporate/about-bp/energy-economics/statistical-review-of-world-energy.html.

Binks, B.P. Particles as surfactants: similarities and differences. Curr. Opin. Colloid Interface Sci. 2002, 7 (1), 21-41.

Binks, B.P.; Horozov, T.S. Aqueous foams stabilized solely by silica nanoparticles. Angew. Chem. 2005, 117 (24), 3788-3791.

Binks, B.P.; Horozov, T.S. Colloidal particles at liquid interfaces. Cambridge Univ. Press 2006, 1-71.

Cervantes Martinez, A.; Rio, E.; Delon, G.; Saint-Jalmes, A.; Langevin, D.; Binks, B.P. On the origin of the remarkable stability of aqueous foams stabilized by nanoparticles: link with microscopic surface properties. Soft Matter 2008, 4, 1531-1535.

Chiang, J.C.; Sanyal, S.K.; Castanier, L.M.; Brigham, W.E.; Sufi, A. Foam as a mobility control agent in steam injection process. Paper SPE 8912 presented at the 50th Annual California Regional Meeting, Los Angeles, April, 9-11, 1980.

Craig, V.S.; Ninham, B.W.; Pashley, R.M. The effect of electrolytes on bubble coalescence in water. J. Phys. Chem. 1993, 97 (39), 10192-10197.

Demiral, M.R.B.; Okandan, E. Experimental analysis of steam foam injection to heavy oil limestone reservoirs. Paper SPE 15734 presented at the 5th SPE Middle East Oil Show, Manama, Bahrain, March 7-10, 1987.

Deschenes, L.A.; Zilaro, P.; Muller, L.J.; Fourkas, J.T.; Mohanty, U. Quantitative measure of hydrophobicity: experiment and theory. J. Phys. Chem. B 1997, 101 (30), 5777-5779.

Dickinson, E.; Ettelaie, R.; Kostakis, T.; Murray, B.S. Factors controlling the formation and stability of air bubbles stabilized by partially hydrophobic silica nanoparticles. Langmuir 2004, 20 (20), 8517-8525.

Espinoza, D.A.; Caldelas, F.M.; Johnston, K.P.; Bryant, S.L.; Huh, C. Nanoparticle-stabilized supercritical CO_2 foams for potential mobility control applications. Paper SPE-129925-MS presented at the SPE Improved Oil Recovery Symposium, Tulsa, Oklahoma, U.S.A., April 24-28, 2010.

Farajzadeh, R.; Andrianov, A.; Krastev, R.; Hirasaki, G. J.; Rossen, W. R. Foam-oil interaction in porous media: implications for foam assisted enhanced oil recovery. Adv. Colloid Interf. Sci. 2012, 183, 1-13.

Farajzadeh, R.; Vincent-Bonnieu, S.; Bourada, B.N. 2014. Effect of gas permeability and solubility on foam. J. Soft Matter Vol. 2014, 1-7.

Fred, A.N. The foam-drive process for increasing the recovery of oil, Bureau of Mines Rept. 1961, 5866.

Grigg, R.B.; Mikhalin, A.A. Effects of flow conditions and surfactant availability on adsorption. Paper SPE-106205-MS presented at SPE Int. Symp. Oilfield Chem., Houston, Texas, U.S.A., February 28- March 2, 2007.

Holm, L.W. The mechanism of gas and liquid flow through porous media in the presence of foam. SPE J. 1968, 8 (4), 359-369.

James, L.A.; Ioannidis, M.A.; Chatzis, I. Experimentally validated model for the determination of concentration-dependent diffusion of a light hydrocarbon in bitumen. Energy Fuels 2012, 26 (10), 6200-6209.

Li, H.; Zheng, S.; Yang, D. Enhanced swelling effect and viscosity reduction of solvent/CO_2/heavy-Oil systems. SPE J. 2013, 18 (4), 695-707.

Luo, P.; Yang, C.; Gu, Y. Enhanced solvent dissolution into in-situ upgraded heavy oil under different temperatures. Fluid Phase Equilibr. 2007, 252, 143-151.

Mannhardt K.; Novosad J.J.; Schramm L.L. Comparative evaluation of foam stability to oil. SPE Res. Eval. Eng. 2003, 3 (1), 23-26.

Pickering S.U. Emulsions. J. Chem. Soc. 1907, 91, 2001–2021

Pugh, P.J. Foaming, foam films, antifoaming and defoaming. Adv. Colloid Interface Sci. 1996, 64, 67-142.

Ramsden W. Separation of solids in the surface layers of solutions and suspensions. Proc. R. Soc. London, 1903, 72, 156-164.

Schott, H. Effect of electrolytes on foaming of nonionic surfactant solutions. J. Am. Oil Chem. Soc. 1988, 65 (10), 1658-1633.

Schramm, L.L. Foam sensitivity to crude oil in porous media. In Foams: fundamentals and applications in the petroleum industry; Schramm, L.L., Ed.; American Chemical Society: Washington, DC, 1994; Chapter 4, pp. 165-197.

Sharma, M.K.; Shah, D.O.; Brigham, W.E. The influence of temperature on surface and microscope properties of surfactant solutions in relation to fluid displacement efficiency in porous media. AIChE J. 1985, 31, 222-228.

Shaw, D.J. Introduction to colloid and surface chemistry (4th Edition). London: Butterworth-Heinemann, 1992.

Simjoo, M.; Rezaei, T.; Andrianov, A.; Zitha, P.L.J. Foam stability in the presence of oil: effect of surfactant concentration and oil type. Colloids and Surfaces A: Physicochem. Eng. Aspect. 2013, 438 (5), 148-158.

Singh, R.; Mohanty, K.K. Synergistic stabilization of foams by a mixture of nanoparticles and surfactants. Paper SPE-169126-MS presented at SPE Improved Oil Recovery Symposium, Tulsa, Oklahoma, U.S.A., April 12-16, 2014.

Smith, D.H. Surfactant-based mobility control: progress in miscible-flood enhanced oil recovery. Washington DC: American Chemical Society, 1988.

Upreti, S.R.; Lohi, A.; Kapadia, R.A.; El-haj, R. Vapor extraction of heavy oil and bitumen: a review. Energy Fuels 2007, 21 (3), 1562-1574.

Wang, L.; Yoon, R.H. Role of hydrophobic force in the thinning of foam films containing a nonionic surfactant. Colloids Surf. A: Physicochem. Eng. Aspects 2006, 282-283, 84-91.

Wang, C.; Li, H. Stability and mobility of foam generated by gas-solvent/surfactant mixtures under reservoir conditions. J. Nat. Sci. Eng. Sci. 2016, 34, 366-375.

Worthen, A.; Bagaria, H.; Chen, Y.; Bryant, S.L.; Huh, C.; Johnston, K.P. Nanoparticle stabilized carbon dioxide in water foams for enhanced oil recovery. Paper SPE-154285-MS presented at SPE Improved Oil Recovery Symposium, Tulsa, Oklahoma, U.S.A., April 14-

18, 2012.
Yang, S.H.; Reed, R.L. Mobility control using CO_2 foams. Paper SPE-19689-MS presented at the SPE Annual Technical Conference and Exhibition, San Antonio, Texas, October 8-11, 1989.
Yu, J.; An, C.; Mo, D.; Liu, N.; Lee, R.L. Foam mobility control for nanoparticle-stabilized supercritical CO_2 foam. Paper SPE-153336-MS presented at SPE Improved Oil Recovery Symposium, Tulsa, Oklahoma, U.S.A., April 14-18, 2012.
Zhang, S.; Sun, D.; Dong, X.; Li, C.; Xu, J. Aqueous foams stabilized with particles and nonionic surfactants. Colloids Surf. 2008, 324 (1-3), 1-8.